



Universitat Autònoma de Barcelona

ADVERTIMENT. L'accés als continguts d'aquesta tesi queda condicionat a l'acceptació de les condicions d'ús establertes per la següent llicència Creative Commons:  http://cat.creativecommons.org/?page_id=184

ADVERTENCIA. El acceso a los contenidos de esta tesis queda condicionado a la aceptación de las condiciones de uso establecidas por la siguiente licencia Creative Commons:  <http://es.creativecommons.org/blog/licencias/>

WARNING. The access to the contents of this doctoral thesis it is limited to the acceptance of the use conditions set by the following Creative Commons license:  <https://creativecommons.org/licenses/?lang=en>

GLOBAL ASSESSMENT OF MARINE PALEOPRODUCTIVITY PROXIES

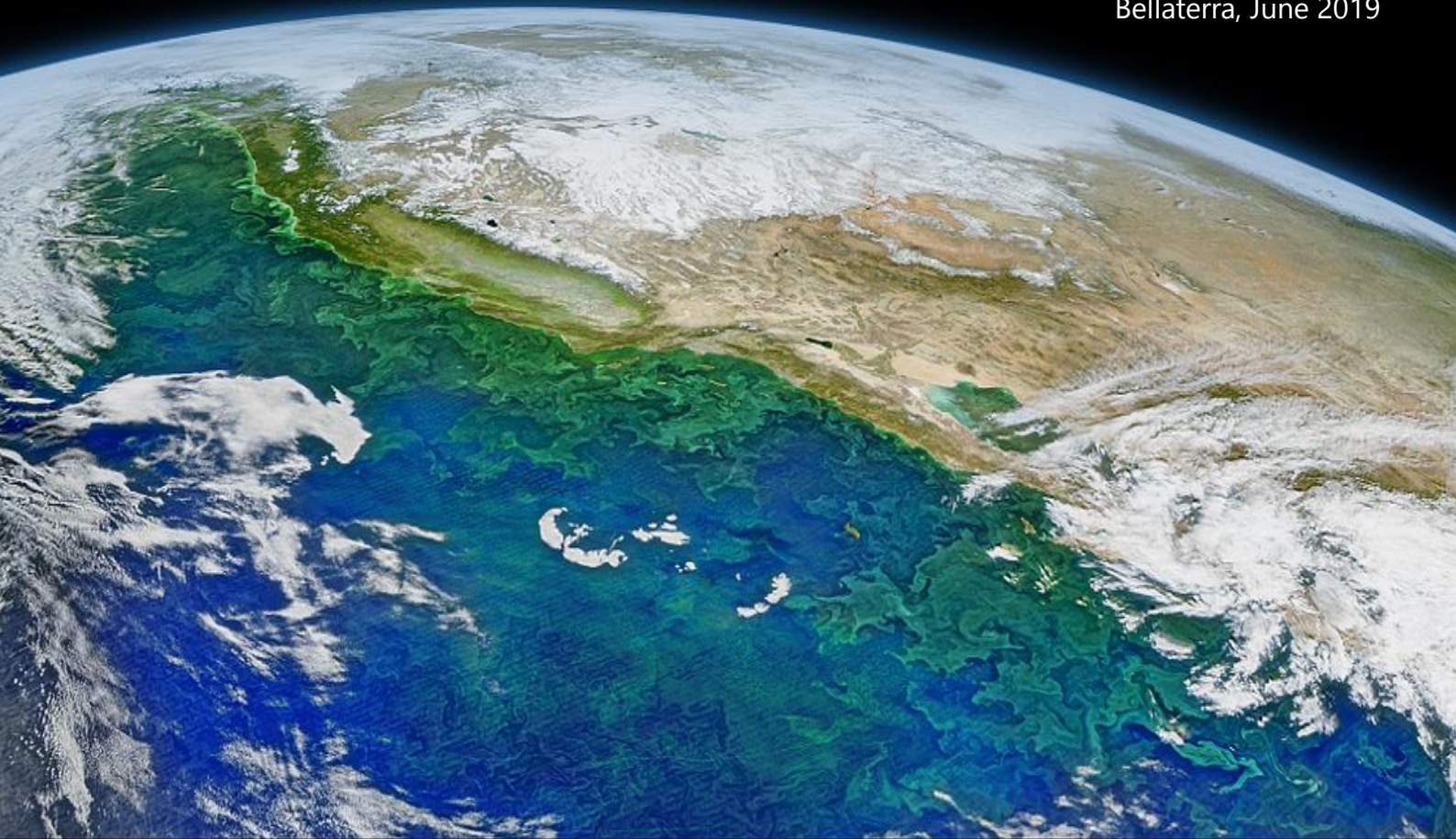
Maria Raja Sanchez

Doctoral Thesis

Supervisors: Dr. Antoni Rosell Melé
Dr. Eric D. Galbraith

Doctoral degree in Environmental Sciences and Technology
Institut de Ciència i Tecnologia Ambiental
Universitat Autònoma de Barcelona

Bellaterra, June 2019



Cover photo from the NASA Earth Observatory.

GLOBAL ASSESSMENT OF MARINE PALEOPRODUCTIVITY PROXIES

Maria Raja Sanchez

Doctoral Thesis

Supervisors: Dr. Antoni Rosell Melé
Dr. Eric D. Galbraith

Doctoral degree in Environmental Sciences and Technology
Institut de Ciència i Tecnologia Ambiental
Universitat Autònoma de Barcelona

Maria Raja Sanchez

Antoni Rosell Melé

Eric D. Galbraith

Bellaterra, June 2019

Als meus pares,

Contents

Abbreviations	I
List of figures	III
List of tables	V
Acknowledgements	VII
Abstract	IX
Resum	XI
CHAPTER 1. Introduction and objectives	3
1.1. Global climate change.....	3
1.2. The soft-tissue pump.....	4
1.3. Primary productivity (PP) and remote sensing.....	6
1.4. Paleoproductivity proxies	8
1.4.1. Introduction to paleoproductivity proxies	8
1.4.2. Export proxies.....	9
1.4.2.1. Biomarkers.....	10
1.4.2.2. Total organic carbon (TOC).....	11
1.4.2.3. Mineral shells.....	12
1.4.2.4. Trace elements.....	12
1.4.3. Nutrient proxies.....	13
1.4.3.1. Isotopic ratios.....	13
1.5. Objectives and outline	14
1.6. References.....	17
CHAPTER 2. Chlorins: quantitative paleoproductivity proxy	31
2.1. Introduction.....	31
2.2. Methods.....	32

2.2.1.	Chlorins abundance	32
2.2.2.	Uncertainties in the sedimentary data.....	33
2.2.3.	SSchla concentration	35
2.2.4.	Uncertainties in the remote sensing data	35
2.3.	Results	36
2.3.1.	The global fraction of the exported and buried chlorophyll- <i>a</i>	36
2.3.2.	Quantifying SSchla from chlorins	37
2.3.3.	Other factors controlling chlorins deposition.....	40
2.4.	Discussion	41
2.4.1.	Chlorins as a quantitative proxy for past PP	41
2.4.2.	Regional and seasonal variability	42
2.4.3.	Depositional factors in the export and burial of surface chlorophyll- <i>a</i>	44
2.5.	Conclusions	44
2.6.	References.....	45
 CHAPTER 3. Alkenones: quantitative paleoproductivity proxy.....		55
3.1.	Introduction.....	55
3.2.	Methods.....	56
3.2.1.	Alkenones abundance.....	56
3.2.2.	SSchla and SSPIC concentration	57
3.3.	Results	59
3.3.1.	Quantifying SSchla from alkenones.....	59
3.3.2.	Quantifying SSPIC from alkenones	61
3.4.	Discussion	63
3.4.1.	Alkenones as a quantitative proxy for past PP	63
3.4.2.	The relevant role of photosynthetic picoeukaryotes (PPE) in the global carbon export.....	65
3.4.3.	Alkenones and SSPIC for studying past PP and the global carbonate pump.....	66

3.5.	Conclusions	67
3.6.	References.....	67
CHAPTER 4. Total organic carbon: quantitative paleoproductivity proxy.....		79
4.1.	Introduction.....	79
4.2.	Methods.....	80
4.2.1.	TOC abundance	80
4.2.2.	SSchla concentration	81
4.3.	Results	82
4.3.1.	Quantifying SSchla from TOC	82
4.3.2.	The link between preservation factors and TOC.....	84
4.4.	Discussion	85
4.4.1.	TOC as a quantitative proxy for global past PP	85
4.4.2.	TOC as a quantitative proxy for regional past PP	89
4.5.	Conclusions	91
4.6.	References.....	92
CHAPTER 5. Nitrogen isotopes: constraints of nutrient proxies.....		103
5.1.	Introduction.....	103
5.2.	Methods.....	104
5.2.1.	Bulk nitrogen isotopic analysis	105
5.2.2.	Chlorin-specific nitrogen isotopic analysis	105
5.3.	Results and discussion	106
5.3.1.	Bulk and chlorin-specific nitrogen isotopes.....	106
5.3.2.	Chlorin-compound specific nitrogen isotopic variability	108
5.4.	Conclusions	111
5.5.	References.....	112

CHAPTER 6. Conclusions and further research	119
6.1. Main conclusions.....	119
6.2. Further implications.....	123
6.2.1. The soft-tissue pump.....	123
6.2.2. The carbonate pump.....	124
6.3. Future research.....	124
6.3.1. Ocean remote sensing validation.....	125
6.3.2. Implications of logarithmic relationship between chlorins and PP.....	125
6.3.3. Constraining $\delta^{15}\text{N}_{\text{chlorin}}$ proxy.....	126
6.4. References.....	126
APPENDIX	131
Appendix 1. Supplementary figures and tables.....	131
Appendix 2. Database references.....	137

Abbreviations

allPhe *a* - Allomer of pheophytin-*a*

BE - Burial efficiency

CCEs - Carotenoid chlorin esters

Chide *a* - Chlorophyllide-*a*

Chl *a* - Chlorophyll-*a*

Chlone *a* - Chlorophyllone-*a*

CPhe *a* - Cyclopheophorbide-*a*-enol

DCM - Dichloromethane

DMF - N,N-dimethylformamide

EA-IRMS - Elemental analysis-isotope ratio mass spectrometry

epPhe *a* - Epimer of pheophytin-*a*

ESA - European Space Agency

GC - Gas chromatography

HPLC - High performance liquid chromatography

MAR - Mass accumulation rate

MARS - Microwave accelerated extraction system

MeOH - Methanol

MERIS - MEdium Resolution Imaging Spectrometer

mesoCPhe *a* - Meso form of cyclopheophorbide-*a*-enol

MODIS - Moderate-Resolution Imaging Spectroradiometer

n - Number of samples

NASA - National Aeronautics and Space Administration

NOAA - National Oceanic and Atmospheric Administration

PDA - Photodiode array detector

PChl *a* - Pyrochlorophyll *a*

Phe *a* - Pheophytin-*a*

Phide *a* - Pheophorbide-*a*

PP - Primary productivity

PPhe *a* - Pyropheophytin-*a*

PPhide *a* - Pyropheophorbide-*a*

R² - Coefficient of determination

RMS log error - Root-mean square logarithmic error

Rrs - Remote sensing reflectance

SA - Subarctic

SCEs - Steryl chlorin esters

SeaWiFS - Sea-viewing Wide Field-of-view Sensor

SO - Southern Ocean

SR - Sedimentation rate

SSchla - Sea-surface chlorophyll-*a*

SSPIC - Sea-surface particulate inorganic carbon

ST - Subtropics

SVI - Seasonal variation index

T - Tropics

TOC - Total organic carbon

VIIRS - Visible and Infrared Imager Radiometer Suite

WD - Water depth

$\delta^{13}\text{C}$ - Carbon isotopic signal

$\delta^{15}\text{N}$ - Nitrogen isotopic signal

$\delta^{15}\text{N}_{\text{bulk}}$ - Bulk nitrogen isotopic signal

$\delta^{15}\text{N}_{\text{chla}}$ - Chlorophyll-*a* nitrogen isotopic signal

$\delta^{15}\text{N}_{\text{chlorin}}$ - Chlorin nitrogen isotopic signal

$\delta^{15}\text{N}_{\text{Phea}}$ - Pheophytin-*a* nitrogen isotopic signal

List of figures

Figure 1. Temperature and CO ₂ concentration from Antarctic ice cores over the past 800.000 years.....	3
Figure 2. Principal processes and compartments of the soft-tissue pump	4
Figure 3. Photographs of the dominant phytoplankton species in the global ocean.....	5
Figure 4. Global annual average sea-surface chlorophyll- <i>a</i> (SSchla) concentration measured by the Sea-viewing Wide Field-of-view Sensor (SeaWiFS) since 1997 to 2010.....	6
Figure 5. Satellite images obtained from phytoplankton blooms.....	7
Figure 6. Global average sea-surface chlorophyll- <i>a</i> (SSchla) concentration obtained by merging the Moderate-Resolution Imaging Spectroradiometer (MODIS) and the Infrared Imager Radiometer Suite (VIIRS) sensors.....	8
Figure 7. Paleoproductivity proxies classification.....	9
Figure 8. Principal chlorins structure and their degradation pathways.....	10
Figure 9. Global core-top sediments distribution for the chlorins study.....	33
Figure 10. Global correlations between sedimentary chlorins concentration and the sum of sea-surface chlorophyll- <i>a</i> (SSchla) concentration from 1997 to 2017.....	37
Figure 11. Regional correlations between sedimentary chlorins concentration and the sum of sea-surface chlorophyll- <i>a</i> (SSchla) concentration from 1997 to 2017.....	39
Figure 12. Global correlation between sedimentary chlorins concentration and the average of sea-surface chlorophyll- <i>a</i> concentration (SSchla) from 1997 to 2017	40
Figure 13. Global correlation between the ratio of the sum of sea-surface chlorophyll- <i>a</i> (SSchla) concentration from 1997 to 2017 and chlorins concentration with depositional factors.....	41
Figure 14. Global core-top sediments distribution for the alkenones study	57
Figure 15. Global correlations between sedimentary C37 alkenones concentration and the sum of sea-surface chlorophyll- <i>a</i> (SSchla) concentration from 1997 to 2017.....	59
Figure 16. Regional correlations between sedimentary alkenones concentration and the sum of sea-surface chlorophyll- <i>a</i> (SSchla) concentration from 1997 to 2017	61
Figure 17. Global correlations between sedimentary alkenones concentration and the sum of sea-surface particulate inorganic carbon concentration (SSPIC) from 1997 to 2017	62
Figure 18. Global core-top sediments distribution for the total organic carbon study	81
Figure 19. Global comparisons between sedimentary total organic carbon (TOC) content and the sum of sea-surface chlorophyll- <i>a</i> (SSchla) concentration from 1997 to 2017.....	83

Figure 20. Global comparisons between sedimentary total organic carbon (TOC) content and depositional factors.....	86
Figure 21. Regional comparisons between sedimentary total organic carbon (TOC) content and the sum of sea-surface chlorophyll- <i>a</i> (SSchla) concentration from 1997 to 2017.....	91
Figure 22. Global sediments distribution for the nitrogen isotopes study.....	105
Figure 23. Comparison between nitrogen isotope proxies.....	107
Figure 24. Chlorin nitrogen isotopic signal ($\delta^{15}\text{N}_{\text{chlorin}}$) from core-top sediment samples	108
Figure 25. The averages and the standard deviations of the differences between chlorophyll- <i>a</i> or pheophytin- <i>a</i> nitrogen isotopic signal ($\delta^{15}\text{N}_{\text{Chla}}$ or $\delta^{15}\text{N}_{\text{Phea}}$) and the rest of chlorins.....	109
Figure 26. Comparison of the differences between chlorophyll- <i>a</i> and chlorin nitrogen isotopic signal ($\delta^{15}\text{N}_{\text{chla}}$ and $\delta^{15}\text{N}_{\text{chlorin}}$) with environmental factors	111
Figure 27. Global comparisons between the sum of sea-surface chlorophyll- <i>a</i> (SSchla) concentration from 1997 to 2017 and export proxies concentration.....	121

List of tables

Table 1. Coefficients and errors of chlorins equations.....	39
Table 2. Coefficients and errors of alkenones equations.....	60
Table 3. Coefficients and errors of total organic carbon (TOC) equations.....	87
Table 4. Coefficients and errors of export proxies equations.....	122

Acknowledgements

En primer lloc, voldria donar les gràcies al meu director de tesi, el Dr. Antoni Rosell, per il·lustrar-me l'immens món que s'amaga sota les aigües profundes de l'oceà. Per la seva orientació al llarg de tota la tesi, les hores de discussió, l'oportunitat de divulgar la nostra recerca en conferències internacionals, i sobretot, per saber transmetre'm la seva motivació en els moments més difícils. I would also like to thank Eric Galbraith for his supervision and stimulating discussions, which have significantly enriched the work presented in this thesis.

One of the best things this project has given me is the opportunity to stay in the Japan Agency for Marine-Earth Science and Technology. I am very thankful to Dr. Nao Ohkouchi for his guidance and support during the 3 months I spent in Japan. I am glad I worked with Nana and Hisami, and all the other lab members. I will always be deeply grateful for your help and making me feel at home. Al Gerard i la Patri, per fer que aquesta aventura acabés de la millor manera possible.

The Integrated Ocean Drilling Program (IODP), the OSU-MGR Collection and the Scripps Institution of Oceanography are acknowledged for providing sediment samples. We are in debt with N. Lahajnar, Z. Chase and J. Carriquiry for providing additional samples, and O. Cartapanis for supplying sedimentation rate maps. O. Cartapanis is also thanked for providing total organic carbon data and collaborating in their regional classification. ODV and QGIS are acknowledged for providing software. GlobColour data (<http://globcolour.info>) used in this study have been developed, validated, and distributed by ACRI-ST, France.

We acknowledge financial support from the Spanish research Ministry (CTM2013-43006-P; and Maria de Maeztu award MDM-2015-0552), the American Chemical Society (54868-ND2) and MAPFRE foundation.

Als meus companys de l'ICTA. Als qui ja hi eren quan vaig arribar, per acollir-me de la millor manera, ensenyar-me i ajudar-me en tot el que vaig necessitar. Especialment a la Núria, pels teus consells i per ser el meu diari al llarg d'aquests quatre anys; i al Ferran, amb qui he compartit mitja vida al laboratori, per escoltar-me i ajudar-me a trobar la calma. Als qui van començar amb mi aquest viatge, per buscar amb mi l'alegria a cada moment. En especial a la Mar, per tota l'energia que m'has donat i per recordar-me la sort que tenim de poder gaudir cada instant. Als qui van arribar més tard i han compartit amb mi els últims temps, per donar-me l'empenta necessària per arribar fins al final. Molt especialment a Sostenipra, per acollir-me i fer-me sentir part del grup, heu fet que seguir amb la lluita valgués la pena. Many thanks to my colleagues from ICTA, for all the moments we shared, especially to Aljosa, Alex and to those "living" in the z-328 office, for your

help and cheer me up every day. A la secretaria de l'ICTA, pel gran equip professional i humà que sou, especialment a la Vane i a la Cristina.

A la gran família que m'ha donat el bàsquet i a Timbalers la Garsa. Per ajudar-me a desconnectar i ser un xute d'energia incalculable. A la Irene i la Gemma, por estar siempre a mi lado y llenar mi vida de risas y locura. A la Maria, per cuidar-me i fer-me saber que tornarà a sortir el sol, cada dia. A l'Esther, per il·lusionar-nos juntes amb la vida i recordar-me qui sóc enmig de la tempesta. A l'Alba i la Sister, per saber entendre'm i omplir-me de moments plens d'amor i alegria, *amistats que t'ajuden a viure*.

Als meus pares, tot el que he fet i el que sóc és gràcies a vosaltres. Em sento molt afortunada de poder aprendre i gaudir de vosaltres cada dia. Gràcies pel vostre suport incondicional, per ser la llum quan tot és negre i per tot el que feu per mi, dia rere dia. Als meus avis, per creure tant en mi i fer-me sentir capaç de tot.

A la resta de familiars i amics. Gràcies!

Abstract

Ocean primary productivity (PP) is a key driver of the global marine carbon cycle and thus, the climate of our planet. Obtaining quantitative information on past PP relies on biogeochemical models since current paleoproductivity proxies are qualitative at best. Moreover, the global scale applicability of such proxies and their constraints remains unclear.

The objective of this thesis is to evaluate the applicability and constraints of some of the most frequently used organic proxies to obtain information on biomass export and surface nutrient conditions, and appraise their potential to deliver quantitative information on global spatial scales.

The central approach followed in this thesis relies on the comparison of remote sensing sea-surface ocean chlorophyll-*a* (SSchla) concentration, as an indicator of marine PP, with global surface sediment data of chlorins, alkenones and total organic carbon (TOC) concentration. In addition, the study on nutrient proxies is based on the comparison of nitrogen isotopic signal ($\delta^{15}\text{N}$) derived from sedimentary bulk and chlorophyllic pigments.

A key result is that the global spatial distribution of chlorins and alkenones is mainly related to SSchla concentration rather than depositional factors (e.g. oxygen and sedimentation rate). However, sedimentary chlorins concentration is linked to SSchla by a non-linear relationship, while alkenones and TOC by a linear equation. Global TOC presents higher scatter than biomarkers on its correlation with global SSchla. Depositional factors do play a role in decomposing organic matter, and we estimate that only 0.33% of SSchla accumulates in sediment. However, we also postulate that the rate of degradation is spatially constant. Hence, our results indicate that chlorins and alkenones can be used to quantitatively reconstruct past PP at global scale. These export proxies would deliver lower errors on past PP quantitative estimation than TOC. Regarding to nutrient proxies, our data show a linear relationship between $\delta^{15}\text{N}$ of bulk and chlorophyllic pigments, which indicate these proxies globally provide equivalent information on past nutrient conditions and past PP. Furthermore, $\delta^{15}\text{N}$ presents considerable differences between pigments, which suggests chlorins might not track chlorophyll-*a* signal, and complicates the application of individual chlorins as nutrient proxies.

This study highlights the limitations on the applicability of TOC as a quantitative paleoproductivity proxy at global scale, and the potential constraints on the use of individual chlorins for reconstructing past nutrient conditions and past PP. Our findings also pave the way for the use of biomarkers as global quantitative proxies of past PP using globally applicable correlations in ocean sediments.

Resum

La productivitat primària (PP) marina és un procés clau en el cicle global del carboni marí i, per tant, en el clima del nostre planeta. L'obtenció d'informació quantitativa de PP en el passat es basa en models biogeoquímics, ja que les proxies de paleoproductivitat actuals són qualitatives. A més, l'aplicabilitat a escala global d'aquestes proxies, i les seves limitacions, romanen incertes.

L'objectiu d'aquesta tesi és avaluar l'aplicabilitat i les limitacions d'algunes de les proxies orgàniques més utilitzades per obtenir informació sobre l'exportació de biomassa i condicions nutricionals en superfície, i avaluar el seu potencial per proporcionar informació quantitativa en escales d'espai globals.

El plantejament central abordat en aquesta tesi es basa en la comparació de la concentració de clorofil·la-*a* a la superfície oceànica (SSchla) mesurada per teledetecció, com a indicador de la PP marina, amb concentracions de sediment superficial de clorines, alquenones i carboni orgànic total (TOC). A més, l'estudi de proxies de nutrients es basa en la comparació de la senyal isotòpica de nitrogen ($\delta^{15}\text{N}$), derivada de sediment total i de pigments clorofil·lics sedimentaris.

Un resultat clau és que la distribució espacial global de clorines i alquenones està principalment relacionada amb la concentració de SSchla, en comptes de factors deposicionals (p. ex. oxigen i taxa de sedimentació). Tanmateix, la concentració de clorines sedimentàries està relacionada amb la SSchla a través d'una relació no lineal, mentre que les alquenones i el TOC, per una equació lineal. El TOC global presenta una major dispersió que els biomarcadors en la seva correlació amb la SSchla global. Els factors deposicionals juguen un paper en la descomposició de matèria orgànica, i hem estimat que només un 0.33% de la SSchla s'acumula en els sediments. Tanmateix, també hem postulat que la velocitat de degradació és constant en l'espai. Per tant, els nostres resultats indiquen que les clorines i les alquenones es poden utilitzar per reconstruir quantitativament PP en el passat a escala global. Aquestes proxies presenten errors més baixos que el TOC en l'estimació de PP quantitativa. Respecte a les proxies nutricionals, les nostres dades mostren una relació lineal entre la $\delta^{15}\text{N}$ derivada de sediment total i de pigments clorofil·lics sedimentaris, el que suggereix que les clorines no reflexen la senyal de la clorofil·la-*a*, i pot complicar l'ús de les clorines individuals com a proxies de nutrients.

Aquest estudi destaca les limitacions de l'aplicabilitat del TOC com a proxy quantitativa de paleoproductivitat a escala global, i les potencials limitacions en l'ús de clorines individuals per reconstruir condicions nutricionals i la PP en el passat. Els nostres resultats també mostren el potencial d'alguns biomarcadors com a proxies quantitatives de PP, a través de correlacions que es poden aplicar a escala global en sediments marins.

Chapter 1

Introduction and objectives



Picture author: Favim

1. Introduction and objectives

1.1. Global climate change

CO₂ concentration in the atmosphere and the oceans directly influences global climate. Its increasing concentration in the atmosphere due to recent human activities is markedly altering the natural global carbon cycle, and leading to global warming and ocean acidification (Archer et al., 2009; Shakun et al., 2012). Figure 1 shows the close link between CO₂ concentration and temperature over the past 800,000 years, and the drastically increase of CO₂ concentration in the present day. Carbon cycle models project CO₂ concentrations of 720 to 1,000 ppm by 2100, which may result in an increase of ~ 2.6 °C in global mean temperature, and a pH decrease of ~ 0.3 in seawater (Kawahata et al., 2019).

In order to undertake mitigation and adaptation actions in response to the anthropogenic climate change, it is essential to understand the global interactions between the geological, biological, physical and chemical mechanisms that govern our climate. One of the main unresolved questions to understand the impact of the anthropogenic emissions of CO₂ are the dynamics of the ocean as a natural sink of atmospheric CO₂, and the role of marine biology on transferring CO₂ from the atmosphere to the deep ocean and sediments.

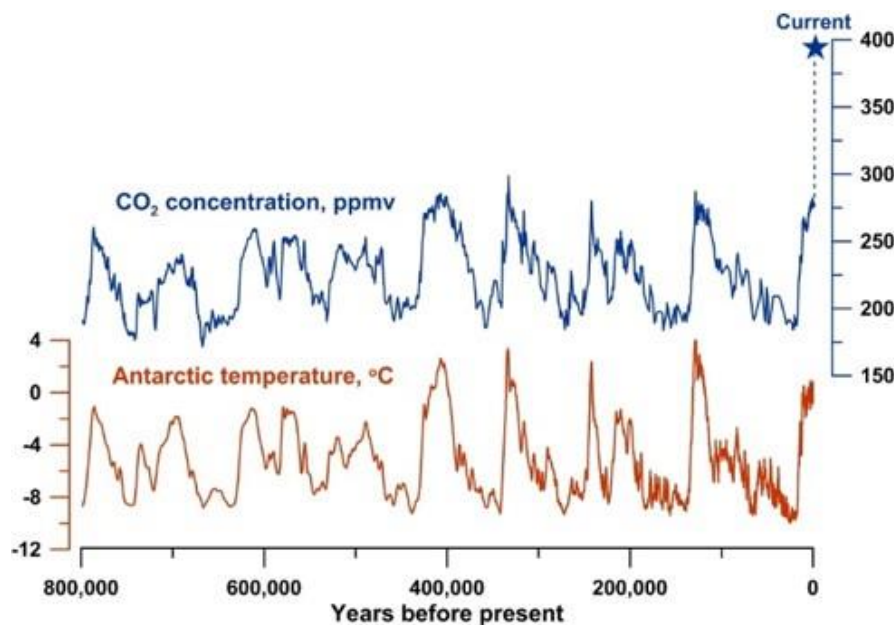


Figure 1. Temperature and CO₂ concentration from Antarctic ice cores over the past 800,000 years. Image extracted from (Shakun et al., 2012).

1.2. The soft-tissue pump

Marine biology influences the global CO₂ cycle by sequestering CO₂ from the atmosphere to the ocean. One of the principal biological mechanisms that transfer atmospheric CO₂ to the deep ocean and marine sediments is the soft-tissue pump.

The soft-tissue pump can be divided in three distinct stages: fixation, export and burial (Figure 2).

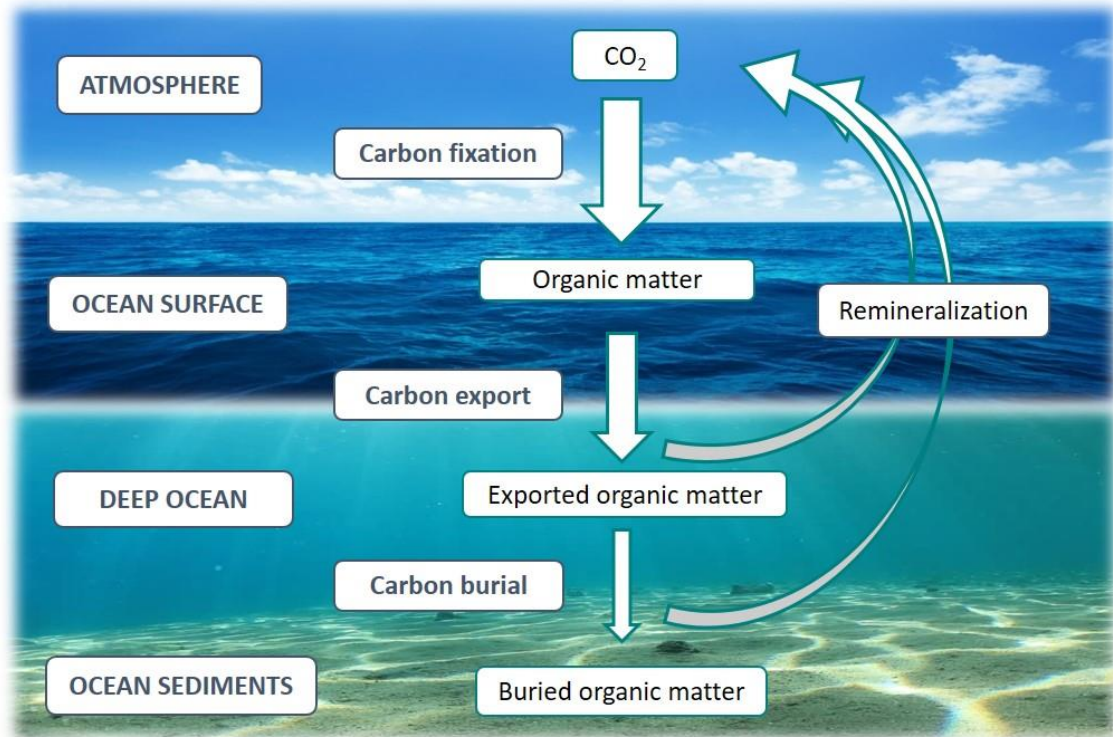


Figure 2. Principal processes and compartments of the soft-tissue pump.

Carbon fixation per unit area per unit time is named primary productivity (PP). Although this process can be developed in the absence of sunlight by oxidation or reduction of inorganic compounds (chemosynthesis), it principally takes place through phytoplankton photosynthesis by using sunlight as the energy source. Photosynthesis reaction is described hereafter:



The phytoplankton community is very diverse, accounting for more than 20,000 species (Sarmiento & Gruber, 2006). However, all species use chlorophyll-a (Chl *a*) as the principal pigment for absorbing sunlight and carrying out photosynthesis. The dominant species over most of the open ocean are diatoms, coccolithophores and dinoflagellates (Figure 3).



Figure 3. Photographs of the dominant phytoplankton species in the global ocean.

Once fixated, the vast majority of organic carbon is converted back into CO_2 in the upper layers of the ocean. This process is known as carbon remineralization, and commonly occurs by heterotrophic and bacteria respiration. Global carbon cycle models predict that only 6 to 10 PgC/yr (Schlitzer, 2002; Siegel et al., 2014) of the 48 PgC/yr that are produced in surface waters (DeVries & Weber, 2017; Sarmiento & Gruber, 2006), are exported from the euphotic zone to the deep ocean.

Many efforts have been made to describe the carbon flux from the surface to the ocean's interior and identify the factors that control this process. The majority of the elaborated equations point out PP and water depth as the main variables in influencing the global carbon flux in the ocean (Betzer et al., 1984; Pace et al., 1987; Sarnthein et al., 1988; Suess, 1980). However, other factors, such as oxygen, ballast, particle size and temperature have also been discussed to have an influence in the organic carbon sinking flux (Cram et al., 2018). Below, the most common carbon flux equations are described:

$$\text{(Suess, 1980): Carbon flux} = \frac{\text{PP}}{0.0238 \cdot \text{WD} + 0.212}$$

$$\text{(Betzer et al., 1984) : Carbon flux} = 0.409 \cdot \text{WD}^{-0.628} \cdot \text{pp}^{1.41}$$

$$\text{(Sarnthein et al., 1988) : Carbon flux} = 20.5361 \cdot \text{PP}_{\text{new}}^{0.6648} \cdot \text{WD}^{-0.5537}$$

$$\text{(Antia et al., 2001) : Carbon flux} = 0.1 \cdot \text{WD}^{-0.68} \cdot \text{pp}^{1.77}$$

Similarly to the remineralization in the water column, benthic organisms, such as worms, clams and bacteria, decomposed organic matter that arrives to the water-sediment interface. Global carbon cycle models estimate only 0.15 PgC/yr are ultimately buried in the surface ocean sediment (Muller-Karger et al., 2005).

Burial efficiency equations, which calculate the fraction of organic carbon that is finally buried in the sediments related to that which reaches the sediment-water interface, indicate sedimentation rate as the principal factor in controlling the accumulation of organic carbon in sediments (Betts & Holland, 1991; Reeburgh & Henrichs, 1987). Nevertheless, oxygen concentration in bottom waters has also been suggested as an important factor in controlling organic matter burial and

preservation (Betts & Holland, 1991; Hartnett et al., 1998). The most common burial efficiency (BE) equations are described hereafter:

$$\text{(Reeburgh \& Henrichs, 1987) : BE} = \frac{(\text{SR} \cdot 1000)^{0.4}}{2.1}$$

$$\text{(Betts \& Holland, 1991) : } \log_{10} \left(\frac{\text{BE}}{100} \right) = \frac{1.39 \cdot \log_{10} \text{SR}}{\log_{10}(\text{SR} + 7.9)} + 0.34$$

In spite of numerous studies demonstrating empirical relationships between organic matter accumulation and several factors, the main control factors of organic matter export and accumulation in sediment are still controversial. Thus, organic carbon accumulated in marine sediments seems to reflect the interplay of PP and several organic matter preservation factors.

1.3. Primary productivity (PP) and remote sensing

Ocean PP is the driving factor in the marine carbon cycle and plays a key role in regulating our global climate. Since almost all marine PP occurs through phytoplankton photosynthesis, it is commonly estimated by determining phytoplankton biomass in the ocean surface (Davies et al., 2018). In turn, phytoplankton biomass is generally estimated from sea-surface chlorophyll-*a* (SSchla) concentration by using oceanic biogeochemical models (Behrenfeld et al., 2005; Lee et al., 2015), as it is the principal pigment used by all phytoplankton during photosynthesis (Figure 4).

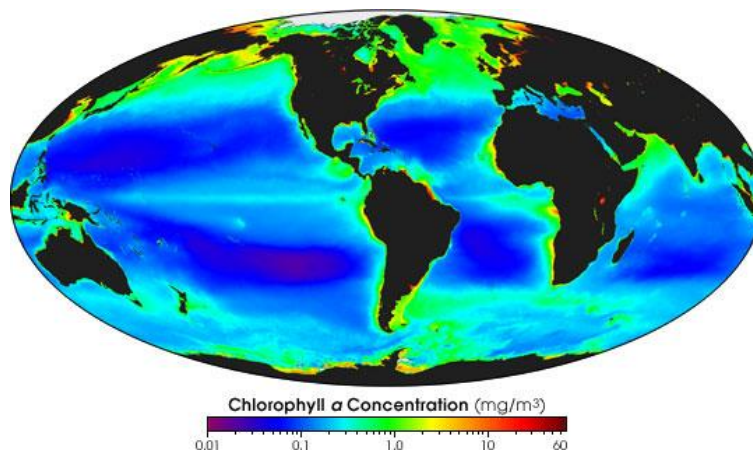


Figure 4. Global annual average sea-surface chlorophyll-*a* (SSchla) concentration measured by the Sea-viewing Wide Field-of-view Sensor (SeaWiFS) since 1997 to 2010. Image from the National Aeronautics and Space Administration (NASA) Earth Observatory.

Remote sensing has been recognized as the only feasible means to estimate SSchla concentration for the global ocean and quantify global PP, as it overcomes spatial and temporal limitations (Lee et al., 2015). Since 1997, remote sensing sensors have been launched to space for collecting global SSchla concentration data. Some examples of sensors from the National Aeronautics and Space Administration (NASA) missions are the Sea-viewing Wide Field-of-view Sensor (SeaWiFS), the

Moderate-Resolution Imaging Spectroradiometer (MODIS) and the Visible and Infrared Imager Radiometer Suite (VIIRS), which collected data from 1997 to 2010, from 2002 to present and from 2012 to present, respectively. Another example from the European Space Agency (ESA) mission is the MEdium Resolution Imaging Spectrometer (MERIS), which registered data from 2002 to 2012. Remote sensors capture ocean colour emitted from phytoplankton blooms by collecting several spectral bands at a $1/24^\circ$ spatial resolution (4.63 km at the equator) meanwhile navigating around the globe (Figure 5). For instance, MODIS views the entire Earth's surface every two days, acquiring data in 36 spectral bands. Merging data for a certain period would improve spatial coverage by avoiding gaps caused by environmental factors, such as clouds and dust. To improve spatial coverage, monthly averaged data is obtained from combining daily data (Figure 6). Besides, studying PP changes at long time-scales would require longer time periods than those registered in a single remote sensing mission. In order to ensure data continuity, reduce data noise and improve spatial and temporal coverage, the GlobColour project merges data from different sensors. The GlobColour project (<http://globcolour.info>) has been developed, validated, and distributed by ACRI-ST, France.

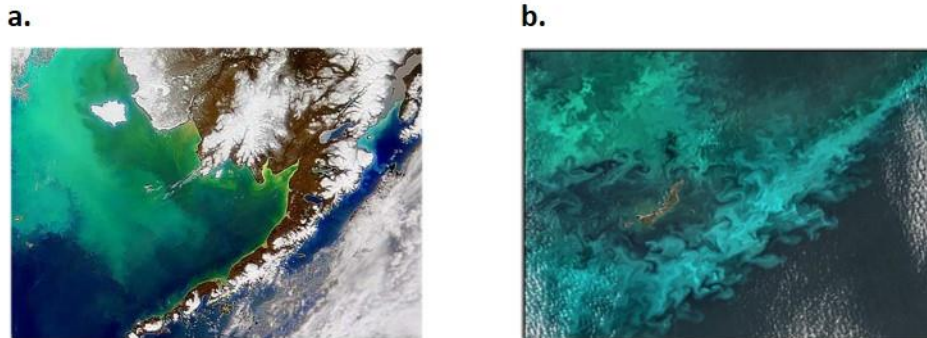


Figure 5. Satellite images obtained from phytoplankton blooms in the Bering Sea in **a.** 1998 and **b.** 2014. Images from the NASA Earth Observatory.

To obtain SSchla concentration from the wavelengths captured by remote sensors, the GlobColour Project uses the OCx algorithm, which is a fourth-order polynomial relationship between a ratio of remote sensing reflectance (Rrs) and SSchla concentration. Coefficients a_0 to a_4 are sensor specific (O'Reilly et al., 2000):

$$\log_{10} ([SSchla]) = a_0 + \sum_{i=1}^4 a_i \log_{10} \left(\frac{Rrs(\text{blue})}{Rrs(\text{green})} \right)^i$$

Despite the great progresses have been achieved over the last decades in estimating global SSchla concentration, there are still some hampers that deviate remote sensing SSchla from *in situ* SSchla measurements at the sea-surface (Lee et al., 2015), especially in those oceanic regions, where optical, physical and biological properties are complex (Blondeau-Patissier et al., 2014; Brown &

Yoder, 1994; Gregg & Casey, 2004; Werdell et al., 2018). The main factors contributing to surface waters complexity are reported to be coloured dissolved organic matter, radiance-absorbing aerosols, phytoplankton species diversity, suspended sediments, clouds, ice, sun glint, and navigation/time space mismatches (Claustre & Maritoner, 2003; Dierssen & Smith, 2000; Sathyendranath et al., 2001; Volpe et al., 2007). Therefore, global standard algorithms, such as the OCx algorithm used in the GlobColour Project, might not reflect accurate SSchla concentrations for some specific oceanic regions that present high complexity surface waters.

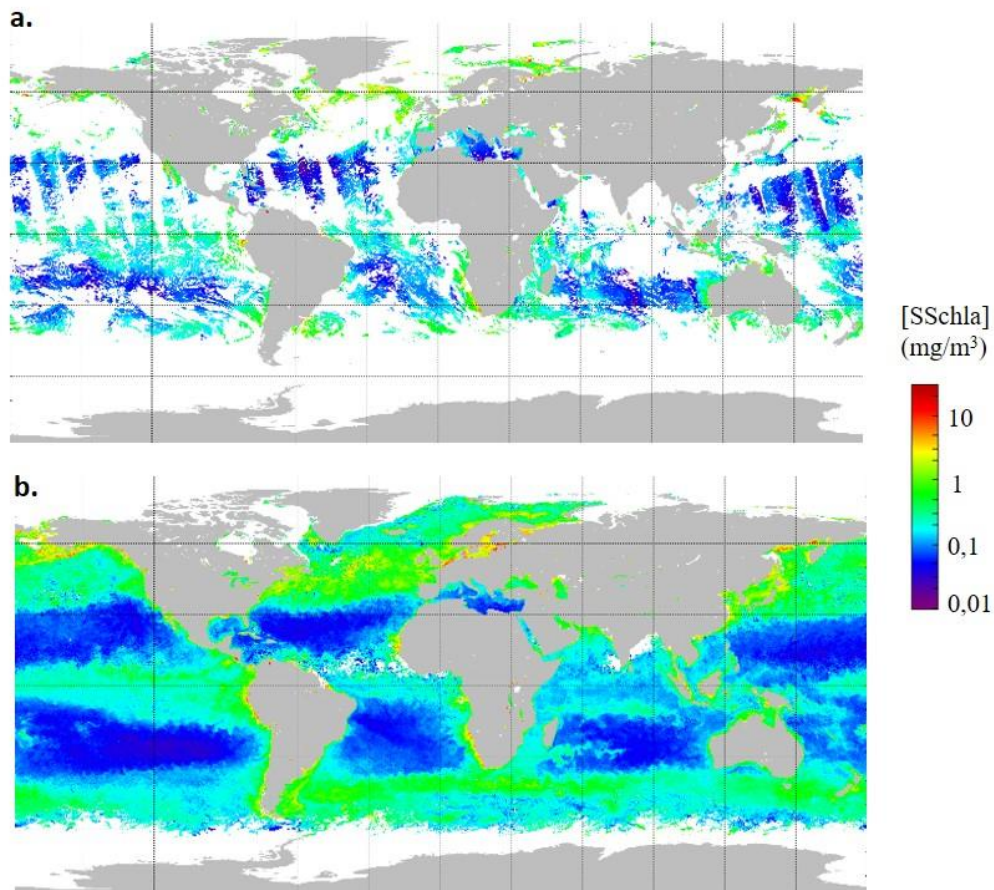


Figure 6. Global average sea-surface chlorophyll-a (SSchla) concentration obtained by merging the Moderate-Resolution Imaging Spectroradiometer (MODIS) and the Infrared Imager Radiometer Suite (VIIRS) sensors. Data collected in **a.** 2017-05-30 (daily data) and **b.** 2017-04-01 to 2017-04-30 (monthly data). Images from the GlobColour Project.

1.4. Paleoproductivity proxies

1.4.1. Introduction to paleoproductivity proxies

Remote sensing provides a powerful tool for studying PP variations in a global scale over the last decades. However, elucidating the principal mechanisms that control the soft-tissue pump and predict future changes in our climate, require larger time-scales than those offered by remote sensing. Therefore, paleoceanographers have developed palaeoproductivity proxies to infer past

PP (Schoepfer et al., 2015; Zhao et al., 2006), and which are usually based in paleontological or geochemical characteristics of sediments. Paleoproductivity proxies can be classified in two major groups: export and nutrient proxies (Berger et al., 1994; Marchitto, 2007) (Figure 7).

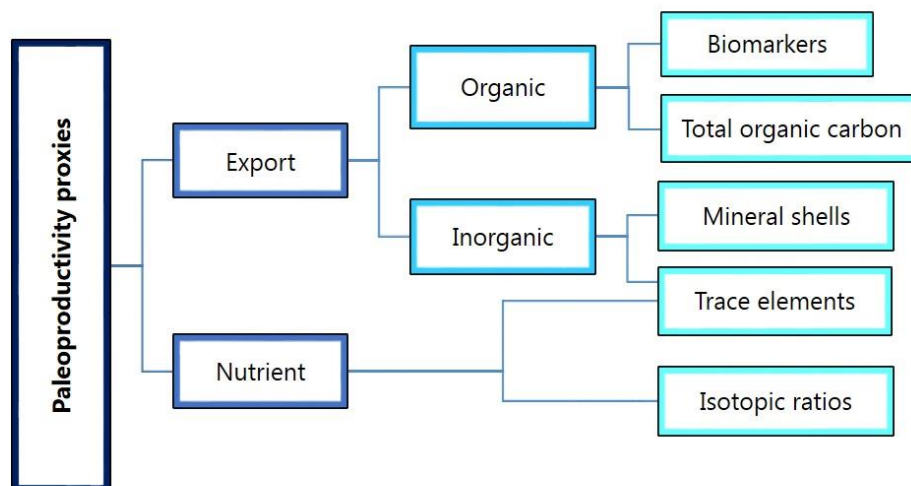


Figure 7. Paleoproductivity proxies classification. This classification is based on (Berger et al., 1994; Marchitto, 2007).

1.4.2. Export proxies

Export proxies are based on the concentration of organic and inorganic molecules accumulated in the ocean sediment. Hence, they are related to export and buried production and affected by export and burial efficiencies. Consequently, one of the major drawbacks of export proxies is that temporal changes in preservation conditions might affect proxies concentration. For instance, enhanced burial of total organic carbon (TOC) in glacial-age sediments from the equatorial Pacific was interpreted as reflecting increased past PP (Pedersen, 1983), but more recently it was reinterpreted as the result of better preservation conditions (Bradtmiller et al., 2010). To solve this problem, several proxies are measured for comparison, which is known as a multiproxy study. It is based on the fact that preservation rarely affects different materials in the same manner.

Another issue that might affect export proxies would be that changes in the accumulation of other compounds present in the sediment can modify the concentration of the proxy. This factor is named the dilution effect, and particularly occurs in coastal margins, where considerably amounts of terrestrial material can achieve marine sedimentary settings, mainly by river input (Bianchi et al., 2018). Mass accumulation rates, which take into account the bulk sedimentation rate (i.e. centimetres of sediment accumulated in a time), are calculated to discard dilution effects. However, sedimentation rate calculation requires an age model based on microfossil datums

and/or magnetic anomalies (Stein et al., 1989), which is not always available. Therefore, mass accumulation rates are not always possible to obtain.

1.4.2.1. Biomarkers

Among export proxies, we can find biomarkers. These are organic compounds that can be linked to specific sources and provide information about past environmental conditions. For instance, chlorins are directly linked to Chl *a*, as they are its degradation products. Since Chl *a* is relatively unstable under oxic and light conditions, chlorins are frequently found instead in the sedimentary record (King & Repeta, 1994; Prowse & Maxwell, 1991; Soma et al., 2001). Chlorins include Chl *a* primary degradation products that can be formed by senescence, such as pheophytin-*a* (Phe *a*), pyropheophytin-*a* (PPhe *a*) and pheophorbide-*a* (Phide *a*) (Chikaraishi et al., 2007), and by zooplankton grazing, such as cyclopheophorbide-*a*-enol (CPhe *a*) and chlorophyllone-*a* (Chlone *a*) (Goericke et al., 2000; Louda et al., 2008). Moreover, chlorins encompass Chl *a* secondary degradation products, which are formed by esterification with steroids and carotenoids, such as carotenoid and steryl chlorin esters (CCEs and SCEs) (Goericke et al., 1999; King & Repeta, 1994) (Figure 8).

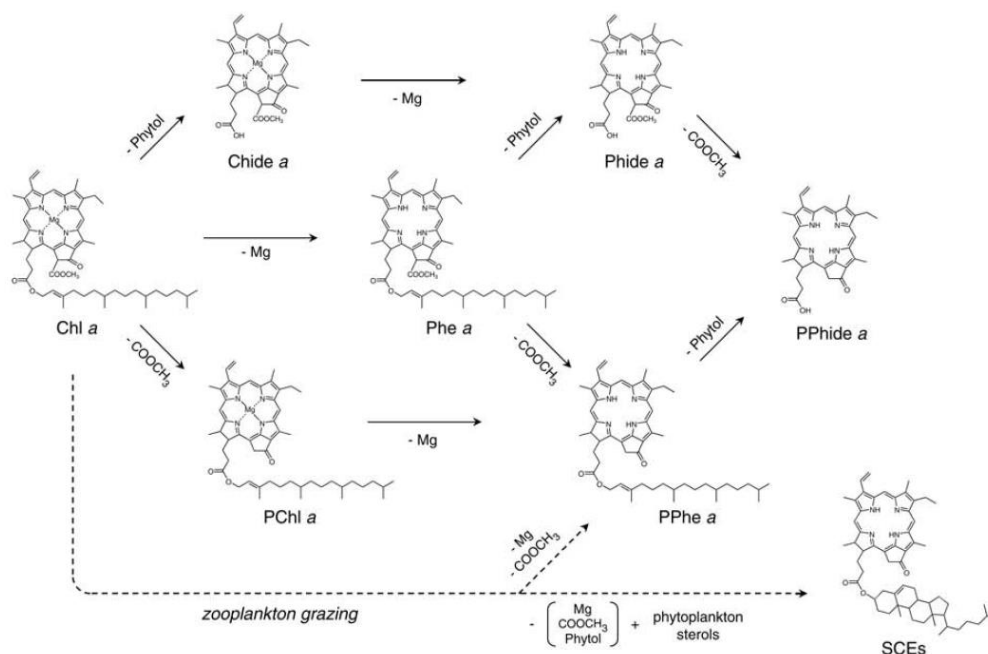


Figure 8. Principal chlorins structure and their degradation pathways. Image from (Chikaraishi et al., 2007). Abbreviations: chlorophyll-*a* (Chl *a*), chlorophyllide-*a* (Chide *a*), pheophorbide-*a* (Phide *a*), pheophytin-*a* (Phe *a*), pyrochlorophyll-*a* (PChl *a*), pyropheophorbide-*a* (PPhide *a*), pyropheophytin-*a* (PPhe *a*), steryl chlorin esters (SCEs).

Since Chl *a* is produced by all phytoplankton species for carrying out photosynthesis, chlorins are commonly used to track total past PP (Finkenbinder et al., 2018; Harris et al., 1996; Higginson et al., 2003; Summerhayes et al., 1995; Szymczak-Zyła et al., 2011). In contrast, alkenones, and to a minor extent long chain alkyl diols and sterols, have been used as biomarkers for inferring past PP of some phytoplankton species (Bolton et al., 2010; Hinrichs et al., 1999; Lawrence, 2006; Moreno et al., 2004; Petrick et al., 2018; Plancq et al., 2014; Prahel et al., 1993; Rostek et al., 1997; Seki et al., 2004; Tyler et al., 2010).

Alkenones are biomarkers of *Emiliania huxleyi*, which is its principal source and the most abundant coccolithophore in the modern pelagic ocean (Conte et al., 1994; Marlowe et al., 1984; Rhodes et al., 1995; Schmidt et al., 2013; Volkman et al., 1980; Volkman et al., 1995). However, *Geophyrocapsa oceanica* and other coccolithophore species from the same genera are also considered important alkenones producers nowadays (Volkman et al., 1995). Long chain alkyl diols are produced by eustigmatophytes and diatoms, but unidentified algal sources might be significant (Méjanelle et al., 2003; Sinninghe Damsté et al., 2003); meanwhile sterols are mainly produced by different species of dinoflagellates, although they also have been found in a few diatoms (Volkman et al., 1998).

1.4.2.2. Total organic carbon (TOC)

TOC englobes all organic material buried in the sediment and has the advantages that is the major component of phytoplankton biomass and provides the most direct proxy for past PP. Therefore, many studies have used TOC as a proxy for reconstructing past PP (Bunzel et al., 2017; Moreno et al., 2004; Nieto-Moreno et al., 2011; Pedersen, 1983; Schoepfer et al., 2015; Schubert et al., 2001; Summerhayes et al., 1995; Xu et al., 2017). However, it has some constraints as a paleoproductivity proxy. For instance, organic matter from terrestrial sources might bias TOC concentrations and thus, obscure the marine signal (i.e. organic matter produced in the surface ocean and exported and buried in the sediments). This limitation primarily affects coastal margins, where almost half of the organic carbon accumulated in the sediments comes from river inputs (Schlünz & Schneider, 2000). Another issue related to TOC proxy would be that it encompasses many different compounds, which would present different degradation pathways. Therefore, TOC as a past PP proxy could be affected by complex changes in preservation conditions, probably more than other export proxies.

Since TOC reflects total buried production, which has important implications in the global carbon cycle, numerous studies have focused on the factors controlling TOC accumulation in sediments. Hence, several equations have been proposed to estimate the carbon flux and burial into the sediments. Common equations include PP, water depth, sedimentation rate and oxygen. However,

the primary control is an ongoing debate (Chen et al., 2016; Fu et al., 2014; Yu et al., 2019; Zonneveld et al., 2010). Therefore, the reliability and applicability of palaeoproductivity proxies that are based on PP as the principal factor controlling organic matter accumulation on the sediment, such as TOC or biomarkers, remains controversial.

1.4.2.3. Mineral shells

Inorganic compounds used by some marine organisms for producing their external skeletons are also generally used as paleoproductivity proxies (Finkenbinder et al., 2018; Plancq et al., 2014). This is the case of carbonate and silice. Carbonate production in the pelagic ocean is dominated by coccolithophores (phytoplankton) and foraminifera (zooplankton), and to a minor extent by calcareous dinoflagellates (phytoplankton) and pteropods (zooplankton) (Rühlemann et al., 1999). On the other hand, silice is mainly produced by diatoms (phytoplankton) and radiolarians (zooplankton) (Hüneke & Henrich, 2011).

Generally, carbonate and silice abundances on the sea-floor correlate with overall patterns of surface water productivity. This fact has been used to justify their value as paleoproductivity proxies. Nevertheless, other processes can obscure their application. For instance, spatial and temporal variation dissolution in the water column and after deposition on the sea floor affect both carbonate and silice proxies. In fact, some studies have suggested carbonate glacial-interglacial cycles are predominantly caused by dissolution rather than productivity changes (Anderson et al., 2008; Le & Shackleton, 1992). Another major limitation factor of the silice proxy is the spatial and temporal variation of silicate supply in the photic zone. Moreover, iron availability regulates diatom growth and silice downward flux in the open ocean (Hüneke & Henrich, 2011). Therefore, silice abundance variation in sediment may also reflect changes in surface waters iron supply rather than productivity. This limitation is particularly severe in high-nutrient-low-chlorophyll (HNLC) regions, such as the Southern Ocean, where silice sedimentation records do not clearly show a glacial increase in export production (Dezileau et al., 2003; Frank et al., 2000), as it is suggested by ice core measurements (Anderson et al., 2002).

1.4.2.4. Trace elements

Some trace elements are delivered to the sediment in association with organic matter, and they may be retained within the sediment after organic matter decay (Tribovillard et al., 2006). For instance, nickel, barium and copper have been found to present similar distributions to organic carbon fluxes (Böning et al., 2015; Paytan & Griffith, 2007; Steiner et al., 2017). Hence, the high tendency of some trace elements to be incorporated into organic matter during export, promote their use as export proxies.

Besides, several trace elements have been reported to present similar fluxes to major nutrients. For instance, cadmium and zinc exhibit an oceanic distribution very close to phosphate and silice, respectively; and nickel correlates with phosphate in the upper waters, and with silice at depth (Bruland, 1980; Marchitto, 2007). Thus, trace elements have also been used to reconstruct past nutrient conditions (Marchitto, 2007).

However, other factors control trace element accumulation in sediments. For instance, redox conditions and seawater saturation level might affect cations re-solubilization from the sediment and allow their transport to other marine settings (Paytan & Griffith, 2007; Steiner et al., 2017; Tribovillard et al., 2006). For instance, recent studies suggest barium might not reflect changes in past PP (Steiner et al., 2017; Tribovillard et al., 2006).

1.4.3. Nutrient proxies

Most of the global ocean is oligotrophic (i.e. low nutrient concentration in surface waters). Therefore, nutrient availability in the surface ocean is an important control on PP, as it is a limiting factor for carrying out photosynthesis. Proxies associated with nutrient conditions in sea-surface waters are known as nutrient proxies.

Nutrient proxies can be divided into two different groups: isotopic ratios and trace element. The basis of isotopic ratio proxies relies on the fact that changes in nutrient conditions produce variations in the ratio between the different stable isotopes of an element, such as nitrogen or carbon. On the other hand, trace element proxies exhibit similar patterns than major nutrients along the water column.

1.4.3.1. Isotopic ratios

PP is limited by the availability of nitrate in most part of the ocean (70%) (Bristow et al., 2017). Therefore, nitrate availability has been frequently inferred to obtain information about nutrient conditions and PP in the global ocean. Since phytoplankton preferentially assimilate ^{14}N relative to ^{15}N in high nutrient availability conditions (Wada & Hattori, 1978), and nitrogen isotopic composition in the surface ocean is uniform ($\delta^{15}\text{N} \approx 5 \text{‰}$) (Sigman et al., 2000), changes in the nitrogen isotopic ratio might reflect changes in nutrient availability conditions (Wada & Hattori, 1976). The nitrogen isotopic ratio or nitrogen isotopic signal is commonly expressed in delta notation by using atmospheric N_2 as a reference.

$$\delta^{15}\text{N} = \left(\frac{(^{15}\text{N}/^{14}\text{N})_{\text{sample}}}{(^{15}\text{N}/^{14}\text{N})_{\text{standard}}} - 1 \right) \cdot 1000$$

For tracking past changes in sea-surface nutrient conditions and infer past PP, paleoceanographers generally measure the nitrogen isotopic signal of total matter accumulated in the sediment ($\delta^{15}\text{N}_{\text{bulk}}$) (Ehlert et al., 2015; Mollier-Vogel et al., 2012), as nitrate surface signal has been found to be transferred and preserved in sediments (Altabet & Francois, 1994). However, $\delta^{15}\text{N}_{\text{bulk}}$ is limited by the heterogeneity and different diagenetic pathways of organic nitrogen accumulated in the sediment (Wada, 1980), which can overprint the nitrogen signal and thus, complicate the interpretation of the proxy (Enders et al., 2008; Junium et al., 2015; Sachs & Repeta, 1999; Tyler et al., 2010).

In order to avoid the effect of multiple sources and diagenetic pathways on the isotopic signal, chlorin-specific nitrogen isotopic signal ($\delta^{15}\text{N}_{\text{chlorin}}$) has been used as an alternative proxy (Enders et al., 2008; Fulton et al., 2012; Fulton et al., 2018; Kusch et al., 2010; Naeher et al., 2016a; Naeher et al., 2016b; Sachs & Repeta, 1999; Tyler et al., 2010). Nevertheless, the interpretation of $\delta^{15}\text{N}_{\text{chlorin}}$ proxy relies on the assumption that $\delta^{15}\text{N}_{\text{chlorin}}$ reflects the original Chl *a* nitrogen isotopic signal ($\delta^{15}\text{N}_{\text{chla}}$). This is based on the fact that the chemical bonds that are involved in the reaction from Chl *a* to the other chlorins do not link nitrogen atoms, so no relative nitrogen isotopic abundances are expected to vary during diagenetic transformation. The variation on the isotopic ratio of a certain element is known as isotope fractionation.

Hence, nitrogen isotope fractionation produced by phytoplankton consumption is commonly used to infer past nutrient conditions and past PP. However, interpretations from $\delta^{15}\text{N}_{\text{bulk}}$ and $\delta^{15}\text{N}_{\text{chlorin}}$ proxies are not always concordant (Junium et al., 2015; Sachs & Repeta, 1999; Tyler et al., 2010) and the contribution of diagenetic processes in modifying the nitrogen isotopic fingerprint is still controversial.

1.5. Objectives and outline

The aim of this thesis is to evaluate the applicability and constraints of some of the most frequently used organic proxies to study the marine carbon cycle through time. Oceanic PP is the driving factor of the global marine carbon cycle. Therefore, estimating modern and past PP for key climatic periods is a main interest for the scientific community. Global SSchl_a concentration, estimated by remote sensing, is used to infer modern PP using biogeochemical models. Meanwhile for tracking past PP, many palaeoproductivity proxies have been proposed. However, proxies limitations and their applicability on a global scale remains unclear in most cases. Besides, the lack of modern PP data on a global scale has hindered the calibration of available proxies and their use to provide quantitative estimates on past PP (Hernández-Almeida et al., 2019). In this

sense, and in order to achieve the main aim of this thesis, the following specific objectives and research questions have been addressed:

Objective 1. To evaluate the use of available organic export proxies for reconstructing ocean past PP at global scale, and their potential as quantitative paleoproductivity proxies (*Chapter 2, 3 and 4*).

In this thesis we have focused our research on the following organic export proxies:

- Chlorins (*Chapter 2*):

Chlorins include Chl *a*, the main pigment used in photosynthesis, and its degradation products. Thus, in contrast to other available proxies, chlorins provide information about total PP. Chlorins abundance in sediment is common used to infer total past PP (Harris et al., 1996; Higginson et al., 2003; Summerhayes et al., 1995; Szymczak-Zyła et al., 2011).

- Alkenones (*Chapter 3*):

Alkenones are biomarkers of *Emiliania huxleyi*, which is the most abundant coccolithophore in the modern pelagic ocean (Conte et al., 1994; Marlowe et al., 1984; Rhodes et al., 1995; Schmidt et al., 2013; Volkman et al., 1980; Volkman et al., 1995;). Hence, alkenones concentration in sediment is one of the most common approaches for estimating past PP (Bolton et al., 2010; Lawrence, 2006; Moreno et al., 2004; Petrick et al., 2018; Prahl et al., 1993; Rostek et al., 1997; Seki et al., 2004). Nevertheless, in contrast to chlorins, alkenones are only produced by some species of phytoplankton.

- TOC (*Chapter 4*):

TOC embraces all organic matter that is accumulated in the sediment. Therefore, TOC is the major component of phytoplankton biomass and provides the most direct proxy for productivity. Consequently, many studies use TOC as a proxy for reconstructing past PP (Bunzel et al., 2017; Moreno et al., 2004; Nieto-Moreno et al., 2011; Pedersen, 1983; Schoepfer et al., 2015; Schubert et al., 2001; Summerhayes et al., 1995; Xu et al., 2017).

Research question 1.1. Are organic export proxies concentration in sediment mainly related to PP?

Only around 0.31% of surface PP is exported and buried onto the sediments (DeVries & Weber, 2017; Muller-Karger et al., 2005; Sarmiento & Gruber, 2006). Therefore, besides PP, other factors influence the concentration of organic matter in sediments. Depositional factors, such as water depth, sedimentation rate and oxygen are discussed to have an important role in controlling organic matter concentration in sediment (Mann & Zweigel, 2008; Müller & Suess, 1979;

Schwarzkopf, 1993). Despite numerous studies have been focused on the factors that control organic matter accumulation, the primary control is an ongoing debate (Chen et al., 2016; Fu et al., 2014; Yu et al., 2019; Zonneveld et al., 2010). Hence, organic export proxies reliability and applicability is still unconstrained.

Research question 1.2. Which organic proxy provides more accurate values on past PP quantitative reconstructions?

Currently, many proxies are available to estimate past PP (Schoepfer et al., 2015; Zhao et al., 2006). However, past PP quantitative reconstruction relies on the use of biogeochemical models as the available proxy approaches are qualitative at best. Therefore, only relative past PP changes through downcore can be currently inferred from sedimentary field data and no comparisons between different locations of the global ocean can be addressed.

Objective 2. To evaluate global constraints of available nutrient proxies used for tracking past nutrient conditions and past PP (*Chapter 5*).

In this thesis we have focused our research on the following nitrogen isotope proxies:

- $\delta^{15}\text{N}_{\text{bulk}}$:

$\delta^{15}\text{N}_{\text{bulk}}$ comprises all nitrogen accumulated in the sediment and present an alternative approach to infer past PP by estimating past nutrient conditions. However, it is limited by the heterogeneity and different diagenetic pathways of sedimentary nitrogen (Wada, 1980), which can complicate the interpretation of the proxy (Enders et al., 2008; Junium et al., 2015; Sachs & Repeta, 1999; Tyler et al., 2010).

- $\delta^{15}\text{N}_{\text{chlorin}}$:

$\delta^{15}\text{N}_{\text{chlorin}}$ includes Chl *a*, the main pigment used in photosynthesis, and its degradation products. In order to avoid the effect of multiple nitrogen sources and diagenetic pathways on the isotopic signal, $\delta^{15}\text{N}_{\text{chlorin}}$ is used as an alternative proxy for past nutrient conditions and past PP (Enders et al., 2008; J. M. Fulton et al., 2018; James M. Fulton et al., 2012; Kusch et al., 2010; Naeher et al., 2016a; Naeher et al., 2016b; Sachs & Repeta, 1999; Tyler et al., 2010).

Research question 2.1. Are nitrogen isotope proxies consistent at a global scale?

Comparisons between $\delta^{15}\text{N}_{\text{bulk}}$ and $\delta^{15}\text{N}_{\text{chlorin}}$ present consistent agreement in some occasions (James M. Fulton et al., 2012; Higgins et al., 2010; Kusch et al., 2010), but show significant differences in others (Junium et al., 2015; Sachs & Repeta, 1999; Tyler et al., 2010). Consequently, the reliability of $\delta^{15}\text{N}_{\text{bulk}}$ has been questioned by arguing its signal is compromised by multiple sources and diagenetic alteration. However, all comparison studies carried out so far are based

on independent regional environments, which might not reflect global environmental conditions governing most of the ocean.

Research question 2.2. Can $\delta^{15}\text{N}_{\text{chlorin}}$ be used to track $\delta^{15}\text{N}_{\text{chla}}$ in sediment?

The interpretation of $\delta^{15}\text{N}_{\text{chlorin}}$ proxy relies on the assumption that $\delta^{15}\text{N}_{\text{chlorin}}$ reflect the original $\delta^{15}\text{N}_{\text{chla}}$. This is based on the fact that the chemical bonds that are involved in the transformation from Chl *a* to the other chlorins do not link nitrogen atoms, so no nitrogen fractionation is expected during the transformation. This assumption has been confirmed in some locations (Tyler et al., 2010), but some discrepancies between the nitrogen isotope signal of Chl *a* and the rest of chlorins, as well as among different chlorins have been found in other studies (Kusch et al., 2010; Naeher et al., 2016b). Hence, the dominant factor that controls $\delta^{15}\text{N}_{\text{chlorin}}$ variability in sediments remains controversial, which might complicate the interpretation of $\delta^{15}\text{N}_{\text{chlorin}}$ proxy for tracking past nutrient conditions and past PP.

1.6. References

- Altabet, M. A., & Francois, R. (1994). Sedimentary nitrogen isotopic ratio as a recorder for surface ocean nitrate utilization. *Global Biogeochemical Cycles*, *8*(1), 103–116. <https://doi.org/10.1029/93GB03396>
- Anderson, R. F., Fleisher, M. Q., Lao, Y., & Winckler, G. (2008). Modern CaCO_3 preservation in equatorial Pacific sediments in the context of late-Pleistocene glacial cycles. *Marine Chemistry*, *111*(1–2), 30–46. <https://doi.org/10.1016/j.marchem.2007.11.011>
- Anderson, R. F., Chase, Z., Fleisher, M. Q., & Sachs, J. (2002). The Southern Ocean's biological pump during the Last Glacial Maximum. *Deep-Sea Research Part II: Topical Studies in Oceanography*, *49*, 1909–1938. [https://doi.org/10.1016/S0967-0645\(02\)00018-8](https://doi.org/10.1016/S0967-0645(02)00018-8)
- Antia, N., Koeve, W., Fischer, G., Blanz, T., Schulz-Bull, D., Scholten, J., et al. (2001). Basin-wide particulate carbon flux in the Atlantic Ocean: Regional export patterns and potential for atmospheric CO_2 sequestration. *Global Biogeochemical Cycles*, *15*(4), 845–862. <https://doi.org/10.1029/2000gb001376>
- Archer, D., Eby, M., Brovkin, V., Ridgwell, A., Cao, L., Mikolajewicz, U., et al. (2009). Atmospheric Lifetime of Fossil Fuel Carbon Dioxide. *Annual Review of Earth and Planetary Sciences*, *37*(1), 117–134. <https://doi.org/10.1146/annurev.earth.031208.100206>
- Behrenfeld, M. J., Boss, E., Siegel, D. A., & Shea, D. M. (2005). Carbon-based ocean productivity and phytoplankton physiology from space. *Global Biogeochemical Cycles*, *19*(1), 1–14. <https://doi.org/10.1029/2004GB002299>

- Berger, W. H., Herguera, J. C., Lange, C. B., & Schneider, R. (1994). Paleoproductivity: Flux Proxies Versus Nutrient Proxies and Other Problems Concerning the Quaternary Productivity Record. *Carbon Cycling in the Glacial Ocean: Constraints on the Ocean's Role in Global Change*, 385–412. https://doi.org/10.1007/978-3-642-78737-9_17
- Betts, J. N., & Holland, H. D. (1991). The oxygen content of ocean bottom waters, the burial efficiency of organic carbon, and the regulation of atmospheric oxygen. *Global and Planetary Change*, 5(1–2), 5–18. [https://doi.org/10.1016/0921-8181\(91\)90123-E](https://doi.org/10.1016/0921-8181(91)90123-E)
- Betzer, P. R., Showers, W. J., Laws, E. A., Winn, C. D., DiTullio, G. R., & Kroopnick, P. M. (1984). Primary productivity and particle fluxes on a transect of the equator at 153°W in the Pacific Ocean. *Deep Sea Research Part A, Oceanographic Research Papers*, 31(1), 1–11. [https://doi.org/10.1016/0198-0149\(84\)90068-2](https://doi.org/10.1016/0198-0149(84)90068-2)
- Bianchi, T. S., Cui, X., Blair, N. E., Burdige, D. J., Eglinton, T. I., & Galy, V. (2018). Centers of organic carbon burial and oxidation at the land-ocean interface. *Organic Geochemistry*, 115, 138–155. <https://doi.org/10.1016/j.orggeochem.2017.09.008>
- Blondeau-Patissier, D., Gower, J. F. R., Dekker, A. G., Phinn, S. R., & Brando, V. E. (2014). A review of ocean color remote sensing methods and statistical techniques for the detection, mapping and analysis of phytoplankton blooms in coastal and open oceans. *Progress in Oceanography*, 123, 123–144. <https://doi.org/10.1016/j.pocean.2013.12.008>
- Bolton, C. T., Lawrence, K. T., Gibbs, S. J., Wilson, P. A., Cleaveland, L. C., & Herbert, T. D. (2010). Glacial-interglacial productivity changes recorded by alkenones and microfossils in late Pliocene eastern equatorial Pacific and Atlantic upwelling zones. *Earth and Planetary Science Letters*, 295(3–4), 401–411. <https://doi.org/10.1016/j.epsl.2010.04.014>
- Böning, P., Shaw, T., Pahnke, K., & Brumsack, H. J. (2015). Nickel as indicator of fresh organic matter in upwelling sediments. *Geochimica et Cosmochimica Acta*, 162, 99–108. <https://doi.org/10.1016/j.gca.2015.04.027>
- Bradtmiller, L. I., Anderson, R. F., Sachs, J. P., & Fleisher, M. Q. (2010). A deeper respired carbon pool in the glacial equatorial Pacific Ocean. *Earth and Planetary Science Letters*, 299(3–4), 417–425. <https://doi.org/10.1016/j.epsl.2010.09.022>
- Bristow, L. A., Mohr, W., Ahmerkamp, S., & Kuypers, M. M. M. (2017). Nutrients that limit growth in the ocean. *Current Biology*, 27(11), R474–R478. <https://doi.org/10.1016/j.cub.2017.03.030>
- Brown, C. W., & Yoder, J. A. (1994). Cocolithophorid blooms in the global ocean. *Journal of Geophysical Research*, 99(C4), 7467–7482. <https://doi.org/10.1029/93JC02156>

- Bruland, K. W. (1980). Oceanographic distributions of cadmium, zinc, nickel, and copper in the North Pacific. *Earth and Planetary Science Letters*, *47*(2), 176–198. [https://doi.org/10.1016/0012-821X\(80\)90035-7](https://doi.org/10.1016/0012-821X(80)90035-7)
- Bunzel, D., Schmiedl, G., Lindhorst, S., Mackensen, A., Reolid, J., Romahn, S., & Betzler, C. (2017). A multi-proxy analysis of late Quaternary Indian monsoon dynamics for the Maldives, Inner Sea. *Climate of the Past Discussions*, (April), 1–35. <https://doi.org/10.5194/cp-2017-54>
- Chen, C., Mu, C. L., Zhou, K. K., Liang, W., Ge, X. Y., Wang, X. P., et al. (2016). The geochemical characteristics and factors controlling the organic matter accumulation of the Late Ordovician-Early Silurian black shale in the Upper Yangtze Basin, South China. *Marine and Petroleum Geology*, *76*, 159–175. <https://doi.org/10.1016/j.marpetgeo.2016.04.022>
- Chikaraishi, Y., Matsumoto, K., Kitazato, H., & Ohkouchi, N. (2007). Sources and transformation processes of pheopigments: Stable carbon and hydrogen isotopic evidence. *Organic Geochemistry*, *38*, 985–1001.
- Claustre, H., & Maritoner, S. (2003). The Many Shades of Ocean Blue. *Ocean Science*, *302*(5650), 1514–1515.
- Conte, M. H., Volkman, J. K., & Eglinton, G. (1994). Lipid biomarkers of the Prymnesiophyceae. *The Haptophyte Algae*, *51*(January), 351–377.
- Cram, J. A., Weber, T., Leung, S. W., Mcdonnell, A. M. P., Liang, J. H., & Deutsch, C. (2018). The Role of Particle Size, Ballast, Temperature, and Oxygen in the Sinking Flux to the Deep Sea. *Global Biogeochemical Cycles*, 858–876. <https://doi.org/10.1029/2017GB005710>
- Davies, C. H., Ajani, P., Armbrecht, L., Atkins, N., Baird, M. E., Beard, J., et al. (2018). A database of chlorophyll a in Australian waters. *Scientific Data*, *5*, 1–8. <https://doi.org/10.1038/sdata.2018.18>
- DeVries, T., & Weber, T. (2017). The export and fate of organic matter in the ocean: New constraints from combining satellite and oceanographic tracer observations. *Global Biogeochemical Cycles*, *31*(3), 535–555. <https://doi.org/10.1002/2016GB005551>
- Dezileau, L., Reyss, J. L., & Lemoine, F. (2003). Late Quaternary changes in biogenic opal fluxes in the Southern Indian Ocean. *Marine Geology*, *202*, 143–158. [https://doi.org/10.1016/S0025-3227\(03\)00283-4](https://doi.org/10.1016/S0025-3227(03)00283-4)
- Dierssen, H. M., & Smith, R. C. (2000). Bio-optical properties and remote sensing ocean color algorithms for Antarctic Peninsula waters, *105*(1999), 26301–26312.
- Ehlert, C., Grasse, P., Gutiérrez, D., Salvatelli, R., & Frank, M. (2015). Nutrient utilisation and

- weathering inputs in the Peruvian upwelling region since the Little Ice Age. *Climate of the Past*, 11, 187–202. <https://doi.org/10.5194/cp-11-187-2015>
- Enders, S. K., Pagani, M., Pantoja, S., Baron, J. S., Wolfe, A. P., Pedentchouk, N., & Nunez, L. (2008). Compound-specific stable isotopes of organic compounds from lake sediments track recent environmental changes in an alpine ecosystem, Rocky Mountain National Park, Colorado. *Limnology and Oceanography*, 53(4), 1468–1478.
- Finkenbinder, M. S., Abbott, M. B., Stoner, J. S., Ortiz, J. D., Finney, B. P., Dorfman, J. M., & Stansell, N. D. (2018). Millennial-scale variability in Holocene aquatic productivity from Burial Lake, Arctic Alaska. *Quaternary Science Reviews*, 187, 220–234. <https://doi.org/10.1016/j.quascirev.2018.03.019>
- Frank, M., Gersonde, R., Rutgers van der Loeff, M., Bohrmann, G., Ntirnberg, C. C., Kubik, P. W., et al. (2000). Similar glacial and interglacial export bioproductivity in the Atlantic sector of the Southern Ocean: Multiproxy evidence and implications for glacial atmospheric Augusto Mangini We present time series of export productivity proxy data including depositi, 15(6), 642–658.
- Fu, X., Tan, F., Feng, X., Wang, D., Chen, W., Song, C., & Zeng, S. (2014). Early Jurassic anoxic conditions and organic accumulation in the eastern Tethys. *International Geology Review*, 56(12), 1450–1465. <https://doi.org/10.1080/00206814.2014.945103>
- Fulton, J. M., Arthur, M. A., Thomas, B., & Freeman, K. H. (2018). Pigment carbon and nitrogen isotopic signatures in euxinic basins. *Geobiology*, 16(4), 429–445. <https://doi.org/10.1111/gbi.12285>
- Fulton, James M., Arthur, M. A., & Freeman, K. H. (2012). Black Sea nitrogen cycling and the preservation of phytoplankton $\delta^{15}\text{N}$ signals during the Holocene. *Global Biogeochemical Cycles*, 26(2), n/a-n/a. <https://doi.org/10.1029/2011GB004196>
- Goericke, R., Shankle, A., & Repeta, D. J. (1999). Novel carotenol chlorin esters in marine sediments and water column particulate matter. *Geochimica et Cosmochimica Acta*, 63(18), 2825–2834. [https://doi.org/10.1016/S0016-7037\(99\)00155-6](https://doi.org/10.1016/S0016-7037(99)00155-6)
- Goericke, R., Strom, S. L., & Bell, M. a. (2000). Distribution and sources of cyclic pheophorbides in the marine environment. *Limnology and Oceanography*, 45(1), 200–211. <https://doi.org/10.4319/lo.2000.45.1.0200>
- Gregg, W. W., & Casey, N. W. (2004). Global and regional evaluation of the SeaWiFS chlorophyll data set. *Remote Sensing of Environment*, 93(4), 463–479.

<https://doi.org/10.1016/j.rse.2003.12.012>

- Harris, P., Zhao, M., & Rosell-Melé, A. (1996). Chlorin accumulation rate as a proxy for Quaternary marine primary productivity. *Nature*. Retrieved from <http://www.nature.com/nature/journal/v383/n6595/abs/383063a0.html>
- Harris, P. G., Zhao, M., Rosell-Melé, A., Tiedemann, R., Sarnthein, M., & Maxwell, J. R. (1996). Chlorin accumulation rate as a proxy for Quaternary marine primary productivity. *Nature*, *383*, 63–65. Retrieved from <http://www.nature.com/nature/journal/v383/n6595/abs/383063a0.html>
- Hartnett, H. E., Keil, R. G., Hedges, J. I., & Devol, A. H. (1998). Influence of oxygen exposure time on organic carbon preservation in continental margin sediments. *Nature*, *391*(February), 572–574.
- Hernández-Almeida, I., Ausín, B., Saavedra-Pellitero, M., Baumann, K. H., & Stoll, H. M. (2019). Quantitative reconstruction of primary productivity in low latitudes during the last glacial maximum and the mid-to-late Holocene from a global *Florisphaera profunda* calibration dataset. *Quaternary Science Reviews*, *205*, 166–181. <https://doi.org/10.1016/j.quascirev.2018.12.016>
- Higgins, M. B., Robinson, R. S., Carter, S. J., & Pearson, A. (2010). Evidence from chlorin nitrogen isotopes for alternating nutrient regimes in the Eastern Mediterranean Sea. *Earth and Planetary Science Letters*, *290*(1–2), 102–107. <https://doi.org/10.1016/j.epsl.2009.12.009>
- Higginson, M. J., Maxwell, J. R., & Altabet, M. A. (2003). Nitrogen isotope and chlorin paleoproductivity records from the Northern South China Sea: Remote vs. local forcing of millennial- and orbital-scale variability. *Marine Geology*, *201*(1–3), 223–250. [https://doi.org/10.1016/S0025-3227\(03\)00218-4](https://doi.org/10.1016/S0025-3227(03)00218-4)
- Hinrichs, K. U., Schneider, R. R., Müller, P. J., & Rullkötter, J. (1999). A biomarker perspective on paleoproductivity variations in two Late Quaternary sediment sections from the Southeast Atlantic Ocean. *Organic Geochemistry*, *30*(5), 341–366. [https://doi.org/10.1016/S0146-6380\(99\)00007-8](https://doi.org/10.1016/S0146-6380(99)00007-8)
- Hüneke, H., & Henrich, R. (2011). Chapter 4 - Pelagic Sedimentation in Modern and Ancient Oceans. In H. HüNeke & T. B. T.-D. in S. Mulder (Eds.), *Deep-Sea Sediments* (Vol. 63, pp. 215–351). Elsevier. <https://doi.org/https://doi.org/10.1016/B978-0-444-53000-4.00004-4>
- Junium, C. K., Arthur, M. A., & Freeman, K. H. (2015). Compound-specific $\delta^{15}\text{N}$ and chlorin preservation in surface sediments of the Peru Margin with implications for ancient bulk $\delta^{15}\text{N}$ records. *Geochimica et Cosmochimica Acta*, *160*, 306–318.

<https://doi.org/10.1016/j.gca.2014.12.018>

- Kawahata, H., Fujita, K., Iguchi, A., Inoue, M., Iwasaki, S., Kuroyanagi, A., et al. (2019). *Perspective on the response of marine calcifiers to global warming and ocean acidification—Behavior of corals and foraminifera in a high CO₂ world “hot house.”* *Progress in Earth and Planetary Science* (Vol. 6). Progress in Earth and Planetary Science. <https://doi.org/10.1186/s40645-018-0239-9>
- King, L. L., & Repeta, D. J. (1994). Phorbol sterol esters in Black Sea sediment traps and sediments: A preliminary evaluation of their paleoceanographic potential. *Geochimica et Cosmochimica Acta*. [https://doi.org/10.1016/0016-7037\(94\)90342-5](https://doi.org/10.1016/0016-7037(94)90342-5)
- Kusch, S., Kashiyama, Y., Ogawa, N. O., Altabet, M., Butzin, M., Friedrich, J., et al. (2010). Implications for chloro- and pheopigment synthesis and preservation from combined compound-specific $\delta^{13}\text{C}$, $\delta^{15}\text{N}$, and $\Delta^{14}\text{C}$ analysis. *Biogeosciences*, *7*(12), 4105–4118. <https://doi.org/10.5194/bg-7-4105-2010>
- Lawrence, K. T. (2006). Evolution of the Eastern Tropical Pacific Through Plio-Pleistocene Glaciation. *Science*, *312*(5770), 79–83. <https://doi.org/10.1126/science.1120395>
- Le, J., & Shackleton, N. J. (1992). Carbonate dissolution fluctuations in the western equatorial Pacific during the late Quaternary. *Quaternary Research*, *7*(1), 21–42.
- Lee, Z., Marra, J., Perry, M. J., & Kahru, M. (2015). Estimating oceanic primary productivity from ocean color remote sensing: A strategic assessment. *Journal of Marine Systems*, *149*, 50–59. <https://doi.org/10.1016/j.jmarsys.2014.11.015>
- Louda, J. W., Neto, R. R., Magalhaes, A. R. M., & Schneider, V. F. (2008). Pigment alterations in the brown mussel *Perna perna*. *Comparative Biochemistry and Physiology - B Biochemistry and Molecular Biology*, *150*(4), 385–394. <https://doi.org/10.1016/j.cbpb.2008.04.008>
- Mann, U., & Zweigel, J. (2008). *Modelling Source-Rock Distribution and Quality Variations: The Organic Facies Modelling Approach. Analogue and Numerical Modelling of Sedimentary Systems: From Understanding to Prediction*. <https://doi.org/10.1002/9781444303131.ch11>
- Marchitto, T. M. (2007). Nutrient Proxies. *Paleoceanography*, 1732–1740.
- Marlowe, I. T., Green, J. C., Neal, A. C., Brassell, S. C., Eglinton, G., & Course, P. A. (1984). Long chain (n-c37-c39) alkenones in the prymnesiophyceae. distribution of alkenones and other lipids and their taxonomic significance. *British Phycological Journal*, *19*(3), 203–216. <https://doi.org/10.1080/00071618400650221>
- Méjanelle, L., Sanchez-Gargallo, A., Bentaleb, I., & Grimalt, J. O. (2003). Long chain n-alkyl diols,

- hydroxy ketones and sterols in a marine eustigmatophyte, *Nannochloropsis gaditana*, and in *Brachionus plicatilis* feeding on the algae. *Organic Geochemistry*, *34*(4), 527–538. [https://doi.org/10.1016/S0146-6380\(02\)00246-2](https://doi.org/10.1016/S0146-6380(02)00246-2)
- Mollier-Vogel, E., Ryabenko, E., Martinez, P., Wallace, D., Altabet, M. A., & Schneider, R. (2012). Nitrogen isotope gradients off Peru and Ecuador related to upwelling, productivity, nutrient uptake and oxygen deficiency. *Deep-Sea Research Part I: Oceanographic Research Papers*, *70*, 14–25. <https://doi.org/10.1016/j.dsr.2012.06.003>
- Moreno, A., Cacho, I., Canals, M., Grimalt, J. O., & Sanchez-Vidal, A. (2004). Millennial-scale variability in the productivity signal from the Alboran Sea record, Western Mediterranean Sea. *Palaeogeography, Palaeoclimatology, Palaeoecology*, *211*(3–4), 205–219. <https://doi.org/10.1016/j.palaeo.2004.05.007>
- Muller-Karger, F. E., Varela, R., Thunell, R., Luerssen, R., Hu, C., & Walsh, J. J. (2005). The importance of continental margins in the global carbon cycle. *Geophysical Research Letters*, *32*(1), 1–4. <https://doi.org/10.1029/2004GL021346>
- Müller, P. J., & Suess, E. (1979). Productivity, sedimentation rate, and sedimentary organic matter in the oceans: I. Organic carbon preservation. *Deep-Sea Research*, *26A*, 1347–1362.
- Naeher, S., Suga, H., Ogawa, N. O., Schubert, C. J., Grice, K., & Ohkouchi, N. (2016a). Compound-specific carbon and nitrogen isotopic compositions of chlorophyll a and its derivatives reveal the eutrophication history of Lake Zurich (Switzerland). *Chemical Geology*, *443*, 210–219. <https://doi.org/10.1016/j.chemgeo.2016.09.005>
- Naeher, S., Suga, H., Ogawa, N. O., Takano, Y., Schubert, C. J., Grice, K., & Ohkouchi, N. (2016b). Distributions and compound-specific isotopic signatures of sedimentary chlorins reflect the composition of photoautotrophic communities and their carbon and nitrogen sources in Swiss lakes and the Black Sea. *Chemical Geology*, *443*, 198–209. <https://doi.org/10.1016/j.chemgeo.2016.04.029>
- Nieto-Moreno, V., Martínez-Ruiz, F., Giral, S., Jiménez-Espejo, F., Gallego-Torres, D., Rodrigo-Gámiz, M., et al. (2011). Tracking climate variability in the western Mediterranean during the Late Holocene: A multiproxy approach. *Climate of the Past*, *7*(4), 1395–1414. <https://doi.org/10.5194/cp-7-1395-2011>
- O'Reilly, J. E., Maritorena, S., O'Brien, M. C., Siegel, D. a, Toole, D., Menzies, D., et al. (2000). SeaWiFS Postlaunch Calibration and Validation Analyses, part 3. *NASA Tech. Memo.*, *11*, 1–49.
- Pace, M. L., Knauer, G. a, Karl, D. M., & Martin, J. H. (1987). Primary production, new production

- and vertical flux in the eastern Pacific Ocean. *Nature*. <https://doi.org/Doi.10.1038/325803a0>
- Paytan, A., & Griffith, E. M. (2007). Marine barite: Recorder of variations in ocean export productivity. *Deep-Sea Research Part II: Topical Studies in Oceanography*, *54*(5–7), 687–705. <https://doi.org/10.1016/j.dsr2.2007.01.007>
- Pedersen, T. F. (1983). Increased productivity in the eastern equatorial Pacific during the last glacial maximum (19000–14000 yr B.P.). *Geology*, *11*(1971), 16–19.
- Petrick, B., McClymont, E. L., Littler, K., Rosell-Melé, A., Clarkson, M. O., Maslin, M., et al. (2018). Oceanographic and climatic evolution of the southeastern subtropical Atlantic over the last 3.5 Ma. *Earth and Planetary Science Letters*, *492*, 12–21. <https://doi.org/10.1016/j.epsl.2018.03.054>
- Plancq, J., Mattioli, E., Pittet, B., Simon, L., & Grossi, V. (2014). Productivity and sea-surface temperature changes recorded during the late Eocene-early Oligocene at DSDP Site 511 (South Atlantic). *Palaeogeography, Palaeoclimatology, Palaeoecology*, *407*, 34–44. <https://doi.org/10.1016/j.palaeo.2014.04.016>
- Prahl, F. G., Collier, R. B., Dymond, J., Lyle, M., & Sparrow, M. A. (1993). A biomarker perspective on prymnesiophyte productivity in the northeast pacific ocean. *Deep-Sea Research Part I*, *40*(10), 2061–2076. [https://doi.org/10.1016/0967-0637\(93\)90045-5](https://doi.org/10.1016/0967-0637(93)90045-5)
- Prowse, W. G., & Maxwell, J. R. (1991). High molecular weight chlorins in a lacustrine shale. *Organic Geochemistry*, *17*(6), 877–886. [https://doi.org/10.1016/0146-6380\(91\)90029-J](https://doi.org/10.1016/0146-6380(91)90029-J)
- Reeburgh, W. S., & Henrichs, S. M. (1987). Anaerobic Mineralization of Marine Sediment Organic-Matter - Rates and the Role of Anaerobic Processes in the Oceanic Carbon Economy. *Geomicrobiology Journal*, *5*(3–4), 191–237.
- Rhodes, L. L., Peake, B. M., MacKenzie, A. L., Simon, M., & Edwards, A. R. (1995). Coccolithophores *Gephyrocapsa oceanica* and *Emiliania huxleyi* (Prymnesiophyceae = Haptophyceae) in New Zealand's coastal waters: Characteristics of blooms and growth in laboratory culture. *New Zealand Journal of Marine and Freshwater Research*, *29*(3), 345–357. <https://doi.org/10.1080/00288330.1995.9516669>
- Rostek, F., Bard, E., Beaufort, L., Sonzogni, C., & Ganssen, G. (1997). Sea surface temperature and productivity records for the past 240kyr in the Arabian Sea. *Deep-Sea Research*, *44*(97), 1461–1480.
- Rühlemann, C., Müller, P. J., & Schneider, R. R. (1999). Organic Carbon and Carbonate as Paleoproductivity Proxies: Examples from High and Low Productivity Areas of the Tropical

- Atlantic. *Use of Proxies in Paleoceanography*, 315–344. https://doi.org/10.1007/978-3-642-58646-0_12
- Sachs, J. P., & Repeta, D. J. (1999). Oligotrophy and Nitrogen Fixation During Eastern Mediterranean Sapropel Events. *Science*, *286*(5449), 2485–2488. <https://doi.org/10.1126/science.286.5449.2485>
- Sarmiento, J. L., & Gruber, N. (2006). *Ocean Biogeochemical Dynamics*. New Jersey: Princeton Univ. Press. <https://doi.org/10.1063/1.2754608>
- Sarnthein, M., Winn, K., Duplessy, J.-C., & Fontugne, M. R. (1988). Global variations of surface ocean productivity in low and mid latitudes: Influence on CO₂ reservoirs of the deep ocean and atmosphere during the last 21,000 years. *Paleoceanography*, *3*(3), 361–399. <https://doi.org/10.1029/PA003i003p00361>
- Sathyendranath, S., Cota, G., Stuart, V., Maass, H., & Platt, T. (2001). Remote sensing of phytoplankton pigments: A comparison of empirical and theoretical approaches. *International Journal of Remote Sensing*, *22*(2–3), 249–273. <https://doi.org/10.1080/014311601449925>
- Schlitzer, R. (2002). Carbon export fluxes in the Southern Ocean: Results from inverse modeling and comparison with satellite-based estimates. *Deep-Sea Research Part II: Topical Studies in Oceanography*, *49*(9–10), 1623–1644. [https://doi.org/10.1016/S0967-0645\(02\)00004-8](https://doi.org/10.1016/S0967-0645(02)00004-8)
- Schlünz, B., & Schneider, R. R. (2000). Transport of terrestrial organic carbon to the oceans by rivers: re-estimating flux- and burial rates. *International Journal of Earth Sciences*, *88*(4), 599–606. <https://doi.org/10.1007/s005310050290>
- Schmidt, S., Harlay, J., Borges, A. V., Groom, S., Delille, B., Røevros, N., et al. (2013). Particle export during a bloom of *Emiliania huxleyi* in the North-West European continental margin. *Journal of Marine Systems*, *109–110*(SUPPL.), S182–S190. <https://doi.org/10.1016/j.jmarsys.2011.12.005>
- Schoepfer, S. D., Shen, J., Wei, H., Tyson, R. V., Ingall, E., & Algeo, T. J. (2015). Total organic carbon, organic phosphorus, and biogenic barium fluxes as proxies for paleomarine productivity. *Earth-Science Reviews*, *149*, 23–52. <https://doi.org/10.1016/j.earscirev.2014.08.017>
- Schubert, C. J., Stein, R., & Calvert, S. E. (2001). Tracking nutrient and productivity variations over the last deglaciation in the Arctic Ocean. *Paleoceanography*, *16*(2), 199–211. <https://doi.org/10.1029/2000PA000503>
- Schwarzkopf, T. A. (1993). Model for prediction of organic carbon content in possible source rocks.

- Marine and Petroleum Geology*, 10(5), 478–492. [https://doi.org/10.1016/0264-8172\(93\)90049-X](https://doi.org/10.1016/0264-8172(93)90049-X)
- Seki, O., Ikehara, M., Kawamura, K., Nakatsuka, T., Ohnishi, K., Wakatsuchi, M., et al. (2004). Reconstruction of paleoproductivity in the Sea of Okhotsk over the last 30 kyr. *Paleoceanography*, 19(1). <https://doi.org/10.1029/2002PA000808>
- Shakun, J. D., Clark, P. U., He, F., Marcott, S. A., Mix, A. C., Liu, Z., et al. (2012). Global warming preceded by increasing carbon dioxide concentrations during the last deglaciation. *Nature*, 484(7392), 49–54. <https://doi.org/10.1038/nature10915>
- Siegel, D. A., Buesseler, K. O., Doney, S. C., Salliey, S. F., Behrenfeld, M. J., & Boyd, P. W. (2014). Global assessment of ocean carbon export by combining satellite observations and food-web models. *Global Biogeochemical Cycles*, 28, 181–196. <https://doi.org/10.1002/2013GB004743>. Received
- Sigman, D. M., Altabet, M. A., Mccorkle, D. C., Francois, R., & Fischer, G. (2000). The d15N of nitrate in the Southern Ocean: Nitrogen cycling and circulation interior. *Journal of Geophysical Research: Oceans*, 105, 19599–19614.
- Sinninghe Damsté, J. S., Rampen, S., Irene, W., Rijpstra, C., Abbas, B., Muyzer, G., & Schouten, S. (2003). A diatomaceous origin for long-chain diols and mid-chain hydroxy methyl alkanoates widely occurring in quaternary marine sediments: Indicators for high-nutrient conditions. *Geochimica et Cosmochimica Acta*, 67(7), 1339–1348. [https://doi.org/10.1016/S0016-7037\(02\)01225-5](https://doi.org/10.1016/S0016-7037(02)01225-5)
- Soma, Y., Tanaka, A., Soma, M., & Kawai, T. (2001). 2.8 million years of phytoplankton history in Lake Baikal recorded by the residual photosynthetic pigments in its sediment core. *Geochemical Journal*, 35(5), 377–383. <https://doi.org/10.2343/geochemj.35.377>
- Stein, R., Haven, H. L., Littke, R., Rullkotter, J., & Welte, D. H. (1989). Accumulation of marine and terrigenous organic carbon at upwelling site 658 and non-upwelling sites 657 and 659: Implications for the reconstruction of paleoenvironments in the eastern subtropical atlantic through late Cenozoic times. *Proceedings of the Ocean Drilling Program, Scientific Results*, 108, 108, 351–360.
- Steiner, Z., Lazar, B., Torfstein, A., & Erez, J. (2017). Testing the utility of geochemical proxies for paleoproductivity in oxic sedimentary marine settings of the Gulf of Aqaba, Red Sea. *Chemical Geology*, 473, 40–49. <https://doi.org/10.1016/j.chemgeo.2017.10.012>
- Suess, E. (1980). Particulate organic carbon flux in the oceans - surface productivity and oxygen

- utilization. *Nature*, *288*(20), 260–263. <https://doi.org/10.1038/288260a0>
- Summerhayes, C. P., Kroon, D., Rosell-Mele, A., Jordan, R. W., Schrader, H.-J., Hearn, R., et al. (1995). Variability in the Benguela Current upwelling system over the past 70,000 years. *Progress in Oceanography*, *35*(3), 207–251. [https://doi.org/10.1016/0079-6611\(95\)00008-5](https://doi.org/10.1016/0079-6611(95)00008-5)
- Szymczak-Zyła, M., Kowalewska, G., & Louda, J. W. (2011). Chlorophyll-a and derivatives in recent sediments as indicators of productivity and depositional conditions. *Marine Chemistry*, *125*(1–4), 39–48. <https://doi.org/10.1016/j.marchem.2011.02.002>
- Tribouillard, N., Algeo, T. J., Lyons, T., & Riboulleau, A. (2006). Trace metals as paleoredox and paleoproductivity proxies: An update. *Chemical Geology*, *232*(1–2), 12–32. <https://doi.org/10.1016/j.chemgeo.2006.02.012>
- Tyler, J., Kashiyama, Y., Ohkouchi, N., Ogawa, N., Yokoyama, Y., Chikaraishi, Y., et al. (2010). Tracking aquatic change using chlorine-specific carbon and nitrogen isotopes: The last glacial-interglacial transition at Lake Suigetsu, Japan. *Geochemistry Geophysics Geosystems*, *11*(9), Q09010. <https://doi.org/10.1029/2010GC003186>
- Volkman, J K, Barrett, S. M., Blackburn, S. I., & Sikes, E. L. (1995). Alkenones in Gephyrocapsa-Oceanica - Implications for Studies of Paleoclimate. *Geochimica et Cosmochimica Acta*, *59*(3), 513–520. [https://doi.org/http://dx.doi.org/10.1016/0016-7037\(95\)00325-T](https://doi.org/http://dx.doi.org/10.1016/0016-7037(95)00325-T)
- Volkman, John K., Eglinton, G., Corner, E. D. S., & Forsberg, T. E. V. (1980). Long-chain alkenes and alkenones in the marine coccolithophorid *Emiliania huxleyi*. *Phytochemistry*, *19*(12), 2619–2622. [https://doi.org/10.1016/S0031-9422\(00\)83930-8](https://doi.org/10.1016/S0031-9422(00)83930-8)
- Volkman, John K., Barrett, S. M., Blackburn, S. I., Mansour, M. P., Sikes, E. L., & Gelin, F. (1998). Microalgal biomarkers: A review of recent research developments. *Organic Geochemistry*, *29*(5-7-7 pt 2), 1163–1179. [https://doi.org/10.1016/S0146-6380\(98\)00062-X](https://doi.org/10.1016/S0146-6380(98)00062-X)
- Volpe, G., Santoleri, R., Vellucci, V., Ribera d'Alcalá, M., Marullo, S., & D'Ortenzio, F. (2007). The colour of the Mediterranean Sea: Global versus regional bio-optical algorithms evaluation and implication for satellite chlorophyll estimates. *Remote Sensing of Environment*, *107*(4), 625–638. <https://doi.org/10.1016/j.rse.2006.10.017>
- Wada, E. (1980). Nitrogen isotope fractionation and its significance in biogeochemical processes occurring in marine environments. *Isotope Marine Chemistry*, 375–398. Retrieved from https://www.jamstec.go.jp/biogeochem/pdf/Wada_1980.pdf
- Wada, E., & Hattori, A. (1976). Natural abundance of ¹⁵N in particulate organic matter in the North Pacific Ocean. *Geochimica et Cosmochimica Acta*, *40*(2), 249–251.

[https://doi.org/10.1016/0016-7037\(76\)90183-6](https://doi.org/10.1016/0016-7037(76)90183-6)

Wada, E., & Hattori, A. (1978). Nitrogen isotope effects in the assimilation of inorganic nitrogenous compounds by marine diatoms. *Geomicrobiology Journal*, 1(1), 85–101.

<https://doi.org/10.1080/01490457809377725>

Werdell, P. J., McKinnna, Lachlan, I. W., Boss, E., Acklesond, S. G., Craig, S. E., Gregg, W. W., et al. (2018). An overview of approaches and challenges for retrieving marine inherent optical properties from ocean color remote sensing. *Treatise on Geomorphology*, 160, 186–212.

<https://doi.org/10.1016/j.pocean.2018.01.001>

Xu, Y., Wang, L., Yin, X., Ye, X., Li, D., Liu, S., et al. (2017). The influence of the Sunda Strait opening on paleoenvironmental changes in the eastern Indian Ocean. *Journal of Asian Earth Sciences*, 146(December 2016), 402–411. <https://doi.org/10.1016/j.jseaes.2017.06.014>

Yu, F., Fu, X., Xu, G., Wang, Z., Chen, W., Zeng, S., et al. (2019). Geochemical, palynological and organic matter characteristics of the Upper Triassic Bagong Formation from the North Qiangtang Basin, Tibetan Plateau. *Palaeogeography, Palaeoclimatology, Palaeoecology*, 515(June 2017), 23–33. <https://doi.org/10.1016/j.palaeo.2017.12.002>

Zhao, M., Mercer, J. L., Eglinton, G., Higginson, M. J., & Huang, C. Y. (2006). Comparative molecular biomarker assessment of phytoplankton paleoproductivity for the last 160 kyr off Cap Blanc, NW Africa. *Organic Geochemistry*, 37(1), 72–97.

<https://doi.org/10.1016/j.orggeochem.2005.08.022>

Zonneveld, K. A. F., Versteegh, G. J. M., Kasten, S., Eglinton, T. I., Emeis, K., Huguet, C., & Koch, B. P. (2010). Selective preservation of OM in marine environment, 2010.pdf, 483–511. <https://doi.org/10.5194/bg-7-483-2010>

Chapter 2

Chlorins: quantitative paleoproductivity proxy



Picture author: Ana Herrera

2. Chlorins: quantitative paleoproductivity proxy

2.1. Introduction

Chlorophyll-*a* is the principal pigment used by plants for carrying out photosynthesis. Its concentration in sea surface waters is commonly used as an indicator of phytoplanktonic abundance in the oceans (Davies et al., 2018). Most oceanic biogeochemical models use sea-surface chlorophyll-*a* (SSchla) concentration as the central metric of phytoplankton biomass to estimate primary productivity (PP) (Behrenfeld et al., 2005). PP establishes the carrying capacities of marine ecosystems, and ultimately regulates the flux of carbon to the deep ocean (Suess, 1980) (i.e. the soft-tissue pump). Understanding how PP varies through space, time, and across global climatic oscillations is a key objective in oceanographic and climate research, as it is a vital living link in the carbon cycle.

Satellite sensors are recognized as the only feasible means to overcome spatial and temporal limitations in the estimation of PP on global scales (Lee et al., 2015). Since 1997, different satellite sensors have been launched to estimate global SSchla concentration. The Sea-viewing Wide Field-of-view Sensor (SeaWiFS; 1997-2010), the Moderate-Resolution Imaging Spectroradiometer (MODIS; 2002-present), and the MEdium Resolution Imaging Spectrometer (MERIS; 2002-2012) are some examples. The data from these different sensors have been merged in the GlobColour project for ensuring data continuity, reducing data noise, and improving spatial and temporal coverage (<http://globcolour.info>). In this way, SSchla concentration can be estimated in a global scale over the last 20 years.

The measurement of SSchla concentration previous to the satellite era, and in the absence of water column data, relies on the study of chlorophyllic pigments in marine sediments. However, chlorophyll-*a*, once released into the environment after algae senescence, quickly breakdowns or transforms into a range of degradation products, named chlorins (Leavitt, 1993). These includes pheophytin-*a*, pyropheophytin-*a*, pheophorbide-*a*, cyclopheophorbide-*a*-enol and steryl chlorin esters, among others. They are diagenetically stable and can persist in sediments over millions of years (King & Repeta, 1994; Prowse & Maxwell, 1991; Soma et al., 2001). Their joint measurement as total chlorins abundance has been used in a number of studies to infer qualitatively past PP variability (Harris et al., 1996; Higginson et al., 2003; Summerhayes et al., 1995; Szymczak-Zyła et al., 2011). Thus, for its very nature and unlike any other paleo-proxies for past PP, it provides a signal that it is exclusively linked to SSchla and PP. However, the occurrence of chlorins, in common with any organic carbon derived proxy in sediments, is in fact a measurement of their export from the surface waters and burial flux, which depends on the depositional conditions

(Bianchi et al., 2016; Niggemann et al., 2007), and complicates the interpretation of the proxy to estimate past PP. For instance, enhanced burial of organic carbon in glacial-age sediments from the nearby equatorial Pacific was interpreted as reflecting increased PP (Pedersen, 1983), but more recently it has been reinterpreted as the result of enhanced organic carbon preservation conditions under reduced oxygenation (Bradtmiller et al., 2010). In fact, there is no global assessment that determines to which extent changes in sedimentary chlorins abundance can be related to PP or depositional conditions. To this end, in this chapter we evaluate on a global scale the link between sedimentary chlorins content and remote sensing SSchl_a concentration as a means to derive a quantitative proxy for estimating marine past PP.

2.2. Methods

2.2.1. Chlorins abundance

We compiled a global suite of 121 core-top sediments, generally corresponding to the upper 2 cm of the sediment core (Figure 9). Sediments were obtained between 1973 and 2014 from diverse core repositories and laboratories. Approximately 45% of the samples were retrieved using box corer or multicorer, while the remaining were obtained with gravity and piston corers. The compilation appears to be dominated by samples along continental margins, since they represent the most intensively studied regions. However, sample sites span a wide range of chlorins concentration distributed in the diverse biogeochemical regions defined in (Weber et al., 2016) around the global ocean (Figure 9). In addition, over 80% of the compiled surface sediments are located in sites with a water column deeper than 1,000 meters, while 95% of the samples were retrieved from waters deeper than 500 meters. Consequently, the compilation is mainly representative of the pelagic zone, i.e. the water column of the open ocean.

Chlorins in sediments (ca. 1 g) were extracted using 10 mL of acetone (HPLC grade, LiChrosolv) in a MARS5 microwave accelerated extraction system (CEM Corporation). During extraction the mixture was stirred continuously with a magnetic bar, while temperature was increased from ambient to 70°C over 5 minutes and left at this temperature for a further 5 minutes. After extraction, samples were left to cool down at room temperature, and the supernatants were decanted into glass tubes and centrifuged. Extracts were then concentrated to 0.5 mL under vacuum and filtered through anhydrous Na₂SO₄ columns. To quantify total chlorin abundance, we used an off-column HPLC system with a photodiode array detector (i.e. PDA; Surveyor, Thermo Finnigan) (Harris & Maxwell, 1995) and fluorescence detector (FL3000; Thermo Finnigan). Absorbance was measured at 665 nm, while for the fluorescence measurement we used the 406 nm and 672 nm bands as the excitation and emission wavelengths, respectively. In order to take

into account the effect of the matrix in the quantification analysis, a control sediment sample, characterized by pheophorbide-*a* standard (Sigma-Aldrich), was processed in every batch of samples (14 samples). The reproducibility of the measurement brings a relative standard deviation of 4%. A subset of the compilation was obtained from (Radke et al., 2017), where the quantification of chlorins was done by using the chlorin index established in (Schubert et al., 2005). The study (Radke et al., 2017) yielded results for the Waters around Australia that have a range of variability equivalent to those generated for the present study on a global scale (Figure A1, Appendix 1).

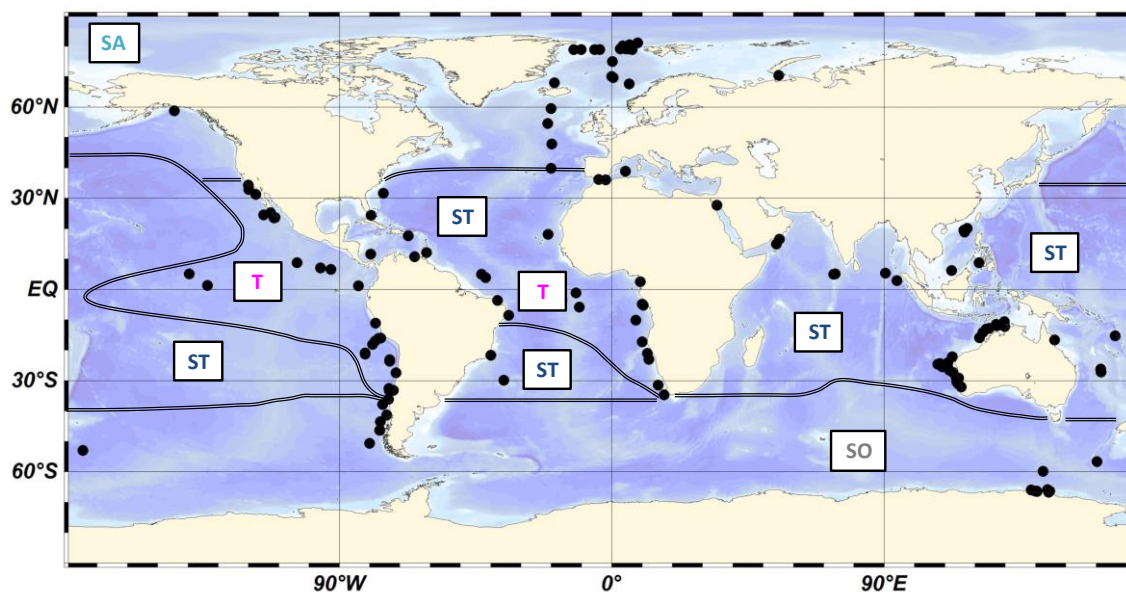


Figure 9. Global core-top sediments distribution. Lines delineate distinct biogeochemical regions defined on the basis of temperature and nutrient concentration (Weber et al., 2016). *Abbreviations: subarctic (SA), subtropics (ST), tropics (T) and Southern Ocean (SO).*

2.2.2. Uncertainties in the sedimentary data

All samples used in the study were obtained from sediment core repositories. We had no control on handling and storage conditions before samples arrived at our laboratory. In fact, the sediment compilation is rather heterogeneous in terms of the retrieval devices used to extract the sediment from the sea-floor, the date when they were retrieved, and the sediment repositories that generously provided the samples. Nevertheless, this diversity in the retrieval ages from the seafloor, the length of storage, and handling conditions probably do not impinge noticeably on chlorins preservation in the sediment. For instance, we did not observe a decrease of sedimentary chlorins concentration with the year of collection from the seafloor (Figure A2, Appendix 1). Arguably, such a decrease could be expected due to the higher exposure of the pigments to light, oxygen and temperature in the core repositories, in comparison to the seafloor. Besides, biogenic agents (i.e. fungi and microorganisms) could also play a role in decomposing chlorins in sediments

during handling and storage. However, this does not appear to be the case, and pigments appear to be stable in the sediments while cores are in storage.

The goal of the study was to analyze modern pigments inputs to seafloor sediments, and thus we considered only the bottom ocean surficial sediments. For this reason, we prioritized the analysis of sediments obtained using box corers and multicorers, which are specially designed for a minimum of disturbance of the sediment surface during coring. To expand the size of the sediment compilation we eventually also included sediments obtained using gravity and piston corers, even though these devices disturb the upper centimetres of the sediment. To assess the variability induced by using different types of corers, we classified the samples in two groups (Figure A2, Appendix 1), and compared their means of sedimentary chlorin concentration. As every group counts with more than 30 observations, we did a z-test. We defined the null hypothesis, $H_0: \mu = \mu_0$, and the alternate hypothesis, $H_1: \mu \neq \mu_0$. The z-statistic obtained was $z_{\text{calc}} = 0.58$, while two tail z-tab is equal to 1.96. Hence, $z_{\text{calc}} < z_{\text{tab}}$, from which it is derived that the means of the values from the two types of corers are statistically indistinguishable. Therefore, the type of coring device does not influence significantly the concentration values in our compilation.

Sedimentation rates could also play a role in driving the concentration of chlorins in sediments. Consequently, to analyse changes in the flux of a chemical or substance to the sea, the mass accumulation rates (MAR) must be used instead of concentrations. Chlorin mass accumulation rates (MAR_{chlorin}) were estimated by multiplying chlorin concentration by sedimentation rate and dry bulk density. In the absence of these data for each sample site, we extracted sedimentation rates from two global maps previously published (Dunne et al., 2012; Jahnke, 1996) and discussed in (Cartapanis et al., 2016). However, sedimentation rates could only be extracted for 71% of the sites. Dry bulk densities were assumed to be $0.9 \text{ g}\cdot\text{cm}^{-3}$, as it corresponds to the mean dry bulk density for marine sediments in the global sediment core database published in (Cartapanis et al., 2016), which has been created by retrieving available data from online data repositories. It is important to point out that these estimated accumulation rates are highly uncertain, given that sedimentation rates can vary significantly over relatively short distances on the seafloor due to winnowing and focusing, and the locations of cores are often biased towards the highest accumulation rates in the search of retrieving records with high temporal resolution. Nonetheless, in the absence of more accurate data, we include the estimates to provide a first-order information on the effect of sedimentation rates in our sedimentary data. We compared MAR_{chlorin} against chlorin concentration in Figure A3 (Appendix 1). The correlation between the two variables is high as attested by their coefficient of determination of $R^2 = 0.93$ and $R^2 = 0.85$, depending on the sources of sedimentation rates (Dunne et al., 2012; Jahnke, 1996). Consequently,

overall for our compilation, the differences in using MARchlorin and chlorin concentration when compared to values of SSchla concentration are not likely to lead to significantly different results. To maximize the size of data points in our compilation we used the chlorin concentration rather than its MAR.

2.2.3. SSchla concentration

SSchla concentration ($\text{mg}\cdot\text{m}^{-3}$) at sediment sample locations were obtained from the Globcolour Project. GlobColour data (<http://globcolour.info>) used in this study has been developed, validated, and distributed by ACRI-ST, France. CHL1 ocean colour L3 is a merged product from different sensors that were in operation from 1997 to present: SeaWiFS (1997-2010), MERIS (2002-2012), MODIS (2002-2017) and VIIRS (2012-2017). The algorithms used to obtain the CHL1 product were OC4v5 for SeaWiFS, OC4Me for MERIS and OC3v5 for MODIS and VIIRS (O'Reilly et al., 2000). The spatial resolution of CHL1 product is $1/24^\circ$ (4.63 km at the equator). Monthly SSchla concentration were extracted for each location from the merged global-scale matrix (2160x4320). A $n=2160$ vector with values from 90 to -90 (steps=0.041667) was created for latitudes and other $m=4320$ vector with values from -180 to 180 (steps=0.041667) was created for longitudes. A search was then conducted for the nearest value in those vectors that coincide with the samples location (latitude and longitude), and to deliver the chlorophyll-*a* concentration values of the matrix that correspond to every location. Each matrix contains monthly data, thus, we obtained chlorophyll-*a* concentration for every location and for every month over the last 20 years. To obtain SSchla concentration for the last 20 years, we added the concentrations from September 1997 to December 2017 for every location.

2.2.4. Uncertainties in the remote sensing data

One of the principal sources of the satellite data scatter might be the poor accuracy of satellite SSchla concentration products in some specific oceanic regions where the complexity of the optical and biological properties are significant. Global standard algorithms are inapplicable in areas with coloured dissolved organic matter, radiance-absorbing aerosols, phytoplankton species diversity, suspended sediments, clouds, ice, sun glint, and navigation/time space mismatches (Claustre & Maritoner, 2003; Dierssen & Smith, 2000; Sathyendranath et al., 2001; Volpe et al., 2007). Moreover, desert dust trapped in the upper layer (Claustre et al., 2002) and bubbles (Stramski & Tegowski, 2001) make the water appear greener. The poor quality of the atmospheric correction still hamper accurate retrievals of optical properties and biogeochemical concentrations (Blondeau-Patissier et al., 2014).

Other sources of scatter that might affect our comparison between SSchla and sedimentary chlorins are the satellite limitation of detecting phytoplankton growing deep in the water column (Cullen, 1982; Huisman et al., 2006), and the different timescales between SSchla observations and sediment measurements. SSchla estimates correspond to 20 years of satellite observations. However, sedimentary data for most of the samples (> 85%) corresponds to about 155 years, as the average of sedimentation rates is around 13 cm/ka, using the map published in (Dunne et al., 2012).

2.3. Results

2.3.1. The global fraction of the exported and buried chlorophyll-*a*

The concentration of chlorins in the sediment is bound to be influenced by the concentration of chlorophyll-*a* in the upper water column (Suess, 1980). However, chemical, physical and biological processes that occur in the water column and/or in the water-sediment interface, such as oxidation, mineral adsorption and bioturbation, may also play a role (Sarmiento & Gruber, 2006). As a result, only a small fraction of the organic matter produced in the sea-surface is finally buried in the sediments. For instance, globally, integrated marine PP at the surface is around 48 PgC/yr (DeVries & Weber, 2017; Sarmiento & Gruber, 2006), while global export production, PP exported out of the photic zone, range from 6 to 10 PgC/yr (Schlitzer, 2002; Siegel et al., 2014). Furthermore, the transfer efficiency, which is the fraction of particulate carbon that is exported from the euphotic zone to the deep ocean, ranges from 5 to 35%. Much less studied is the global fraction of organic matter that reaches the sea-floor, which is estimated to be 0.93 PgC/yr (Muller-Karger et al., 2005). Finally, only 5% of the organic carbon that reaches the sea-floor becomes buried in the sediments. Global fluxes from the sea-surface to the deep ocean or sea-floor, and global burial fluxes that take place in the sediment-water interface are estimated by ocean biogeochemical models (Lutz et al., 2002; Martin et al., 1987; Suess, 1980) and early diagenetic models (Boudreau, 1996; Soetaert et al., 1996; Stolpovsky et al., 2018), respectively.

However, the percentage of the global amount of organic matter produced in the sea-surface that is eventually buried into the sediments is less frequently evaluated. Estimations from models indicate that the amount of carbon that is buried globally in the sediments is around 0.15 Pg (Muller-Karger et al., 2005), which represents around 0.31% of the carbon at the sea-surface. Using our chlorin and SSchla concentration data, we estimate that globally the average fraction of the SSchla that is finally buried in the sediments in the form of chlorins is 0.33%, which is consistent with the fraction of global buried carbon estimated by modelling (Muller-Karger et al., 2005). This

value is derived from the ratio between the amount of chlorins that are buried in the sediment every year, and the annual rate of production of sea-surface chlorophyll-*a* at each core site.

2.3.2. Quantifying SSchla from chlorins

The global comparison between sedimentary chlorins and SSchla concentration estimated over the last 20 years is shown in Figure 10. We represented the data on a logarithmic scale based on the natural distribution of ocean chlorophyll, which is lognormal (Campbell, 1995).

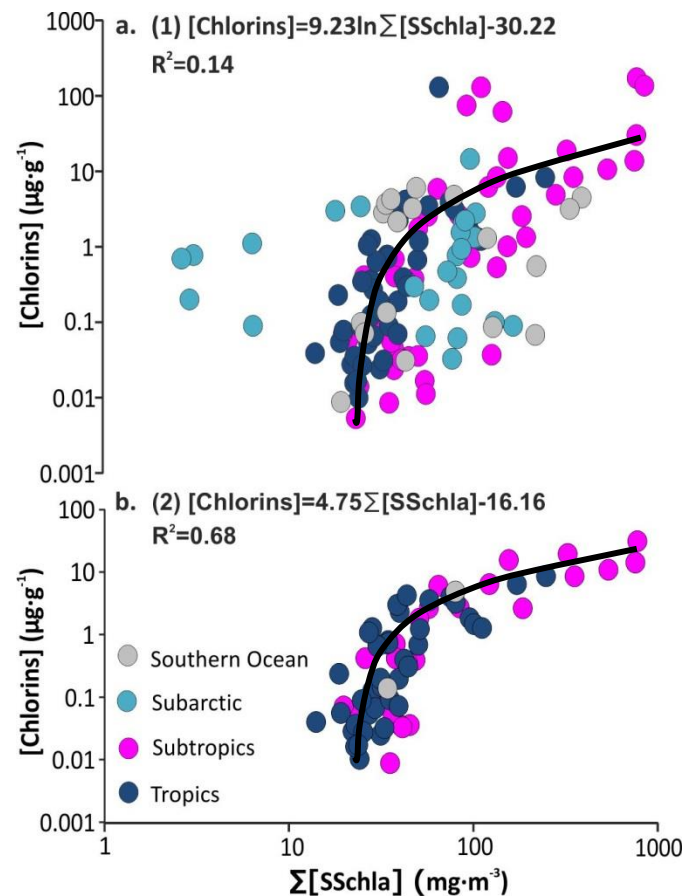


Figure 10. Global correlations between sedimentary chlorins concentration and the sum of sea-surface chlorophyll-*a* (SSchla) concentration from 1997 to 2017. **a.** includes the whole compilation, and **b.** includes regions presenting RMS log errors lower than 31% between remote sensing and *in situ* SSchla. Samples are classified by biogeochemical regions as defined in Figure 9.

For reducing the uncertainty derived from the use of SSchla concentration global standard algorithms, we only considered regions reported to present RMS log errors lower than 31% between remote sensing and *in situ* SSchla concentration, as this threshold has been used to define well-performing regions in global and regional remote sensing SSchla evaluation studies (Gregg & Casey, 2004). Consequently, the North Atlantic (Gregg & Casey, 2004; Mendonça et al., 2010; Stramska et al., 2003), the Antarctic (Barbini et al., 2001; Dierssen & Smith, 2000; Gregg & Casey, 2004; Marrari et al., 2006; Moore et al., 1999) and the California current for high SSchla

concentration ($>1\text{mg}\cdot\text{m}^{-3}$) (Kahru et al., 2012, 2014), which present RMS log errors higher than 31%, are not included in Figure 10 b. Nor the western South American margin, as the error of this region has not been thoroughly studied. Although the equatorial Atlantic presents a RMS log error of 48%, it drops to 23% when removing samples located offshore of the north-eastern coast of South America (Gregg & Casey, 2004). Since our samples are not located in this region, we included samples from the equatorial Atlantic in Figure 10 b.

As it is shown in Figure 10 b, the scatter in the global correlation between sedimentary chlorins and SSchla concentration drop significantly when no considering the regions explained above. The obtained correlation follows a logarithmic relationship with a root mean square error of 26% and R^2 of 0.68. This indicates global SSchla concentration is the dominant factor controlling chlorins content in sediments and suggest sedimentary chlorins as a reliable proxy for quantifying SSchla concentration.

However, several studies suggest regional variability in the organic matter flux from surface to deep ocean (Henson et al., 2012; Lam et al., 2011; Marsay et al., 2015; Weber et al., 2016), which may lead to different correlations between sedimentary chlorins and SSchla concentration depending on the region. To investigate the influence of spatial variability in our data set, we divided the global ocean in the different regions defined in (Weber et al., 2016), which are classified by factors influencing transfer efficiency, such as phytoplankton community, nutrient concentration and temperature. The defined regions are as follows: the tropics, the subtropics, the subarctic and the Southern Ocean. However, due to lack of sufficient data we did not appraise all the biogeographic regions. As can be seen in Figure 11, we did not found significant differences in the correlation between the two regions appraised, the tropics and the subtropics, and the RMS log error range from 19 to 29 % (Table 1). Our data support the results obtained in (Lutz et al., 2002), which showed that spatial variability in the vertical flux of particulate organic carbon decreases with increasing water column depth. Our results are also in agreement with (Jahnke, 1996), where the author indicate, using data from the North Atlantic, that the proportion of primary production that reaches the deep sea does not vary greatly with latitude.

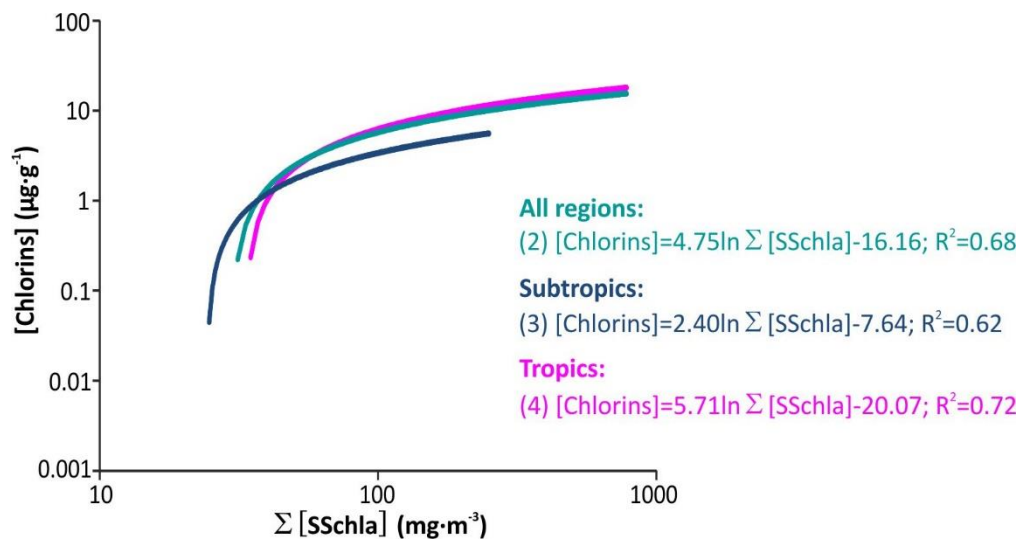


Figure 11. Regional correlations between sedimentary chlorins concentration and the sum of sea-surface chlorophyll-*a* (SSchla) concentration from 1997 to 2017. Different colours for lines and text indicate the evaluated biogeochemical regions, which are defined in Figure 9.

Equation	a	b	R ²	RMS log error (%)	n
1	9.23	-30.22	0.14	109	140
2	4.75	-16.16	0.68	25	70
3	2.40	-7.64	0.62	19	42
4	5.71	-20.07	0.72	29	26
5	4.01	8.25	0.63	33	70
6	3.69	6.41	0.62	36	70
7	3.25	5.39	0.58	43	70

Table 1. Coefficients and errors of chlorins equations. $[\text{Chlorins}] = a \cdot \Sigma [\text{SSchla}] + b$. Abbreviations: coefficient of determination (R^2), root-mean square logarithmic error (RMS log error), number of samples (n).

Not only spatial, but also temporal variability of SSchla concentration can modify the sedimentary chlorin content by influencing the relative amount of organic matter exported from the surface ocean to depth (Berger & Wefer, 1990; Dunne et al., 2005). To approach the temporal variability, we looked into the correlation between the seasonal variation index (SVI) (Lutz et al., 2007), as an indicator of temporal variability, and sedimentary chlorins concentration. We determined the SVI for every location by calculating the average of every month for the whole period of satellite available data, and then the average and the standard deviation of the calculated averages. Both SVI and sedimentary chlorins were logarithmically transformed before statistical analysis for obtaining a normal distribution. We obtained a p-value of 0.004 (for a confidence level of 95%), which indicates that there is a significant correlation between SVI and sedimentary chlorins

concentration. However, the R^2 of 0.12 indicates a minor role of the SVI in controlling sedimentary chlorins concentration.

To further evaluate the extent of the seasonality of SSchla concentration in our study, we also compared the correlation between sedimentary chlorins concentration and the SSchla *i)* annual, *ii)* the seasonal maxima, and *iii)* the monthly maxima, averaged over the last 20 years. The annual SSchla was determined by averaging all months during the last 20 years; and the seasonal or monthly maxima by averaging only the most productive seasons or months of each year, respectively. As it is shown in Figure 12, there are no significant differences between any of the correlations. The coefficients of determination range from 0.58 to 0.63 and the RMS log errors between 33 and 43% (Table 1).

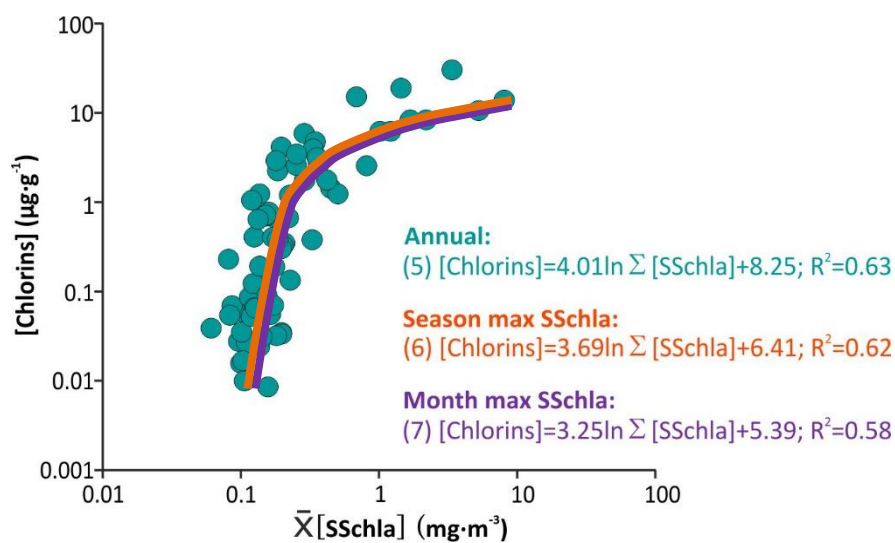


Figure 12. Global correlation between sedimentary chlorins concentration and the average of sea-surface chlorophyll-*a* concentration (SSchla) from 1997 to 2017. Different colours for the lines and text indicate, *i)* annual SSchla: average of all months (green dots), *ii)* seasonal maxima average SSchla: the most productive season (orange line), and *iii)* monthly maxima average SSchla: the most productive month (purple line).

2.3.3. Other factors controlling chlorins deposition

Besides PP, other factors, such as water depth, sedimentation rate and oxygen have been discussed to play an important role in controlling organic matter flux and deposition in sediments (Betts & Holland, 1991; Betzer et al., 1984; Müller & Suess, 1979; Pace et al., 1987; Suess, 1980). To study the influence of these factors in altering chlorins content in sediments, we correlated the SSchla-chlorins ratio, as a measurement of chlorins transfer efficiency from surface to sediments, with water column depth, sedimentation rates and oxygen concentration in bottom waters (Figure 13). Sedimentation rates were extracted from the map published in (Dunne et al., 2012) and oxygen concentration in bottom waters from NOAA database.

The obtained p-values (with a confidence level of 95%) for the correlation between SSchla-chlorins ratio and oxygen, sedimentation rates and water depth were 0.21, 0.60 and 0.03, respectively. These results indicate that there is no significant correlation between SSchla-chlorins ratio and neither oxygen nor sedimentation rates, but it is significant against water depth. The R^2 obtained for the latter correlation was, however, of 0.05.

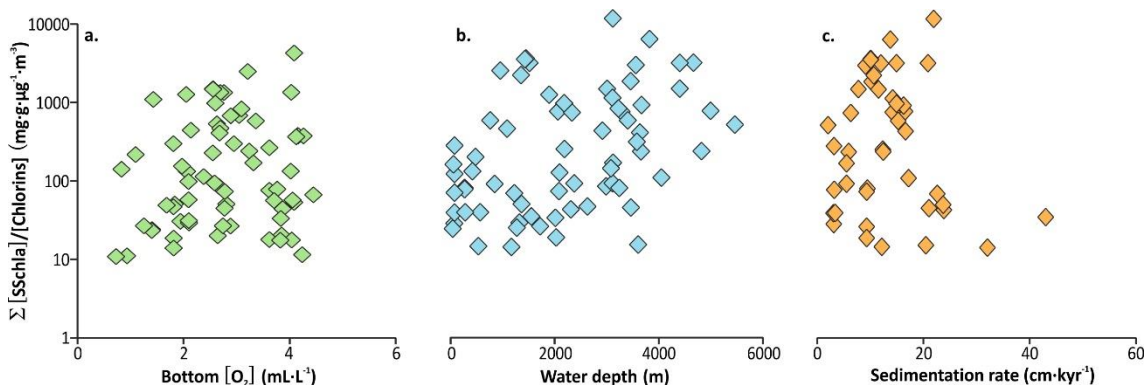


Figure 13. Global correlations between the ratio of the sum of sea-surface chlorophyll-*a* (SSchla) concentration from 1997 to 2017 and chlorins concentration, with depositional factors: **a.** bottom oxygen concentration, **b.** water depth and **c.** sedimentation rate.

2.4. Discussion

2.4.1. Chlorins as a quantitative proxy for past PP

The presence of chlorins in sediments is the outcome of their export from surface waters and sedimentary burial rates, which is driven by PP and the production of SSchla, as well as depositional conditions. As chlorins are labile compounds, arguably, their concentration might have a higher dependence on depositional conditions than other paleoproductivity proxies, such as barium. This would constrain their application as a past PP proxy. However, in paleoceanographic studies, sedimentary chlorins concentration maxima were found concordant with other paleoproductivity proxies, such as biogenic opal and organic carbon (Harris et al., 1996; Schubert et al., 1998), which suggests that chlorins can track past PP variations in some settings, particularly such as upwellings where PP is very high.

To constrain the link between SSchla and sedimentary chlorins concentration, we appraised their global scale correlation (Figure 10). The data span several oceanic biogeochemical regions (Weber et al., 2016), and show that the spatial variability in sedimentary chlorins is indeed related to changes in SSchla, following a logarithmic trend with a root mean square (RMS) log error of 26%, and a coefficient of determination (R^2) of 0.68. Thus, depositional conditions, are not globally the primary variables explaining the spatial distribution of sedimentary chlorins concentration, but rather SSchla concentration which is related to past PP.

The consideration of a logarithmic relationship between SSchl_a and sedimentary chlorins concentration has important implications in the interpretation of paleoceanographic archives. In previous studies, a linear relationship between SSchl_a and chlorins proxy was assumed, which in fact might have led to an under- or overestimation of past PP changes. It may be also particularly relevant that in the Figure 10 b relationship there is an inflection point at 1 µg/g in sedimentary chlorins concentration. Below this apparent threshold, a large change in sedimentary chlorins concentration corresponds to small change in SSchl_a concentration, and the opposite occurs above 1 µg/g in sedimentary chlorins concentration. Therefore, chlorins time series which encompass values above and below the 1 µg/g threshold are estimating magnitudes of relative past PP changes (i.e. Δ SSchl_a concentration) that are different per unit of change of chlorin concentration.

For instance, in one of the seminal studies using chlorins undertaken in lake Biwa (Ishiwatari et al., 2009) this is exactly what was observed. The downcore pattern of chlorins had higher values of 1-4.5 µg/g in the upper sedimentary sections corresponding to the Holocene, and lower values (ca. 0.5 µg/g) in the glacial sections. The interpretation of the results was that the difference in chlorins PP between the Holocene and the glacial was greater than in the organic carbon PP. PP using the organic carbon proxy was approximately the double in the Holocene than in the glacial, but the difference was more than 4 times greater when using the chlorins proxy. Using our regression in Figure 10 b, the difference between estimated SSchl_a concentration between the two periods is approximately the double (69.7 mg/m³ in the glacial and 33.3 mg/m³ in the Holocene), in agreement with the organic carbon estimates in the original paper. In contrast, in studies carried out in the Benguela and the Canary current (Harris et al., 1996; Summerhayes et al., 1995), chlorins concentration were higher than 1 µg/g throughout the glacial and the Holocene. In these settings, a linear relationship can be assumed between SSchl_a and chlorins concentration as their range in the records corresponds to the part of the relationship above the 1 µg/g inflection point. As a consequence, chlorins and organic carbon proxies of these studies were found to estimate similar PP changes between both periods. Another important implication derived from our study is that the Figure 10 b equation will allow the quantification of past SSchl_a concentration, with a RMS log error of 26%, and therefore offers a means for inferring past PP using estimates of SSchl_a concentration.

2.4.2. Regional and seasonal variability

A number of authors have argued that the export efficiency of surface biomass to the deep ocean is spatially variable, and depends on the latitude or biogeographical regions. The issue, however, is not devoid of controversy. Several studies indicate that there are no significant latitudinal trends

in water column fluxes of organic matter (Lampitt & Antia, 1997; Martin et al., 1987; Suess, 1980). In contrast, others suggest a regional variability in the efficiency of the biological pump to transport organic carbon from surface to the ocean's interior (Henson et al., 2012; Lam et al., 2011; Marsay et al., 2015; Weber et al., 2016).

To approach regional differences in the global correlation between sedimentary chlorins and SSchla, we did individual correlations between sedimentary chlorins and SSchla concentration for each defined region in Figure 9. Our comparison between the tropics and the subtropics correlations does not show significant differences (Figure 11), suggesting no significant regional differences in the export and burial efficiency of organic matter to the sediments. Our findings are consistent with previous observations, which found that variability decreases in the intermediate and deep ocean with increasing depth (Lutz et al., 2002). Hence, chemical, physical and biological processes that take place through the deep-water column and in the water-sediment interface seem to play a key role in spatially homogenising the amount of organic matter that is finally buried in the sediment at any site. These results are relevant in paleoclimate reconstructions as biogeochemical regions change through time in some locations. Therefore, finding no significant differences between regions in the evaluated scales suggest that past PP can be inferred using the relationship in Figure 10 b without concerns about changes in the biogeochemical conditions through time.

Besides biogeochemical region conditions, temporal variability of SSchla concentration might also alter chlorins export from surface to sediments and thus, sedimentary chlorins concentration. More episodic PP regions are believed to export a greater amount of particulate organic matter than regions which show lower seasonal variability in past PP (Berger & Wefer, 1990; Dunne et al., 2005).

Our results from the correlation between the seasonal variation index (SVI) (Lutz et al., 2007), as an indicator of temporal variability, and sedimentary chlorins concentration indicates a minor role of the temporal variability in altering sedimentary chlorins concentration ($R^2=0.12$). Moreover, we did not find significant differences between the following correlations: sedimentary chlorins and *i*) annual SSchla, *ii*) the seasonal maxima SSchla, and *iii*) the monthly maxima SSchla (Figure 12). These results suggest that the transfer efficiency from the surface to sediment burial is not significantly higher during episodes of higher PP (i.e. phytoplankton blooms) in comparison to the rest of the year. Hence, although seasonality might lead to changes in export fluxes, this variability is not the predominant cause of variations in sedimentary chlorins concentration, and has not a significant effect in the correlation between SSchla and sedimentary chlorins concentration for the samples evaluated in this study.

2.4.3. Depositional factors in the export and burial of surface chlorophyll-*a*

We have shown that SSchl_a concentration explains most of the spatial variability of chlorins concentration in surface sediments worldwide. However, there are other factors that influence chlorins fluxes to sediments spatially, which arguably could be water depth, sedimentation rate and oxygen (Betts & Holland, 1991; Betzer et al., 1984; Müller & Suess, 1979; Pace et al., 1987; Suess, 1980).

The results from the correlation between the SSchl_a-chlorins ratio (i.e. a measurement of the transfer efficiency and chlorophyll-*a* degradation) and bottom oxygen concentration (p -value=0.21), sedimentation rates (p -value=0.60) and water column depth (R^2 =0.05) suggest that depositional processes in the water column do not greatly affect the global spatial variability of sedimentary chlorins concentration (Figure 13). This agrees with previous studies on experimental and field observations that claimed that oxygen is not a primary control on the degradation of labile organic material (Canfield, 1994), and from sinking particle models which found that the influence of oxygen on remineralization does not contribute significantly to the large-scale patterns of organic carbon transfer efficiency (Cram et al., 2018). Other studies have also asserted that water column depth is not a relevant factor in controlling organic matter concentration in sediments as the majority of organic matter is remineralized above 500 meters depth, and deeper down there is almost no degradation (Pace et al., 1987; Yamanaka & Tajika, 1997). However, it remains to be assessed the combined role of various depositional processes in controlling sedimentary organic matter concentration (Cram et al., 2018).

2.5. Conclusions

In summary, the primary driver that explains the spatial distribution of sedimentary chlorins concentration is SSchl_a concentration and PP, rather than depositional factors. The latter process degrades 99.7% of the SSchl_a during sedimentation until its derivatives are buried in sediments, but is arguably globally constant. As a consequence, this study provides the first space-based calibration for quantifying global PP through the past estimation of SSchl_a concentration. This calibration is independent of the biogeographic region, and seasonality of production, which implies that it is applicable globally despite any changes in biogeochemical regimes in a given site through time. The data generated in this study would also serve as a new tool for validating remote sensing chlorophyll and identifying oceanographic areas with optical properties that diverge from the global and needs specific algorithms for estimating surface chlorophyll concentration and PP. Moreover, these results also provide new constraints, i.e. past SSchl_a and chlorins values, against which is possible to validate and improve ocean biogeochemical models and their estimates of PP and organic carbon sedimentary burial.

2.6. References

- Barbini, R., Colao, F., Fantoni, R., Fiorani, L., & Palucci, A. (2001). Remote sensing of the Southern Ocean: techniques and results. *Journal of Optoelectronics and Advanced Materials*, *3*(4), 817–830.
- Behrenfeld, M. J., Boss, E., Siegel, D. A., & Shea, D. M. (2005). Carbon-based ocean productivity and phytoplankton physiology from space. *Global Biogeochemical Cycles*, *19*(1), 1–14. <https://doi.org/10.1029/2004GB002299>
- Berger, W. H., & Wefer, G. (1990). Export production: seasonality and intermittency, and paleoceanographic implications. *Global and Planetary Change*, *3*(3), 245–254. [https://doi.org/10.1016/0921-8181\(90\)90020-D](https://doi.org/10.1016/0921-8181(90)90020-D)
- Betts, J. N., & Holland, H. D. (1991). The oxygen content of ocean bottom waters, the burial efficiency of organic carbon, and the regulation of atmospheric oxygen. *Global and Planetary Change*, *5*(1–2), 5–18. [https://doi.org/10.1016/0921-8181\(91\)90123-E](https://doi.org/10.1016/0921-8181(91)90123-E)
- Betzer, P. R., Showers, W. J., Laws, E. A., Winn, C. D., DiTullio, G. R., & Kroopnick, P. M. (1984). Primary productivity and particle fluxes on a transect of the equator at 153°W in the Pacific Ocean. *Deep Sea Research Part A, Oceanographic Research Papers*, *31*(1), 1–11. [https://doi.org/10.1016/0198-0149\(84\)90068-2](https://doi.org/10.1016/0198-0149(84)90068-2)
- Bianchi, T. S., Schreiner, K. M., Smith, R. W., Burdige, D. J., Woodard, S., & Conley, D. J. (2016). Redox effects on organic matter storage in coastal sediments during the Holocene: a biomarker/proxy perspective. *Annual Review of Earth and Planetary Sciences*, *44*, 295–319. <https://doi.org/10.1146/annurev-earth-060614-105417>
- Blondeau-Patissier, D., Gower, J. F. R., Dekker, A. G., Phinn, S. R., & Brando, V. E. (2014). A review of ocean color remote sensing methods and statistical techniques for the detection, mapping and analysis of phytoplankton blooms in coastal and open oceans. *Progress in Oceanography*, *123*, 123–144. <https://doi.org/10.1016/j.pocean.2013.12.008>
- Boudreau, B. P. (1996). A method-of-line code for carbon and nutrient diagenesis in aquatic sediments. *Computer & Geosciences*, *22*(5), 479–496.
- Bradtmiller, L. I., Anderson, R. F., Sachs, J. P., & Fleisher, M. Q. (2010). A deeper respired carbon pool in the glacial equatorial Pacific Ocean. *Earth and Planetary Science Letters*, *299*(3–4), 417–425. <https://doi.org/10.1016/j.epsl.2010.09.022>
- Calbet, A., & Landry, M. R. (2004). Phytoplankton growth, microzooplankton grazing, and carbon cycling in marine systems, *49*(1), 51–57.

- Campbell, J. W. (1995). The lognormal distribution as a model for bio-optical variability in the sea. *Journal of Geophysical Research*, *100*(95), 13237–13254. <https://doi.org/10.1029/95JC00458>
- Canfield, D. E. (1994). Factors influencing organic carbon preservation in marine sediments. *Chemical Geology*, *114*(3–4), 315–329. [https://doi.org/10.1016/0009-2541\(94\)90061-2](https://doi.org/10.1016/0009-2541(94)90061-2)
- Cartapanis, O., Bianchi, D., Jaccard, S. L., & Galbraith, E. D. (2016). Global pulses of organic carbon burial in deep-sea sediments during glacial maxima. *Nature Communications*, *7*, 10796. <https://doi.org/10.1038/ncomms10796>
- Ceballos-Romero, E., Le Moigne, F. A. C., Henson, S., Marsay, C. M., Sanders, R. J., Garcíá-Tenorio, R., & Villa-Alfageme, M. (2016). Influence of bloom dynamics on Particle Export Efficiency in the North Atlantic: a comparative study of radioanalytical techniques and sediment traps. *Marine Chemistry*, *186*, 198–210. <https://doi.org/10.1016/j.marchem.2016.10.001>
- Claustre, H., & Maritoner, S. (2003). The Many Shades of Ocean Blue. *Ocean Science*, *302*(5650), 1514–1515.
- Claustre, H., Morel, A., Hooker, S. B., Babin, M., Antoine, D., Oubelkheir, K., et al. (2002). Is desert dust making oligotrophic waters greener? *Geophysical Research Letters*, *29*(10), 107-1-107-4. <https://doi.org/10.1029/2001GL014056>
- Cram, J. A., Weber, T., Leung, S. W., McDonnell, A. M. P., Liang, J. H., & Deutsch, C. (2018). The Role of Particle Size, Ballast, Temperature, and Oxygen in the Sinking Flux to the Deep Sea. *Global Biogeochemical Cycles*, 858–876. <https://doi.org/10.1029/2017GB005710>
- Cullen, J. J. (1982). The deep chlorophyll maximum: Comparing vertical profiles of chlorophyll a. *Canadian Journal of Fisheries and Aquatic Sciences*, *39*, 791–803.
- Davies, C. H., Ajani, P., Armbrrecht, L., Atkins, N., Baird, M. E., Beard, J., et al. (2018). A database of chlorophyll a in Australian waters. *Scientific Data*, *5*, 1–8. <https://doi.org/10.1038/sdata.2018.18>
- DeVries, T., & Weber, T. (2017). The export and fate of organic matter in the ocean: New constraints from combining satellite and oceanographic tracer observations. *Global Biogeochemical Cycles*, *31*(3), 535–555. <https://doi.org/10.1002/2016GB005551>
- Dierssen, H. M., & Smith, R. C. (2000). Bio-optical properties and remote sensing ocean color algorithms for Antarctic Peninsula waters, *105*(1999), 26301–26312.
- Dunne, J. P., Armstrong, R. A., Gnnadesikan, A., & Sarmiento, J. L. (2005). Empirical and mechanistic models for the particle export ratio. *Global Biogeochemical Cycles*, *19*(4), 1–16.

- <https://doi.org/10.1029/2004GB002390>
- Dunne, J. P., Hales, B., & Toggweiler, J. R. (2012). Global calcite cycling constrained by sediment preservation controls. *Global Biogeochemical Cycles*, *26*(3), 1–14.
<https://doi.org/10.1029/2010GB003935>
- Gregg, W. W., & Casey, N. W. (2004). Global and regional evaluation of the SeaWiFS chlorophyll data set. *Remote Sensing of Environment*, *93*(4), 463–479.
<https://doi.org/10.1016/j.rse.2003.12.012>
- Harris, P., Zhao, M., & Rosell-Melé, A. (1996). Chlorin accumulation rate as a proxy for Quaternary marine primary productivity. *Nature*. Retrieved from
<http://www.nature.com/nature/journal/v383/n6595/abs/383063a0.html>
- Harris, P. G., & Maxwell, J. R. (1995). A novel method for the rapid determination of chlorin concentrations at high stratigraphic resolution in marine sediments. *Organic Geochemistry*, *23*(9), 853–856. [https://doi.org/10.1016/0146-6380\(95\)80007-E](https://doi.org/10.1016/0146-6380(95)80007-E)
- Henson, S. A., Sanders, R., & Madsen, E. (2012). Global patterns in efficiency of particulate organic carbon export and transfer to the deep ocean. *Global Biogeochemical Cycles*, *26*(1), 1–14.
<https://doi.org/10.1029/2011GB004099>
- Higginson, M. J., Maxwell, J. R., & Altabet, M. A. (2003). Nitrogen isotope and chlorin paleoproductivity records from the Northern South China Sea: Remote vs. local forcing of millennial- and orbital-scale variability. *Marine Geology*, *201*(1–3), 223–250.
[https://doi.org/10.1016/S0025-3227\(03\)00218-4](https://doi.org/10.1016/S0025-3227(03)00218-4)
- Huisman, J., Pham Thi, N. N., Karl, D. M., & Sommeijer, B. (2006). Reduced mixing generates oscillations and chaos in the oceanic deep chlorophyll maximum. *Nature*, *439*(7074), 322–325. <https://doi.org/10.1038/nature04245>
- Ishiwatari, R., Negishi, K., Yoshikawa, H., & Yamamoto, S. (2009). Glacial-interglacial productivity and environmental changes in Lake Biwa, Japan: A sediment core study of organic carbon, chlorins and biomarkers. *Organic Geochemistry*, *40*(4), 520–530.
<https://doi.org/10.1016/j.orggeochem.2009.01.002>
- Jahnke, R. A. (1996). The global ocean flux of particulate organic carbon: Areal distribution and magnitude, *1*(1), 71–88.
- Kahru, M., Kudela, R. M., Manzano-Sarabia, M., & Mitchell, B. G. (2012). Trends in the surface chlorophyll of the California Current: Merging data from multiple ocean color satellites. *Deep-Sea Research Part II: Topical Studies in Oceanography*, *77–80*, 89–98.

- <https://doi.org/10.1016/j.dsr2.2012.04.007>
- Kahru, M., Kudela, R. M., Anderson, C. R., Manzano-Sarabia, M., & Mitchell, B. G. (2014). Evaluation of satellite retrievals of ocean chlorophyll-a in the California current. *Remote Sensing*, *6*(9), 8524–8540. <https://doi.org/10.3390/rs6098524>
- King, L. L., & Repeta, D. J. (1994). Phorbol sterol esters in Black Sea sediment traps and sediments: A preliminary evaluation of their paleoceanographic potential. *Geochimica et Cosmochimica Acta*. [https://doi.org/10.1016/0016-7037\(94\)90342-5](https://doi.org/10.1016/0016-7037(94)90342-5)
- Lam, P. J., Doney, S. C., & Bishop, J. K. B. (2011). The dynamic ocean biological pump: Insights from a global compilation of particulate organic carbon, CaCO₃, and opal concentration profiles from the mesopelagic. *Global Biogeochemical Cycles*, *25*(3), 1–14. <https://doi.org/10.1029/2010GB003868>
- Lampitt, R. S., & Antia, A. N. (1997). Particle flux in deep seas: Regional characteristics and temporal variability. *Deep-Sea Research Part I: Oceanographic Research Papers*, *44*(8), 1377–1403. [https://doi.org/10.1016/S0967-0637\(97\)00020-4](https://doi.org/10.1016/S0967-0637(97)00020-4)
- Leavitt, P. R. (1993). A review of factors that regulate carotenoid and chlorophyll deposition and fossil pigment abundance. *Journal of Paleolimnology*, *9*(2), 109–127. <https://doi.org/10.1007/BF00677513>
- Lee, Z., Marra, J., Perry, M. J., & Kahru, M. (2015). Estimating oceanic primary productivity from ocean color remote sensing: A strategic assessment. *Journal of Marine Systems*, *149*, 50–59. <https://doi.org/10.1016/j.jmarsys.2014.11.015>
- Lutz, M., Dunbar, R., & Caldeira, K. (2002). Regional variability in the vertical flux of particulate organic carbon in the ocean interior. *Global Biogeochemical Cycles*, *16*(3), 11–11–18. <https://doi.org/10.1029/2000GB001383>
- Lutz, M. J., Caldeira, K., Dunbar, R. B., & Behrenfeld, M. J. (2007). Seasonal rhythms of net primary production and particulate organic carbon flux to depth describe the efficiency of biological pump in the global ocean. *Journal of Geophysical Research: Oceans*, *112*(10), C10011. <https://doi.org/10.1029/2006JC003706>
- Marrari, M., Hu, C., & Daly, K. (2006). Validation of SeaWiFS chlorophyll a concentrations in the Southern Ocean: A revisit. *Remote Sensing of Environment*, *105*(4), 367–375. <https://doi.org/10.1016/j.rse.2006.07.008>
- Marsay, C. M., Sanders, R. J., Henson, S. A., Pabortsava, K., Achterberg, E. P., & Lampitt, R. S. (2015). Attenuation of sinking particulate organic carbon flux through the mesopelagic ocean.

- Proceedings of the National Academy of Sciences*, 112(4), 1089–1094.
<https://doi.org/10.1073/pnas.1415311112>
- Martin, J. H., Knauer, G. A., Karl, D. M., & Broenkow, W. W. (1987). VERTEX: carbon cycling in the northast Pacific, *34*(2), 267–285.
- Mendonça, A., Martins, A., Figueiredo, M., Bashmachnikov, I., Couto, A., Lafon, V., & Aristegui, J. (2010). Evaluation of ocean color and sea surface temperature sensors algorithms using in situ data: a case study of temporal and spatial variability on two northeast Atlantic seamounts. *Journal of Applied Remote Sensing*, 4(1), 043506.
<https://doi.org/10.1117/1.3328872>
- Moore, J. K., Abbott, M. R., Richman, J. G., Smith, W. O., Cowles, T. J., Coale, K. H., et al. (1999). SeaWiFS satellite ocean color data from the Southern Ocean. *Geophysical Research Letters*, 26(10), 1465–1468. <https://doi.org/10.1029/1999GL900242>
- Muller-Karger, F. E., Varela, R., Thunell, R., Luerssen, R., Hu, C., & Walsh, J. J. (2005). The importance of continental margins in the global carbon cycle. *Geophysical Research Letters*, 32(1), 1–4.
<https://doi.org/10.1029/2004GL021346>
- Müller, P. J., & Suess, E. (1979). Productivity, sedimentation rate, and sedimentary organic matter in the oceans: I. Organic carbon preservation. *Deep-Sea Research*, 26A, 1347–1362.
- Niggemann, J., Ferdelman, T. G., Lomstein, B. A., Kallmeyer, J., & Schubert, C. J. (2007). How depositional conditions control input, composition, and degradation of organic matter in sediments from the Chilean coastal upwelling region. *Geochimica et Cosmochimica Acta*, 71(6), 1513–1527. <https://doi.org/10.1016/j.gca.2006.12.012>
- O'Reilly, J. E., Maritorena, S., O'Brien, M. C., Siegel, D. a, Toole, D., Menzies, D., et al. (2000). SeaWiFS Postlaunch Calibration and Validation Analyses, part 3. *NASA Tech. Memo.*, 11, 1–49.
- Pace, M. L., Knauer, G. a, Karl, D. M., & Martin, J. H. (1987). Primary production, new production and vertical flux in the eastern Pacific Ocean. *Nature*. <https://doi.org/Doi 10.1038/325803a0>
- Pedersen, T. F. (1983). Increased productivity in the eastern equatorial Pacific during the last glacial maximum (19,000 to 14,000 yr B.P.). *Geology*, 11, 16–19. [https://doi.org/10.1130/0091-7613\(1983\)11<16](https://doi.org/10.1130/0091-7613(1983)11<16)
- Prowse, W. G., & Maxwell, J. R. (1991). High molecular weight chlorins in a lacustrine shale. *Organic Geochemistry*, 17(6), 877–886. [https://doi.org/10.1016/0146-6380\(91\)90029-J](https://doi.org/10.1016/0146-6380(91)90029-J)
- Radke, L., Nicholas, T., Thompson, P. A., Li, J., Raes, E., Carey, M., et al. (2017). Baseline biogeochemical data from Australia's continental margin links seabed sediments to water

- column characteristics. *Marine and Freshwater Research*, *68*(9), 1593–1617. <https://doi.org/10.1071/MF16219>
- Sarmiento, J. L., & Gruber, N. (2006). *Ocean Biogeochemical Dynamics*. New Jersey: Princeton Univ. Press. <https://doi.org/10.1063/1.2754608>
- Sathyendranath, S., Cota, G., Stuart, V., Maass, H., & Platt, T. (2001). Remote sensing of phytoplankton pigments: A comparison of empirical and theoretical approaches. *International Journal of Remote Sensing*, *22*(2–3), 249–273. <https://doi.org/10.1080/014311601449925>
- Schlitzer, R. (2002). Carbon export fluxes in the Southern Ocean: Results from inverse modeling and comparison with satellite-based estimates. *Deep-Sea Research Part II: Topical Studies in Oceanography*, *49*(9–10), 1623–1644. [https://doi.org/10.1016/S0967-0645\(02\)00004-8](https://doi.org/10.1016/S0967-0645(02)00004-8)
- Schubert, C.J., Villanueva, J., Calvert, S. E., Cowie, G. L., von Rad, U., Schulz, H., et al. (1998). Stable phytoplankton community structure in the Arabian Sea over the past 200,000 years. *Nature*, *394*, 563–566. <https://doi.org/10.1038/nature01282.1>
- Schubert, Carsten J., Niggemann, J., Klockgether, G., & Ferdelman, T. G. (2005). Chlorin Index: A new parameter for organic matter freshness in sediments. *Geochemistry, Geophysics, Geosystems*, *6*(3). <https://doi.org/10.1029/2004GC000837>
- Siegel, D. A., Buesseler, K. O., Doney, S. C., Salliey, S. F., Behrenfeld, M. J., & Boyd, P. W. (2014). Global assessment of ocean carbon export by combining satellite observations and food-web models. *Global Biogeochemical Cycles*, *28*, 181–196. <https://doi.org/10.1002/2013GB004743>. Received
- Soetaert, K., Herman, P. M. J., & Middelburg, J. J. (1996). A model of early diagenetic processes from the shelf to abyssal depths. *Geochimica et Cosmochimica Acta*, *60*(6), 1019–1040. [https://doi.org/10.1016/0016-7037\(96\)00013-0](https://doi.org/10.1016/0016-7037(96)00013-0)
- Soma, Y., Tanaka, A., Soma, M., & Kawai, T. (2001). 2.8 million years of phytoplankton history in Lake Baikal recorded by the residual photosynthetic pigments in its sediment core. *Geochemical Journal*, *35*(5), 377–383. <https://doi.org/10.2343/geochemj.35.377>
- Stolpovsky, K., Dale, A. W., & Wallmann, K. (2018). A new look at the multi-G model for organic carbon degradation in surface marine sediments for coupled benthic-pelagic simulations of the global ocean, (September), 1–26. <https://doi.org/10.5194/bg-15-3391-2018>
- Stramska, M., Stramski, D., Ryszard, H., Kaczmarek, S., & Joanna, S. (2003). Bio-optical relationships and ocean color algorithms for the north polar region of the Atlantic. *Journal of Geophysical*

- Research*, 108(C5), 3143. <https://doi.org/10.1029/2001JC001195>
- Stramski, D., & Tegowski, J. (2001). Effects of intermittent entrainment of air bubbles by breaking wind waves on ocean reflectance and underwater light field. *Journal of Geophysical Research*, 106(C12), 31345–31360. <https://doi.org/10.1029/2000JC000461>
- Suess, E. (1980). Particulate organic carbon flux in the oceans—surface productivity and oxygen utilization. *Nature*, 288(5788), 260–263. <https://doi.org/10.1038/288260a0>
- Summerhayes, C. P., Kroon, D., Rosell-Mele, A., Jordan, R. W., Schrader, H.-J., Hearn, R., et al. (1995). Variability in the Benguela Current upwelling system over the past 70,000 years. *Progress in Oceanography*, 35(3), 207–251. [https://doi.org/10.1016/0079-6611\(95\)00008-5](https://doi.org/10.1016/0079-6611(95)00008-5)
- Szymczak-Zyła, M., Kowalewska, G., & Louda, J. W. (2011). Chlorophyll-a and derivatives in recent sediments as indicators of productivity and depositional conditions. *Marine Chemistry*, 125(1–4), 39–48. <https://doi.org/10.1016/j.marchem.2011.02.002>
- Volpe, G., Santoleri, R., Vellucci, V., Ribera d'Alcalá, M., Marullo, S., & D'Ortenzio, F. (2007). The colour of the Mediterranean Sea: Global versus regional bio-optical algorithms evaluation and implication for satellite chlorophyll estimates. *Remote Sensing of Environment*, 107(4), 625–638. <https://doi.org/10.1016/j.rse.2006.10.017>
- Weber, T., Cram, J. A., Leung, S. W., DeVries, T., & Deutsch, C. (2016). Deep ocean nutrients imply large latitudinal variation in particle transfer efficiency. *Proceedings of the National Academy of Sciences*, 113(31), 8606–8611. <https://doi.org/10.1073/pnas.1604414113>
- Yamanaka, Y., & Tajika, E. (1997). Role of dissolved organic matter in the marine biogeochemical cycle: Studies using an ocean biogeochemical general circulation model. *Global Biogeochemical Cycles*, 11(4), 599–612. <https://doi.org/10.1029/97GB02301>

Chapter 3

Alkenones: quantitative paleoproductivity proxy



Picture author: Reddit

3. Alkenones: quantitative paleoproductivity proxy

3.1. Introduction

Chlorophyll-*a* is the principal pigment used by all phytoplankton for carrying out photosynthesis. Its concentration in surface waters is commonly used as an indicator of phytoplankton biomass and to infer primary productivity (PP) (Davies et al., 2018). On a global scale, sea-surface chlorophyll-*a* (SSchl_a) concentration is estimated by remote sensing (Lee et al., 2015), and the first sensor that estimated global SSchl_a concentration was the Sea-viewing Wide Field-of-view Sensor (SeaWiFS), launched in 1997. Since then, other missions have taken place and their data have been merged in the GlobColour project, which combines measurements from the SeaWiFS, the MEdium Resolution Imaging Spectrometer (MERIS), the Moderate-Resolution Imaging Spectroradiometer (MODIS), and the Visible and Infrared Imager Radiometer Suite (VIIRS). Consequently, at present the available data on satellite surface ocean chlorophyll-*a* spans the last 20 years.

To infer past PP for periods before the existence satellite observation programs, on decadal to millennial time-scales, a range of organic proxies are available, which are based on the study of organic molecules that can be found in the sedimentary records (Schoepfer et al., 2015; Zhao et al., 2006). However, besides PP, many other factors, such as oxygen, temperature, ballasting effect and remineralization, are suggested to be important in controlling transfer and burial efficiency of organic matter (DeVries & Weber, 2017; Francois et al., 2002; Henson et al., 2012) and thus, organic proxies concentration. The relative weights of the factors that control the spatial variability of organic matter concentration in sediments are still unconstrained, which leads to some uncertainty on the applicability of organic matter proxies to estimate past PP. Consequently, available proxies do not yield absolute quantitative information, and only allow for the estimation of downcore relative productivity changes for a given location.

One of the most common approaches relies on the measurement of alkenones concentration in sediments (Bolton et al., 2010; Lawrence, 2006; Moreno et al., 2004; Petrick et al., 2018; Prahl et al., 1993; Rostek et al., 1997; Seki et al., 2004). These organic molecules are biomarkers of *Emiliania huxleyi*, which is the principal source of alkenones and the most abundant coccolithophore in the modern pelagic ocean (Conte et al., 1994; Marlowe et al., 1984; Rhodes et al., 1995; Schmidt et al., 2013; Volkman et al., 1980; Volkman et al., 1995). *Geophyrocapsa oceanica* and other coccolithophore species from the same genera are also considered important alkenones producers nowadays (Volkman et al., 1995). Hence, in contrast to chlorophyll-*a*, alkenones are only produced by some species of phytoplankton.

In this study, we evaluate the use of sedimentary alkenones as a quantitative proxy to estimate the global spatial variability of SSchla concentration, and hence as a tool for estimating past PP. The study is based on a global compilation of C37 di-, tri and tetraunsaturated methyl ketones (C37 alkenones) concentration in core-top sediments, and compared it with remote sensing SSchla concentration. As alkenones are exclusively produced by some phytoplankton species and the main alkenones producers are coccolithophores, we also used sea-surface particulate inorganic carbon (SSPIC) concentration, as a metric for detecting global coccolithophore blooms (Holligan et al., 1983), to better constrain the use and applicability of alkenones as a productivity proxy.

3.2. Methods

3.2.1. Alkenones abundance

Our database contains C37 alkenones concentration from 227 locations widely distributed around the global ocean across diverse biogeochemical regions as defined in (Weber et al., 2016) (Figure 14). Generally, the samples correspond to the upper 1 cm of the sediment core and approximately the 90% of them have been retrieved using devices specially designed for a minimum of disturbance of the sediment surface, i.e. box corer or multicorer. Most of the data (95% of the compilation) are obtained from previous published studies (Appendix 2), while the rest have been analysed in our laboratory following the methodology explained hereafter. Since this study combines data from several laboratories that used somewhat different methodologies, the different analytical techniques used for quantifying alkenones can be a possible concern. However, interlaboratory reproducibility of the different available methods to measure the absolute alkenone abundance in sediments was found to be 32% (Rosell-Melé et al., 2001). Consequently, greater differences between C37 alkenones concentration and remote sensing data (SSchla or SSPIC) can be evaluated in this study without concerns.

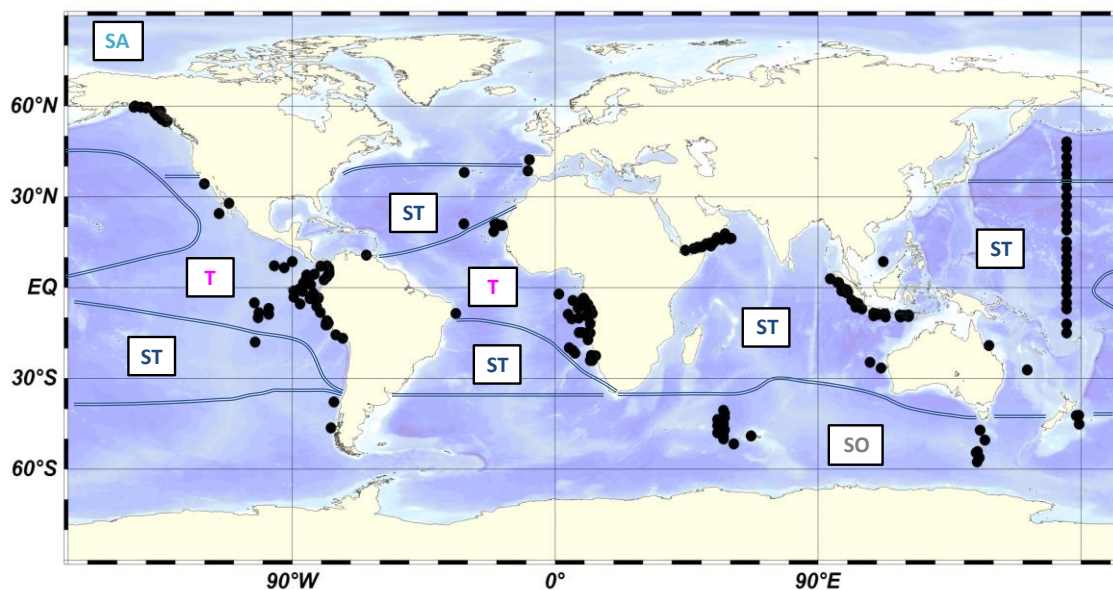


Figure 14. Global core-top sediments distribution. Lines delineate distinct biogeochemical regions defined on the basis of temperature and nutrient concentration (Weber et al., 2016). *Abbreviations: subarctic (SA), subtropics (ST), tropics (T) and Southern Ocean (SO).*

Alkenones in sediments (1-4g) were extracted using 10 mL of DCM:MeOH (3:1) (GC grade, Suprasolv) in a MARS5 microwave accelerated extraction system (CEM Corporation). Before extraction, 25 ng/ μ L of the internal standard 2-nonadecanone (Fluka, purity 0.97%) was added. During extraction the mixture was stirred continuously with a magnetic bar, while temperature was increased from ambient to 70°C over 2.5 minutes and left at this temperature for 5 minutes. After extraction, samples were left to cool down at room temperature, and the supernatants were decanted into glass tubes and centrifuged. Extracts were then dried under vacuum and fractionated through SiO₂ columns using hexane (first fraction) and dichloromethane (second fraction) as eluents. Extracts were dried again and 50 μ L of isooctane was added to the second fraction for the gas chromatography (GC) analysis.

Samples were injected in splitless mode in a GC column (Agilent 19091Z-436 column, 60m \times 250 μ m \times 0.25 μ m) with a flow rate of 1.5 mL/min. The GC method consists of 2 ramps, the first one from 80°C to 120°C with a temperature rate of 30 °C/min, followed by a second ramp that increases temperature at 6°C/min until 320°C. Then, the conditions were held during 21 minutes and the signal was detected by a flame ionization detector at 320°C (Agilent Technologies 7820A GC System).

3.2.2. SSchla and SSPIC concentration

SSchla and SSPIC concentration values for every location were extracted from merged global-scale matrixes of the Globcolour Project (<http://globcolour.info>), which contain monthly data for

the last 20 years. To obtain both SSchla and SSPIC concentration for the last 20 years, we added the concentrations from September 1997 to December 2017 for every location. GlobColour data used in this study has been developed, validated, and distributed by ACRI-ST, France. The sensors used for estimating SSPIC concentration are as follows: SeaWiFS (1997-2010), MODIS (2002-2017) and VIIRS (2012-2017). The previous sensors plus MERIS (2002-2012) have been used to estimate SSchla concentration. The spatial resolution for both parameters is $1/24^\circ$ (4.63 km at the equator). The algorithms used for SSchla concentration are OC4v5 for SeaWiFS, OC4Me for MERIS, and OC3v5 for MODIS and VIIRS (O'Reilly et al., 2000). The SSPIC concentration algorithm is a hybrid of two independent approaches described in (Balch et al., 2005) and (Gordon et al., 2001).

A number of factors might affect our comparison between remote sensing and sedimentary data, including the limitation of detecting SSchla and SSPIC in the deep water column (Cullen, 1982; Huisman et al., 2006), lateral transport of organic matter and the different timescales between remote sensing observations (20 years) and sediment (c.a. 71 years). The age range of sediment samples have been calculated from the sedimentation rate average of all sediments (14 cm/ka) by using the map published in (Dunne et al., 2012).

However, one of the main sources of uncertainty of the remote sensing data might be the poor accuracy of satellite retrievals in some specific oceanic regions, where the optical and biological properties are complex (Blondeau-Patissier et al., 2014; Brown & Yoder, 1994). In those regions, global standard algorithms used in global scale studies, such as this one, might provide biased estimations. Some of the factors that affect the properties of the surface waters are as follows: coloured dissolved organic matter, radiance-absorbing aerosols, phytoplankton species diversity, suspended sediments, clouds, ice, sun glint, and navigation/time space mismatches (Claustre & Maritoner, 2003; Dierssen & Smith, 2000; Sathyendranath et al., 2001; Volpe et al., 2007). Furthermore, desert dust (Claustre et al., 2002) and bubbles (Stramski & Tegowski, 2001) make the water appear greener. It is also important to note that although the main alkenones producers are coccolithophores, there are also other organisms that produce them. Besides, not every coccolithophore organism produces alkenones. Consequently, the correlation between SSPIC and C37 alkenones concentration might be impacted by this mismatch between alkenones and coccolithophores.

3.3. Results

3.3.1. Quantifying SSchla from alkenones

To study the role of C37 alkenones in tracking global SSchla concentration, we appraised their global scale correlation in Figure 15. Our samples cover several oceanic biogeochemical regions, which are defined following the classification described in (Weber et al., 2016), that is based on temperature, phytoplankton community and nutrient concentration. We obtained a linear correlation between the logarithms of C37 alkenones and SSchla concentration with a coefficient of determination (R^2) of 0.45 and a root mean square (RMS) log error of 45%.

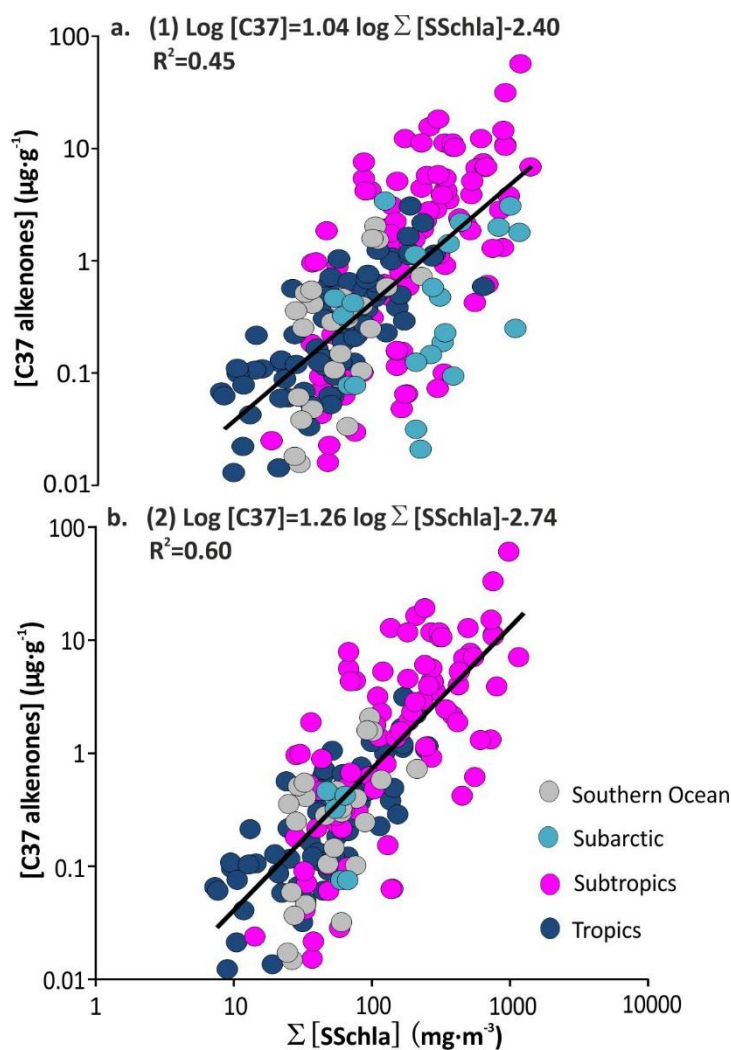


Figure 15. Global correlations between sedimentary C37 alkenones concentration and the sum of sea-surface chlorophyll-*a* (SSchla) concentration from 1997 to 2017. **a.** includes the whole compilation, and **b.** includes regions presenting RMS log errors lower than 31% between remote sensing and *in situ* SSchla. Samples are classified by biogeochemical regions as defined in Figure 14.

In order to minimize the uncertainty derived from the use of SSchla global standard algorithms, we only considered regions reported to present RMS log errors lower than 31% between remote sensing and *in situ* SSchla concentration, as this threshold has been used to define well-performing regions in global and regional remote sensing SSchla evaluation studies (Gregg & Casey, 2004). Consequently, the North Atlantic (Gregg & Casey, 2004; Mendonça et al., 2010; Stramska et al., 2003) and the Gulf of Alaska (Waite & Mueter, 2013), which present RMS log errors higher than 31%, are not included in Figure 15 b. Nor the western South American margin, as the error of this region has not been thoroughly studied. Although the equatorial Atlantic presents a RMS log error of 48%, it drops to 23% when removing samples located offshore of the north-eastern coast of South America (Gregg & Casey, 2004), as our samples are not located in this region, we included samples from the equatorial Atlantic in Figure 15 b. The correlation obtained in Figure 15 b between C37 alkenones and SSchla concentration shows that the spatial variability in C37 alkenones concentration can explain 60% of SSchla concentration variability ($R^2=0.60$) with a RMS log error of 38% (Table 2). Hence, changes in C37 alkenones concentration are mainly related to changes in SSchla concentration.

Equation	a	b	R ²	RMS log error (%)	n
1	1.04	-2.40	0.45	53	226
2	1.26	-2.74	0.60	38	194
3	1.01	-2.35	0.59	31	75
4	1.24	-2.62	0.49	46	88
5	1.32	-2.95	0.33	35	26
6	0.35	0.28	0.03	212	226
7	0.34	0.32	0.03	209	211

Table 2. Coefficients and errors of alkenones equations. $\text{Log}[C37]=a\text{-log}\sum[\text{SSchla}]+b$. *Abbreviations: coefficient of determination (R^2), root-mean square logarithmic error (RMS log error), number of samples (n).*

The global compilation represented in Figure 15 b (C37 alkenones and SSchla concentration) englobes different oceanic biogeochemical regions that present different ranges of PP (mainly due to differences in nutrient circulation, solar irradiance, temperature and phytoplankton community) and organic export efficiencies from the sea-surface to the surface sediment (Weber et al., 2016). In order to study the possible variations that the different oceanic biogeochemical regions might reflect in the correlation between C37 alkenones and SSchla concentration, we obtained a specific correlation for each region described in (Weber et al., 2016) (Figure 14 and

Table 2). The defined regions are as follows: the tropics, the subtropics, the subarctic and the Southern Ocean. Note that the correlation for the subarctic region has been not established due to lack of data. The subtropics show the lower RMS log error (31%) and is the region that can explain more SSchla concentration variability (59%). The tropics present the higher RMS log error (46%), with a coefficient of determination of 0.49, and the Southern Ocean is the region that can explain less SSchla concentration variability (33%), with a log RMS error of 35%. However, no significant differences between oceanic biogeochemical regional correlations were found, as it is shown in Figure 16.

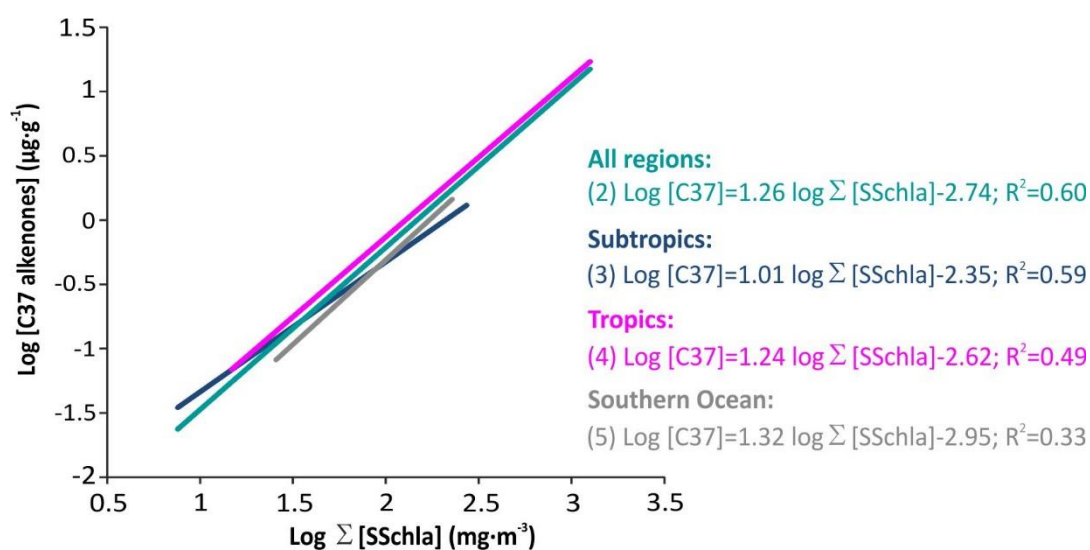


Figure 16. Regional correlations between sedimentary alkenones concentration and the sum of sea-surface chlorophyll-*a* (SSchla) concentration from 1997 to 2017. Different colours for lines and text indicate the evaluated biogeochemical regions, which are defined in Figure 14.

3.3.2. Quantifying SSPIC from alkenones

The main alkenones producers are coccolithophores (Conte et al., 1994; Marlowe et al., 1984; Rhodes et al., 1995; Schmidt et al., 2013; Volkman et al., 1980; Volkman et al., 1995) and the most common parameter for detecting global coccolithophore blooms is remote sensing SSPIC (Brown & Yoder, 1994; Kondrik et al., 2017; Moore et al., 2012; Neukermans et al., 2018; Sadeghi et al., 2012). Therefore, to better assess the use of alkenones as a PP proxy we also study the global correlation between the logarithms of C37 alkenones and SSPIC concentration (Figure 17). Samples were classified by oceanic biogeochemical regions described in (Weber et al., 2016), as in the case of C37 alkenones and SSchla correlation. We obtained a p-value of 0.01 (95% confidence interval), which indicates that exist a significant correlation between C37 alkenones and SSPIC concentration. However, a R^2 of 0.03 and RMS log error of 212% indicate a low degree of correlation.

Similarly, to the C37 alkenones and SSchla correlation, we excluded specific regions where the global standard algorithms are reported to not reflect SSPIC concentration in agreement to *in situ* SSPIC measurements, for reducing the uncertainty associated with the use of SSPIC global standard algorithms in this study. However, we found much less studies that validate remote sensing SSPIC than SSchla estimations. Remote sensing SSPIC were reported to be lower than the average shipboard value in the Pacific equatorial divergence province (Balch et al., 2005) and greatly overestimated in Antarctic waters near the south of Australia (Trull et al., 2018). Consequently, we excluded data from these two sites in Figure 17 b. The p-value obtained for the samples in Figure 17 b was 0.01 (95% confidence interval), which indicates correlation between C37 alkenones and SSPIC concentration. However, a R^2 of 0.03 and a RMS log error of 209% indicate a low degree of correlation (Table 2). Hence, variability in C37 alkenones concentration only can explain 3% of SSPIC concentration variability, with a RMS log error of 209%.

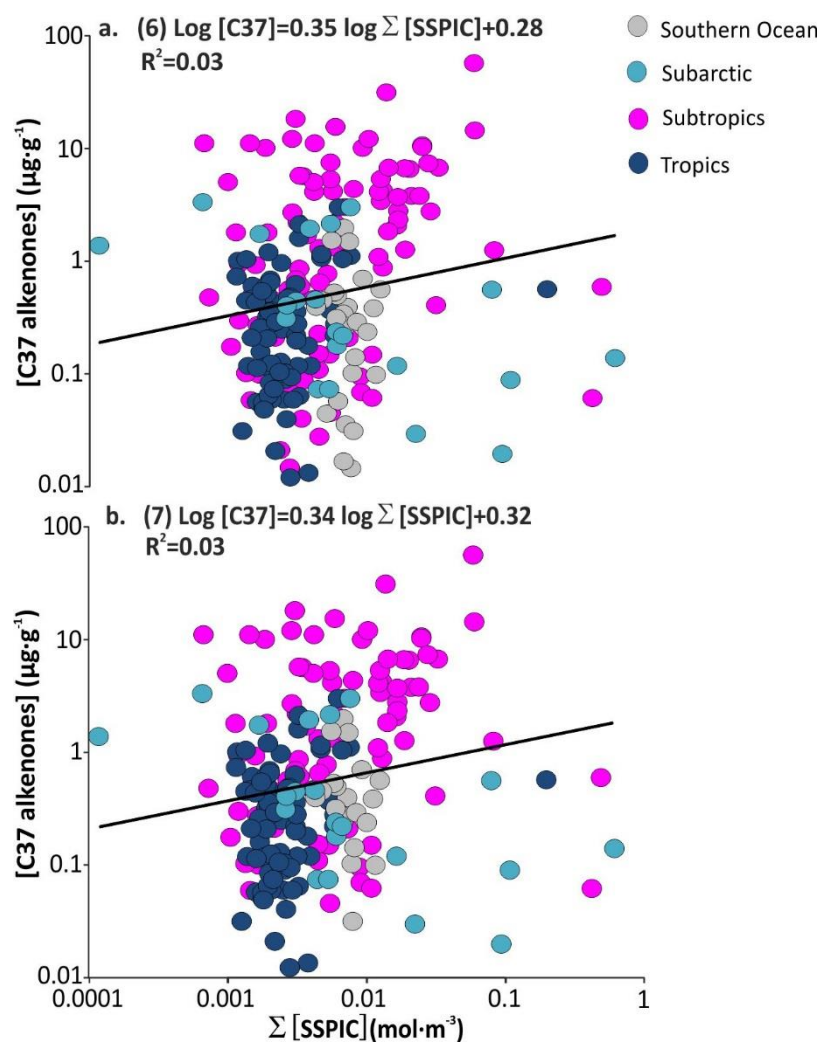


Figure 17. Global correlations between sedimentary alkenones concentration and the sum of sea-surface particulate inorganic carbon (SSPIC) concentration from 1997 to 2017. **a.** includes the whole compilation, and **b.** includes regions presenting RMS log errors lower than 31% between remote sensing and *in situ* SSchla. Samples are classified by biogeochemical regions as defined in Figure 14.

The global correlation represented in Figure 17 englobes different oceanic biogeochemical regions that are related to different ranges of PP and organic matter export efficiencies, as in the case of the global correlation between C37 alkenones and SSchl_a concentration. In order to study the SSPIC variability that can be explained by variations in C37 alkenones concentration, we followed the same procedure as in the case of C37 alkenones and SSchl_a correlation, and studied the correlation between C37 alkenones and SSchl_a concentration for each oceanic biogeochemical region defined in (Weber et al., 2016). None of the regions shows a significant correlation (p -value >0.05). Hence, changes in the SSPIC concentration of any of the oceanic biogeochemical regions defined in (Weber et al., 2016) cannot be explained by changes in C37 alkenones concentration estimated from the corresponding region.

3.4. Discussion

3.4.1. Alkenones as a quantitative proxy for past PP

Alkenones abundance has been used in many studies as a proxy for past PP. For instance, alkenones concentration were used to qualitatively reconstruct past PP variations in the Sea of Okhotsk over the last 30 kyr (Seki et al., 2004), in the Western Mediterranean for 48,000-28,000 years before present (Moreno et al., 2004) and in the southeastern Arabian Sea for the study of the Indian monsoon during previous climatic cycles (Rostek et al., 1997). PP reconstructions derived from C37 alkenones concentration proxy assume a linear relationship between PP and C37 alkenones abundance in sediment. However, besides PP, other factors such as oxygen, temperature, ballasting effect and remineralization control export PP and burial efficiencies (DeVries & Weber, 2017; Francois et al., 2002; Henson et al., 2012) and, consequently sedimentary C37 alkenones abundance.

The global correlation between C37 alkenones and SSchl_a concentration confirms there is a linear relationship between these two variables (Figure 15 b). This study also reveals that SSchl_a concentration is the dominant factor controlling C37 alkenones abundance in sediment, being the latter able to explain 60% of the global SSchl_a concentration spatial variability (Figure 15 b). Therefore, we validate the use of sedimentary alkenones as a proxy to estimate global spatial variability of SSchl_a, and thus, as a tool for estimating past PP.

However, alkenones concentration has been considered as an exclusive coccolithophore PP proxy and information derived from alkenones concentration is generally interpreted as coccolithophore PP (Higginson & Altabet, 2004; Pelejero et al., 1999; Petrick et al., 2018; Seki et al., 2004). In contrast, Bolton et al. (2010) suggested that in upwelling tropic areas, C37 alkenones

concentration tracks PP not only from coccolithophores, but also from the wider phytoplankton community. Later, Bolton et al. (2011) corroborate the last interpretation at two more sites: ODP Site 982 in the North Atlantic and ODP Site 846 in the eastern tropical Pacific. Our results are in agreement with those from (Bolton et al., 2010, 2011) and shows C37 alkenones can be interpreted as a proxy for total PP in very different biogeochemical conditions and thus, independently from the dominated phytoplankton community (Figure 15 b).

We also studied the use of C37 alkenones concentration proxy particularly in oligotrophic areas, as it was suggested to not expect a relationship between C37 alkenones concentration and total PP because the alkenone-synthesising coccolithophores in such regimes constitute a small proportion of the coccolithophore population (Bolton et al., 2010). We calculated the RMS log error in the global correlation considering only samples located in oligotrophic (SSchla annual average concentration $<0.1\text{mg}\cdot\text{m}^{-3}$) and no oligotrophic areas (Figure A4, Appendix 1). The RMS log error considering only oligotrophic areas (33%) is lower than both, considering only no oligotrophic areas (39%) and all samples (38%). Hence, although only 9% of our samples correspond to oligotrophic areas, our results suggest C37 alkenones concentration can be interpreted as a proxy for total PP in a global scale, including oligotrophic areas.

Moreover, in contrast to current available paleoproductivity proxies, the linear relationship obtained from our global correlation between C37 alkenones and SSchla concentration (Figure 15) will permit to obtain absolute values of SSchla concentration in past periods with a RMS log error of 38% (Table 1) and thus, quantitatively estimate past PP. Therefore, besides relative past PP changes through downcore, past PP changes will be able for comparison between different locations at any site in the global ocean.

Obtaining a global correlation between C37 alkenones and SSchla concentration (Figure 15) suggests a proportional organic matter flux rate from sea-surface to sediments over different biogeochemical regions in the global ocean. Previous studies indicate there are no regional differences in the water column organic matter fluxes (Lampitt & Antia, 1997; Martin et al., 1987; Suess, 1980), but later studies found spatial variability in the export efficiency of surface biomass to the deep ocean (Henson et al., 2012; Lam et al., 2011; Marsay et al., 2015; Weber et al., 2016). The correlations between C37 alkenones and SSchla concentration obtained for the different oceanic biogeochemical regions defined in (Weber et al., 2016) were no significantly different as it is shown in Figure 16. Hence, our data support the results obtained in (Lutz et al., 2002), which showed that spatial variability in the vertical flux of particulate organic carbon decreases with increasing water column depth. Our results are also in agreement with (Jahnke, 1996), where the

author concluded the proportion of primary production that reaches the deep sea does not vary greatly with latitude by extrapolating data from the North Atlantic.

3.4.2. The relevant role of photosynthetic picoeukaryotes (PPE) in the global carbon export

Global carbon export to sediments was recognised to be dominated by large phytoplankton, such as diatoms (Sancetta et al., 1989; Smetacek, 1985), and picophytoplankton, which basically englobes cyanobacteria and photosynthetic picoeukaryotes (PPE), was claimed to not contribute significantly to carbon export because of their small size (Michaels & Silver, 1988). Nevertheless, more recent studies enhanced the role of picoplankton in sedimentary carbon fluxes. For instance, massive picoplankton sedimentation in east of New Zealand (Waite et al., 2000), and picophytoplankton export carbon fluxes dominance were found in the eastern equatorial Pacific (Richardson et al., 2004) and in the Arabian sea (Richardson et al., 2006). Later studies showed that the downward flux of organic carbon via small particles often constitute the bulk of the total particulate organic carbon flux in the North Atlantic (Giering et al., 2016), and the export in the Norwegian Sea was most likely due to small particles and contributed to long-term carbon sequestration (Dall'Olmo & Mork, 2014). Therefore, global carbon flux seems to be dominated by picoplankton, either cyanobacteria or PPE.

As mainly alkenones producers (*Emiliania huxleyi* and *Geophyrocapsa oceanica*) are PPE, our results are in agreement with later studies, and suggest PPE as the dominant phytoplankton in terms of global carbon sequestration and burial in the sea-floor. Figure 15 shows a global linear correlation between SSchl_a and sedimentary C37 alkenones concentration. These results are not surprising as although cyanobacteria dominates phytoplankton abundance in the ocean (Worden et al., 2004; Zubkov et al., 2000), PPE dominate biomass (Liu et al., 2009; Teira et al., 2005).

Our results also indicate that PPE export contribution is proportional to total PP at global scale (Figure 15). These results can be explained by the high contribution to total PP by PPE, which has been found to be more than half in several oceanic regions. For instance, in the North Atlantic (68%) (Li, 1995), the southern California Bight (76%) (Worden et al., 2004), the eastern North Atlantic subtropical gyre (54%) (Teira et al., 2005), the southern Bay of Biscay (51%) (Morán, 2007) and the South East Pacific Ocean (>60%) (Rii et al., 2016). Besides, our data are consistent with results obtained in (Richardson & Jackson, 2007) that show the contribution of picoplankton to export is proportional to their contribution to PP. Therefore, the study of C37 alkenones abundance in sediments gives information not only about past PP in the sea-surface, but also about the soft-tissue pump.

3.4.3. Alkenones and SSPIC for studying past PP and the global carbonate pump

Main alkenones producers are coccolithophores (*Emiliana huxleyi* and *Geophyrocapsa oceanica*) (Conte et al., 1994; Marlowe et al., 1984; Rhodes et al., 1995; Schmidt et al., 2013; Volkman et al., 1980; Volkman et al., 1995), which are covered by CaCO₃ plates or coccoliths. Hence, we studied the global carbonate pump by correlating our global compilation of C37 alkenones concentration with remote sensing SSPIC concentration, which is the most common parameter for detecting global coccolithophore blooms (Brown & Yoder, 1994; Kondrik et al., 2017; Moore et al., 2012; Neukermans et al., 2018; Sadeghi et al., 2012). In contrast to SSPIC, SSchla is representative of total phytoplankton community. Hence, we also used SSPIC concentration for better assessing the use of C37 alkenones concentration as a paleoproductivity proxy.

Our results indicate correlation between C37 alkenones and SSPIC concentration (p-value=0.01), but the variability in C37 alkenones can only explain 3% of SSPIC variability, with a RMS log error of 209% (Figure 17 and Table 2). Therefore, the study of C37 alkenones abundance does not provide information about coccolithophore fluxes from sea-surface to sediments and thus, neither about the global carbonate pump nor past PP changes.

The poor correlation found between C37 alkenones and SSPIC concentration might be explained by the fact that in latter stages of bloom, several hundred detached coccoliths are present for each live *Emiliana huxleyi* cell, in addition to empty coccospheres (van der Wal et al., 1995). Actually, the increase in reflectance observed by satellite was attributable specifically to light scatter by detached coccoliths rather than cells of *Emiliana huxleyi* (Holligan et al., 1993). Therefore, SSPIC concentration seems not to be a good indicator of coccolithophore PP, as PP is carried out by living cells rather than detached coccoliths. In contrast, chlorophyll-*a* is produced by living cells during photosynthesis, which makes possible to estimate PP from SSchla (Davies et al., 2018). An alternative way to estimate coccolithophore PP could be to study the coccospheres in the sea-surface rather than SSPIC. Although in the latter stages of a coccolithophore bloom there would be some empty coccospheres that would not contribute to PP, coccospheres flux profile, in contrast to coccoliths, were found similar to alkenones flux profiles (Rosell-Melé et al., 2000). However, remote sensing techniques, which cannot discern between coccospheres and coccoliths, are needed for global scale and decadal time studies, such as this one.

3.5. Conclusions

In this study, we validate the use of C37 alkenones abundance as a proxy to estimate global spatial variability of SSchla concentration, and thus, as a tool for estimating past PP changes. In a global scale, C37 alkenones abundance can be interpreted as a proxy for total PP and thus, independently from the dominated phytoplankton community. Our data suggest C37 alkenones concentration proxy can also be used to infer past PP changes in oligotrophic areas.

In contrast to current available paleoproductivity proxies, the global linear correlation obtained in this study between C37 alkenones and SSchla concentration, will permit to obtain absolute values of SSchla concentration in past periods and thus, quantitatively estimate past PP. Therefore, besides relative past PP changes through downcore, past PP changes will be able for comparison between different locations at any site in the global ocean. The global correlation between C37 alkenones and SSchla concentration also suggest that spatial variability of surface organic matter is homogenised during export through the water column by physical and biogeochemical processes, driving to a spatially constant carbon flux from sea-surface to sediments.

As alkenones are mainly produced by PPE, our data suggest PPE as the dominant phytoplankton in terms of global carbon sequestration and burial in the sea-floor. Our results also indicate that PPE export contribution is proportional to total PP at global scale, which can be explained by the high contribution to total PP by PPE (>50% of total PP). Therefore, the study of C37 alkenones abundance in sediments gives information not only about PP in the sea-surface, but also about the soft-tissue pump.

Besides, the study of C37 alkenones abundance and remote sensing SSPIIC concentration does not provide information about coccolithophore fluxes from sea-surface to sediments and thus, neither about the global carbonate pump nor changes in coccolithophore past PP. Therefore, remote sensing SSPIIC concentration seems not to be a good indicator of coccolithophore PP, probably because it is associated with detached coccoliths rather than living cells. In contrast, chlorophyll-*a* is produced by living cells during photosynthesis, which makes possible to estimate PP from remote sensing SSchla.

3.6. References

- Balch, W. M., Gordon, H. R., Bowler, B. C., Drapeau, D. T., & Booth, E. S. (2005). Calcium carbonate measurements in the surface global ocean based on Moderate-Resolution Imaging Spectroradiometer data. *Journal of Geophysical Research C: Oceans*, 110(7), 1–21. <https://doi.org/10.1029/2004JC002560>
- Blondeau-Patissier, D., Gower, J. F. R., Dekker, A. G., Phinn, S. R., & Brando, V. E. (2014). A review

- of ocean color remote sensing methods and statistical techniques for the detection, mapping and analysis of phytoplankton blooms in coastal and open oceans. *Progress in Oceanography*, 123, 123–144. <https://doi.org/10.1016/j.pocean.2013.12.008>
- Bolton, C. T., Lawrence, K. T., Gibbs, S. J., Wilson, P. A., Cleaveland, L. C., & Herbert, T. D. (2010). Glacial-interglacial productivity changes recorded by alkenones and microfossils in late Pliocene eastern equatorial Pacific and Atlantic upwelling zones. *Earth and Planetary Science Letters*, 295(3–4), 401–411. <https://doi.org/10.1016/j.epsl.2010.04.014>
- Bolton, C. T., Lawrence, K. T., Gibbs, S. J., Wilson, P. A., & Herbert, T. D. (2011). Biotic and geochemical evidence for a global latitudinal shift in ocean biogeochemistry and export productivity during the late Pliocene. *Earth and Planetary Science Letters*, 308(1–2), 200–210. <https://doi.org/10.1016/j.epsl.2011.05.046>
- Brown, C. W., & Yoder, J. A. (1994). Cocolithophorid blooms in the global ocean. *Journal of Geophysical Research*, 99(C4), 7467–7482. <https://doi.org/10.1029/93JC02156>
- Claustre, H., & Maritoner, S. (2003). The Many Shades of Ocean Blue. *Ocean Science*, 302(5650), 1514–1515.
- Claustre, H., Morel, A., Hooker, S. B., Babin, M., Antoine, D., Oubelkheir, K., et al. (2002). Is desert dust making oligotrophic waters greener? *Geophysical Research Letters*, 29(10), 107-1-107-4. <https://doi.org/10.1029/2001GL014056>
- Conte, M. H., Volkman, J. K., & Eglinton, G. (1994). Lipid biomarkers of the Prymnesiophyceae. *The Haptophyte Algae*, 51(January), 351–377.
- Cullen, J. J. (1982). The deep chlorophyll maximum: Comparing vertical profiles of chlorophyll a. *Canadian Journal of Fisheries and Aquatic Sciences*, 39, 791–803.
- Dall’Olmo, G., & Mork, K. A. (2014). Carbon export by small particles in the Norwegian Sea. *Geophysical Research Letters*, 1–6. <https://doi.org/10.1002/2014GL059244.1>.
- Davies, C. H., Ajani, P., Armbrrecht, L., Atkins, N., Baird, M. E., Beard, J., et al. (2018). A database of chlorophyll a in Australian waters. *Scientific Data*, 5, 1–8. <https://doi.org/10.1038/sdata.2018.18>
- DeVries, T., & Weber, T. (2017). The export and fate of organic matter in the ocean: New constraints from combining satellite and oceanographic tracer observations. *Global Biogeochemical Cycles*, 31(3), 535–555. <https://doi.org/10.1002/2016GB005551>
- Dierssen, H. M., & Smith, R. C. (2000). Bio-optical properties and remote sensing ocean color algorithms for Antarctic Peninsula waters, *105*(1999), 26301–26312.

- Dunne, J. P., Hales, B., & Toggweiler, J. R. (2012). Global calcite cycling constrained by sediment preservation controls. *Global Biogeochemical Cycles*, *26*(3), 1–14.
<https://doi.org/10.1029/2010GB003935>
- Francois, R., Honjo, S., Krishfield, R., & Manganini, S. (2002). Factors controlling the flux of organic carbon to the bathypelagic zone of the ocean. *Global Biogeochem. Cycles*, *16*(4), 1087.
<https://doi.org/10.1029/2001gb001722>
- Giering, S. L. C., Sanders, R., Martin, A. P., Lindemann, C., Möller, K. O., Daniels, C. J., et al. (2016). High export via small particles before the onset of the North Atlantic spring bloom. *Journal of Geophysical Research: Oceans*, *121*, 2268–2285.
<https://doi.org/10.1002/2016JC011882>.Received
- Gordon, R., Boynton, G. C., Balch, W. M., Harbour, D. S., Smyth, T. J., & Bay, W. B. (2001). Retrieval of Coccolithophore from SeaWiFS Imagery Calcite Concentration radiance, *28*(8), 1587–1590.
- Gregg, W. W., & Casey, N. W. (2004). Global and regional evaluation of the SeaWiFS chlorophyll data set. *Remote Sensing of Environment*, *93*(4), 463–479.
<https://doi.org/10.1016/j.rse.2003.12.012>
- Henson, S. A., Sanders, R., & Madsen, E. (2012). Global patterns in efficiency of particulate organic carbon export and transfer to the deep ocean. *Global Biogeochemical Cycles*, *26*(1), 1–14.
<https://doi.org/10.1029/2011GB004099>
- Higginson, M. J., & Altabet, M. A. (2004). Initial test of the silicic acid leakage hypothesis using sedimentary biomarkers. *Geophysical Research Letters*, *31*(18), 4–7.
<https://doi.org/10.1029/2004GL020511>
- Holligan, P. M., Viollier, M., Harbour, D. S., Camus, P., & Champagne-Philippe, M. (1983). Satellite and ship studies of coccolithophore production along a continental shelf edge. *Nature*, *304*(5924), 339–342. <https://doi.org/10.1038/304339a0>
- Holligan, Patrick M, Fcrrmindcz, E., Balch, W. M., Boyd, P., Peter, H., Finch, M., et al. (1993). A biogeochemical study of the coccolithophore, *Emiliana huxleyi*, in the North Atlantic, *7*(4), 879–900.
- Huisman, J., Pham Thi, N. N., Karl, D. M., & Sommeijer, B. (2006). Reduced mixing generates oscillations and chaos in the oceanic deep chlorophyll maximum. *Nature*, *439*(7074), 322–325. <https://doi.org/10.1038/nature04245>
- Jahnke, R. A. (1996). The global ocean flux of particulate organic carbon : Areal distribution and magnitude, *1*(1), 71–88.

- Kondrik, D., Pozdnyakov, D., & Pettersson, L. (2017). Particulate inorganic carbon production within *E. huxleyi* blooms in subpolar and polar seas: a satellite time series study (1998–2013). *International Journal of Remote Sensing*, *38*(22), 6179–6205.
<https://doi.org/10.1080/01431161.2017.1350304>
- Lam, P. J., Doney, S. C., & Bishop, J. K. B. (2011). The dynamic ocean biological pump: Insights from a global compilation of particulate organic carbon, CaCO₃, and opal concentration profiles from the mesopelagic. *Global Biogeochemical Cycles*, *25*(3), 1–14.
<https://doi.org/10.1029/2010GB003868>
- Lampitt, R. S., & Antia, A. N. (1997). Particle flux in deep seas: Regional characteristics and temporal variability. *Deep-Sea Research Part I: Oceanographic Research Papers*, *44*(8), 1377–1403.
[https://doi.org/10.1016/S0967-0637\(97\)00020-4](https://doi.org/10.1016/S0967-0637(97)00020-4)
- Lawrence, K. T. (2006). Evolution of the Eastern Tropical Pacific Through Plio-Pleistocene Glaciation. *Science*, *312*(5770), 79–83. <https://doi.org/10.1126/science.1120395>
- Lee, Z., Marra, J., Perry, M. J., & Kahru, M. (2015). Estimating oceanic primary productivity from ocean color remote sensing: A strategic assessment. *Journal of Marine Systems*, *149*, 50–59.
<https://doi.org/10.1016/j.jmarsys.2014.11.015>
- Li, W. K. W. (1995). Composition of ultraphytoplankton in the central North Atlantic, *122*, 1–8.
- Liu, H., Probert, I., Uitz, J., Claustre, H., Aris-Brosou, S., Frada, M., et al. (2009). Extreme diversity in noncalcifying haptophytes explains a major pigment paradox in open oceans. *Proceedings of the National Academy of Sciences*, *106*(31), 12803–12808.
<https://doi.org/10.1073/pnas.0905841106>
- Lutz, M., Dunbar, R., & Caldeira, K. (2002). Regional variability in the vertical flux of particulate organic carbon in the ocean interior. *Global Biogeochemical Cycles*, *16*(3), 11-1-11–18.
<https://doi.org/10.1029/2000GB001383>
- Marlowe, I. T., Green, J. C., Neal, A. C., Brassell, S. C., Eglinton, G., & Course, P. A. (1984). Long chain (n-c37-c39) alkenones in the prymnesiophyceae. distribution of alkenones and other lipids and their taxonomic significance. *British Phycological Journal*, *19*(3), 203–216.
<https://doi.org/10.1080/00071618400650221>
- Marsay, C. M., Sanders, R. J., Henson, S. A., Pabortsava, K., Achterberg, E. P., & Lampitt, R. S. (2015). Attenuation of sinking particulate organic carbon flux through the mesopelagic ocean. *Proceedings of the National Academy of Sciences*, *112*(4), 1089–1094.
<https://doi.org/10.1073/pnas.1415311112>

- Martin, J. H., Knauer, G. A., Karl, D. M., & Broenkow, W. W. (1987). VERTEX: carbon cycling in the northast Pacific, *34*(2), 267–285.
- Mendonça, A., Martins, A., Figueiredo, M., Bashmachnikov, I., Couto, A., Lafon, V., & Aristegui, J. (2010). Evaluation of ocean color and sea surface temperature sensors algorithms using in situ data: a case study of temporal and spatial variability on two northeast Atlantic seamounts. *Journal of Applied Remote Sensing*, *4*(1), 043506.
<https://doi.org/10.1117/1.3328872>
- Michaels, A. F., & Silver, M. W. (1988). Primary production, sinking fluxes and the microbial food web. *Deep-Sea Research*, *35*(4), 473–490.
- Moore, T. S., Dowell, M. D., & Franz, B. A. (2012). Detection of coccolithophore blooms in ocean color satellite imagery: A generalized approach for use with multiple sensors. *Remote Sensing of Environment*, *117*, 249–263. <https://doi.org/10.1016/j.rse.2011.10.001>
- Morán, X. A. G. (2007). Annual cycle of picophytoplankton photosynthesis and growth rates in a temperate coastal ecosystem: A major contribution to carbon fluxes. *Aquatic Microbial Ecology*, *49*(3), 267–279. <https://doi.org/10.3354/ame01151>
- Moreno, A., Cacho, I., Canals, M., Grimalt, J. O., & Sanchez-Vidal, A. (2004). Millennial-scale variability in the productivity signal from the Alboran Sea record, Western Mediterranean Sea. *Palaeogeography, Palaeoclimatology, Palaeoecology*, *211*(3–4), 205–219.
<https://doi.org/10.1016/j.palaeo.2004.05.007>
- Neukermans, G., Oziel, L., & Babin, M. (2018). Increased intrusion of warming Atlantic water leads to rapid expansion of temperate phytoplankton in the Arctic. *Global Change Biology*, *24*(6), 2545–2553. <https://doi.org/10.1111/gcb.14075>
- O'Reilly, J. E., Maritorena, S., O'Brien, M. C., Siegel, D. a, Toole, D., Menzies, D., et al. (2000). SeaWiFS Postlaunch Calibration and Validation Analyses, part 3. *NASA Tech. Memo.*, *11*, 1–49.
- Pelejero, C., Grimalt, J. O., Sarnthein, M., Wang, L., & Flores, J. A. (1999). Molecular biomarker record of sea surface temperature and climatic change in the South China Sea during the last 140,000 years. *Marine Geology*, *156*(1–4), 109–121. [https://doi.org/10.1016/S0025-3227\(98\)00175-3](https://doi.org/10.1016/S0025-3227(98)00175-3)
- Petrick, B., McClymont, E. L., Littler, K., Rosell-Melé, A., Clarkson, M. O., Maslin, M., et al. (2018). Oceanographic and climatic evolution of the southeastern subtropical Atlantic over the last 3.5 Ma. *Earth and Planetary Science Letters*, *492*, 12–21.
<https://doi.org/10.1016/j.epsl.2018.03.054>

- Prahl, F. G., Collier, R. B., Dymond, J., Lyle, M., & Sparrow, M. A. (1993). A biomarker perspective on prymnesiophyte productivity in the northeast pacific ocean. *Deep-Sea Research Part I*, *40*(10), 2061–2076. [https://doi.org/10.1016/0967-0637\(93\)90045-5](https://doi.org/10.1016/0967-0637(93)90045-5)
- Rhodes, L. L., Peake, B. M., MacKenzie, A. L., Simon, M., & Edwards, A. R. (1995). Coccolithophores *Gephyrocapsa oceanica* and *Emiliania huxleyi* (Prymnesiophyceae = Haptophyceae) in New Zealand's coastal waters: Characteristics of blooms and growth in laboratory culture. *New Zealand Journal of Marine and Freshwater Research*, *29*(3), 345–357. <https://doi.org/10.1080/00288330.1995.9516669>
- Richardson, T. L., & Jackson, G. A. (2007). Small Phytoplankton and Carbon Export from the Surface Ocean. *Science*, (February), 838–840. <https://doi.org/10.1126/science.1133471>
- Richardson, T. L., Jackson, G. A., Ducklow, H. W., & Roman, M. R. (2004). Carbon fluxes through food webs of the eastern equatorial Pacific: An inverse approach. *Deep-Sea Research Part I: Oceanographic Research Papers*, *51*(9), 1245–1274. <https://doi.org/10.1016/j.dsr.2004.05.005>
- Richardson, T. L., Jackson, G. A., Ducklow, H. W., & Roman, M. R. (2006). Spatial and seasonal patterns of carbon cycling through planktonic food webs of the Arabian Sea determined by inverse analysis. *Deep-Sea Research Part II: Topical Studies in Oceanography*, *53*(5–7), 555–575. <https://doi.org/10.1016/j.dsr2.2006.01.015>
- Rii, Y. M., Duhamel, S., Bidigare, R. R., Karl, D. M., Repeta, D. J., & Church, M. J. (2016). Diversity and productivity of photosynthetic picoeukaryotes in biogeochemically distinct regions of the South East Pacific Ocean. *Limnology and Oceanography*, *61*(3), 806–824. <https://doi.org/10.1002/lno.10255>
- Rosell-Melé, A., Comes, P., Müller, P. J., & Ziveri, P. (2000). Alkenone fluxes and anomalous U37/(K)' values during 1989-1990 in the Northeast Atlantic (48°N 21°W). *Marine Chemistry*, *71*(3–4), 251–264. [https://doi.org/10.1016/S0304-4203\(00\)00052-9](https://doi.org/10.1016/S0304-4203(00)00052-9)
- Rosell-Melé, A., Bard, E., Emeis, K., Grimalt, J. O., Müller, P. J., & Schneider, R. R. (2001). Precision of the current methods to measure the 0 alkenone proxy U. *Geochemistry, Geophysics, Geosystems*, *2*, n/a-n/a.
- Rostek, F., Bard, E., Beaufort, L., Sonzogni, C., & Ganssen, G. (1997). Sea surface temperature and productivity records for the past 240kyr in the Arabian Sea. *Deep-Sea Research*, *44*(97), 1461–1480.
- Sadeghi, A., Dinter, T., Vountas, M., Taylor, B. B., Altenburg-Soppa, M., Peeken, I., & Bracher, A.

- (2012). Improvement to the PhytoDOAS method for identification of coccolithophores using hyper-spectral satellite data. *Ocean Science*, 8(6), 1055–1070. <https://doi.org/10.5194/os-8-1055-2012>
- Sancetta, C., Villareal, T., & Falkowski, P. (1989). Massive fluxes of rhizosolenid diatoms : A common occurrence ? *Notes*, 1452–1457.
- Sathyendranath, S., Cota, G., Stuart, V., Maass, H., & Platt, T. (2001). Remote sensing of phytoplankton pigments: A comparison of empirical and theoretical approaches. *International Journal of Remote Sensing*, 22(2–3), 249–273. <https://doi.org/10.1080/014311601449925>
- Schmidt, S., Harlay, J., Borges, A. V., Groom, S., Delille, B., Røevros, N., et al. (2013). Particle export during a bloom of *Emiliania huxleyi* in the North-West European continental margin. *Journal of Marine Systems*, 109–110(SUPPL.), S182–S190. <https://doi.org/10.1016/j.jmarsys.2011.12.005>
- Schoepfer, S. D., Shen, J., Wei, H., Tyson, R. V., Ingall, E., & Algeo, T. J. (2015). Total organic carbon, organic phosphorus, and biogenic barium fluxes as proxies for paleomarine productivity. *Earth-Science Reviews*, 149, 23–52. <https://doi.org/10.1016/j.earscirev.2014.08.017>
- Seki, O., Ikehara, M., Kawamura, K., Nakatsuka, T., Ohnishi, K., Wakatsuchi, M., et al. (2004). Reconstruction of paleoproductivity in the Sea of Okhotsk over the last 30 kyr. *Paleoceanography*, 19(1). <https://doi.org/10.1029/2002PA000808>
- Smetacek, V. S. (1985). Role of sinking in diatom life-history cycles: ecological, evolutionary and geological significance. *Marine Biology*, 84(3), 239–251. <https://doi.org/10.1007/BF00392493>
- Stramska, M., Stramski, D., Ryszard, H., Kaczmarek, S., & Joanna, S. (2003). Bio-optical relationships and ocean color algorithms for the north polar region of the Atlantic. *Journal of Geophysical Research*, 108(C5), 3143. <https://doi.org/10.1029/2001JC001195>
- Stramski, D., & Tegowski, J. (2001). Effects of intermittent entrainment of air bubbles by breaking wind waves on ocean reflectance and underwater light field. *Journal of Geophysical Research*, 106(C12), 31345–31360. <https://doi.org/10.1029/2000JC000461>
- Suess, E. (1980). Particulate organic carbon flux in the oceans—surface productivity and oxygen utilization. *Nature*, 288(5788), 260–263. <https://doi.org/10.1038/288260a0>
- Teira, E., Mouriño, B., Marañón, E., Pérez, V., Pazó, M. J., Serret, P., et al. (2005). Variability of chlorophyll and primary production in the Eastern North Atlantic Subtropical Gyre: Potential

- factors affecting phytoplankton activity. *Deep-Sea Research Part I: Oceanographic Research Papers*, 52(4), 569–588. <https://doi.org/10.1016/j.dsr.2004.11.007>
- Trull, T. W., Passmore, A., Davies, D. M., Smit, T., Berry, K., & Tilbrook, B. (2018). Distribution of planktonic biogenic carbonate organisms in the Southern Ocean south of Australia: A baseline for ocean acidification impact assessment. *Biogeosciences*, 15(1), 31–49. <https://doi.org/10.5194/bg-15-31-2018>
- Volkman, J. K., Barrett, S. M., Blackburn, S. I., & Sikes, E. L. (1995). Alkenones in *Gephyrocapsa Oceanica* - Implications for Studies of Paleoclimate. *Geochimica et Cosmochimica Acta*, 59(3), 513–520. [https://doi.org/http://dx.doi.org/10.1016/0016-7037\(95\)00325-T](https://doi.org/http://dx.doi.org/10.1016/0016-7037(95)00325-T)
- Volkman, John K., Eglinton, G., Corner, E. D. S., & Forsberg, T. E. V. (1980). Long-chain alkenes and alkenones in the marine coccolithophorid *Emiliana huxleyi*. *Phytochemistry*, 19(12), 2619–2622. [https://doi.org/10.1016/S0031-9422\(00\)83930-8](https://doi.org/10.1016/S0031-9422(00)83930-8)
- Volpe, G., Santoleri, R., Vellucci, V., Ribera d'Alcalá, M., Marullo, S., & D'Ortenzio, F. (2007). The colour of the Mediterranean Sea: Global versus regional bio-optical algorithms evaluation and implication for satellite chlorophyll estimates. *Remote Sensing of Environment*, 107(4), 625–638. <https://doi.org/10.1016/j.rse.2006.10.017>
- Waite, A. M., Safi, K. A., Hall, J. A., & Nodder, S. D. (2000). Mass sedimentation of picoplankton embedded in organic aggregates. *Limnology and Oceanography*, 45(1), 87–97. <https://doi.org/10.4319/lo.2000.45.1.0087>
- Waite, J. N., & Mueter, F. J. (2013). Spatial and temporal variability of chlorophyll-a concentrations in the coastal Gulf of Alaska, 1998-2011, using cloud-free reconstructions of SeaWiFS and MODIS-Aqua data. *Progress in Oceanography*, 116, 179–192. <https://doi.org/10.1016/j.pocean.2013.07.006>
- van der Wal, P., S. Kempers, R., & J. W. Veldhuis, M. (1995). Production and downward flux of organic matter and calcite in a North Sea bloom of the coccolithophore *Emiliana huxleyi*. *Marine Ecology Progress Series*, 126, 247–265. <https://doi.org/10.1002/dev.420100406>
- Weber, T., Cram, J. A., Leung, S. W., DeVries, T., & Deutsch, C. (2016). Deep ocean nutrients imply large latitudinal variation in particle transfer efficiency. *Proceedings of the National Academy of Sciences*, 113(31), 8606–8611. <https://doi.org/10.1073/pnas.1604414113>
- Worden, A. Z., Nolan, J. K., & Palenik, B. (2004). Assessing the dynamic and ecology of marine picoplankton: the importance of eukaryotic component. *Limnol. Oceanogr.*, 49(1), 168–79.
- Zhao, M., Mercer, J. L., Eglinton, G., Higginson, M. J., & Huang, C. Y. (2006). Comparative molecular

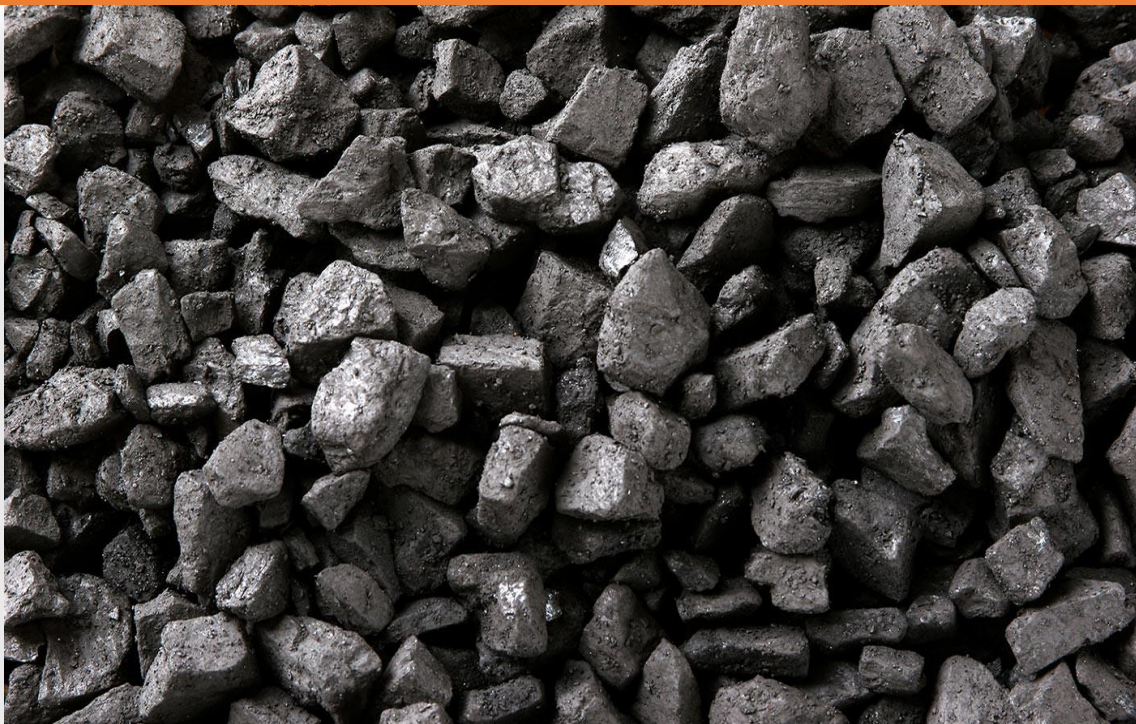
biomarker assessment of phytoplankton paleoproductivity for the last 160 kyr off Cap Blanc, NW Africa. *Organic Geochemistry*, 37(1), 72–97.

<https://doi.org/10.1016/j.orggeochem.2005.08.022>

Zubkov, M. V., Sleigh, M. A., Burkill, P. H., & Leakey, R. J. G. (2000). Picoplankton community structure on the Atlantic Meridional Transect: a comparison between season. *Progress in Oceanography*, 45: 369-386., 45, 369–386.

Chapter 4

Total organic carbon: quantitative paleoproductivity proxy



Picture author: Carbon Market Watch

4. Total organic carbon: quantitative paleoproductivity proxy

4.1. Introduction

Chlorophyll-*a* is the main pigment used by phytoplankton for carrying out photosynthesis. Consequently, sea-surface chlorophyll-*a* (SSchla) concentration, which can be globally estimated by remote sensing, is the most common indicator of total phytoplankton biomass and serves to infer primary productivity (PP) in the global ocean by using oceanic biogeochemical models (Lee et al., 2015).

In 1997, NASA launched the first sensor to estimate SSchla concentration for the global ocean, the Sea-viewing Wide Field-of-view Sensor (SeaWiFS), which offers remote sensing data until 2010. However, many other sensors have been launched to space for collecting global SSchla data. For instance, the MEdium Resolution Imaging Spectrometer (MERIS), from 2002 to 2012, and the Moderate-Resolution Imaging Spectroradiometer (MODIS), from 2002 to present. In order to ensure data continuity, reduce data noise and improve spatial and temporal coverage, data from the above mentioned and other sensors have been merged in the GlobColour project (<http://globcolour.info>). In this way, remote sensing SSchla concentration can be obtained in a global scale from 1997 to present.

To infer past PP for periods before available remote sensing data, paleoceanographers measure sedimentary total organic carbon (TOC) and specific compounds, such as alkenones, silice and barium (Schoepfer et al., 2015; Zhao et al., 2006). Organic carbon has the advantage that is the major component of phytoplankton biomass and provides the most direct proxy for past PP. Hence, many studies use TOC as a proxy for reconstructing past PP (Bunzel et al., 2017; Moreno et al., 2004; Nieto-Moreno et al., 2011; Pedersen, 1983; Schoepfer et al., 2015; Schubert et al., 2001; Summerhayes et al., 1995; Xu et al., 2017).

However, the major part of the organic matter that is produced in surface waters, which is around 48 PgC/yr (DeVries & Weber, 2017; Sarmiento & Gruber, 2006), is converted back into CO₂ in the upper layers. Only 6 to 10 PgC/yr are exported from the euphotic zone to the deep ocean (Schlitzer, 2002; Siegel et al., 2014), and 0.15 PgC/yr are ultimately buried in the sediments (Muller-Karger et al., 2005). Therefore, besides PP, other factors influence the amount of organic matter accumulated in the sediments. Water depth, sedimentation rate and oxygen are discussed to have an important role in controlling TOC in sediments and are frequently included in multivariate and process-based equations used to calculate TOC values (Mann & Zweigel, 2008; Müller & Suess,

1979; Schwarzkopf, 1993). Consequently, the link between PP and TOC can be altered by multiple factors and processes that occur during organic matter deposition and burial.

Although numerous studies have focused on the factors that control organic matter accumulation in sediments, the primary control is an ongoing debate (Chen et al., 2016; Fu et al., 2014; Yu et al., 2019; Zonneveld et al., 2010). Therefore, the reliability and applicability of organic matter proxies, such as TOC, remain controversial. For instance, enhanced burial of organic carbon in glacial-age sediments from the nearby equatorial Pacific was interpreted as reflecting increased PP (Pedersen, 1983), but more recently it has been reinterpreted as the result of enhanced organic carbon preservation conditions under reduced oxygenation (Bradtmiller et al., 2010). In this study, we assess the use of TOC as a quantitative proxy for estimating SSchl_a concentration, and hence as a tool to estimate past PP. The study is based on a global compilation of TOC content in core-top sediments, and compared it with remote sensing SSchl_a concentration.

4.2. Methods

4.2.1. TOC abundance

Our database contains TOC content from 7,783 locations widely distributed around the global ocean (Figure 18), which have been obtained from previous studies (Appendix 2). Since the distribution of the samples is not spatially homogeneous around the global ocean, we checked the representability of our global compilation. For this, we created a 1°x1° grid layer and combined it with our samples location layer, obtaining average values of TOC and SSchl_a concentration for each 1°x1° cell that contain at least one sample (Figure A5, Appendix 1). As we obtained the same equation and coefficient of determination (R^2) for the individual and the gridded locations (average values) when correlating TOC and SSchl_a concentration, we assume the most sampled regions do not introduce significant biases in our global compilation and thus, it is representative of the global ocean.

Generally, the samples correspond to the upper 5 cm of the sediment core and TOC values are obtained from previous studies. Hence, the different routine methods used by the diverse laboratories to obtain TOC content in marine sediment samples might be a possible concern. However, the interlaboratory reproducibility of total carbon in sediment samples was found to be 3% (King et al., 1998). Consequently, greater differences between TOC and SSchl_a concentration can be evaluated in this study without concerns.

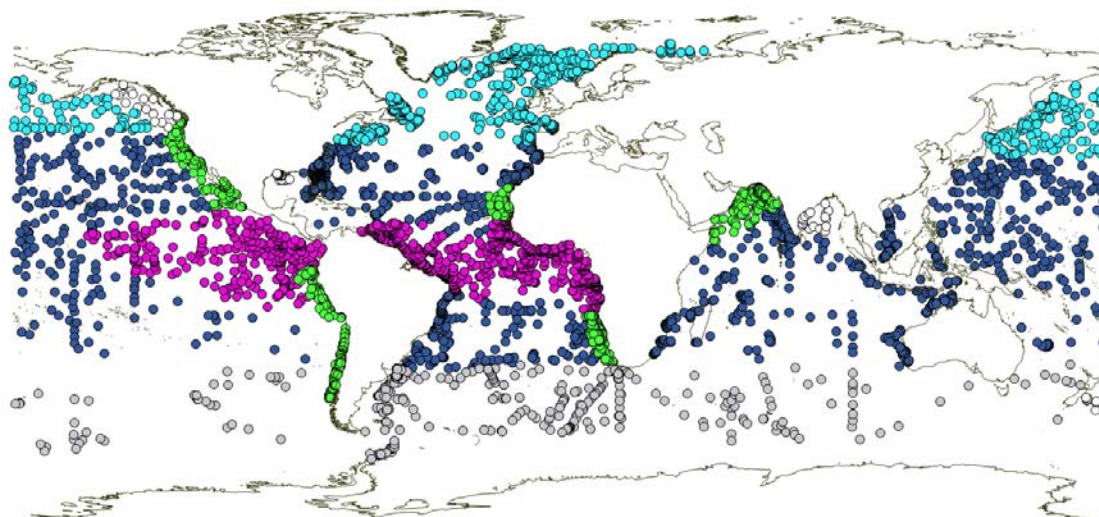


Figure 18. Global core-top sediments distribution. Different colours indicate distinct biogeochemical regions defined on the basis of temperature and nutrient concentration (Weber et al., 2016). The defined regions are as follows: northern latitudes (cyan), low latitudes (dark blue), southern latitudes (grey), equatorial upwellings (pink), coastal upwellings (green) and regions with significant higher river inputs (white).

4.2.2. SSchla concentration

SSchla concentration values for every location were extracted from merged global-scale matrixes of the Globcolour Project (<http://globcolour.info>), which contain monthly data. To obtain SSchla concentration for the last 21 years, we added the concentration from September 1997 to September 2018 for every location. GlobColour data used in this study has been developed, validated, and distributed by ACRI-ST, France. The sensors used for estimating SSchla concentration are as follows: SeaWiFS (1997-2010), MERIS (2002-2012), MODIS (2002-2017) and VIIRS (2012-2017). The spatial resolution is $1/24^\circ$ (4.63 km at the equator), and the algorithms are OC4v5 for SeaWiFS, OC4Me for MERIS, and OC3v5 for MODIS and VIIRS (O'Reilly et al., 2000).

A number of factors might affect our comparison between remote sensing and sedimentary data, including the limitation of detecting SSchla concentration in the deep water column (Cullen, 1982; Huisman et al., 2006), lateral transport of organic matter and the different timescales between remote sensing observations (21 years) and sediment (c.a. 333 years). The age range of sediment samples have been calculated from the sedimentation rate average of all sediments (15 cm/ka) by using the map published in (Dunne et al., 2012), and the maximum core depth (5 cm).

However, one of the principal sources of uncertainty on SSchla concentration data might be the poor accuracy of SSchla remote sensing products in some specific oceanic regions, where optical, physical and biological properties are complex (Blondeau-Patissier et al., 2014; Brown & Yoder, 1994; Gregg & Casey, 2004; Werdell et al., 2018). In those regions, global standard algorithms might provide biased estimations. The main factors affecting surface waters properties are

reported to be coloured dissolved organic matter, radiance-absorbing aerosols, phytoplankton species diversity, suspended sediments, clouds, ice, sun glint, and navigation/time space mismatches (Claustre & Maritoner, 2003; Dierssen & Smith, 2000; Sathyendranath et al., 2001; Volpe et al., 2007). Besides, desert dust (Claustre et al., 2002) and bubbles (Stramski & Tegowski, 2001) make the water appear greener.

4.3. Results

4.3.1. Quantifying SSchla from TOC

To assess the link between TOC and SSchla concentration, we appraised their global scale correlation in Figure 19. We represented the data on logarithmic scale based on the natural distribution of ocean chlorophyll, which is lognormal (Campbell, 1995). The coefficient of determination (R^2) and root mean square (RMS) log error obtained for the linear correlation between the logarithms of TOC and SSchla concentration were 0.17 and 22%, respectively.

In order to reduce the uncertainty derived from the use of SSchla global standard algorithms, we only considered regions reported to present RMS log errors lower than 31% between remote sensing and *in situ* SSchla concentration, as this threshold has been used to define well-performing regions in global and regional remote sensing SSchla evaluation studies (Gregg & Casey, 2004). Consequently, polar regions (Barbini et al., 2001; Dierssen & Smith, 2000; Gregg & Casey, 2004; Lewis et al., 2016; Matsuoka et al., 2007; Matsuoka et al., 2011; Mitchell, 1992; Mustapha et al., 2012; Wang & Cota, 2003), the North Atlantic (Gregg & Casey, 2004; Mendonça et al., 2010; Moulin et al., 2001; Stramska et al., 2003), the Gulf of Alaska (Waite & Mueter, 2013) and the California current for high SSchla concentration ($>1\text{mg}\cdot\text{m}^{-3}$) (Kahru et al., 2012, 2014), which present RMS log errors higher than 31%, are not included in Figure 19 b. Nor the western South American margin, as the error of this region has not been thoroughly studied.

Despite not considering remote sensing SSchla non-validated regions, the correlation obtained between TOC and SSchla concentration (Figure 19 b) shows that spatial variations in TOC content can explain less than half spatial variations in SSchla concentration at a global scale ($R^2=0.25$, Table A1, Appendix 1). Hence, changes in SSchla concentration cannot be identified as the principal factor altering TOC content in sediments. Our global comparison between TOC and SSchla concentration, showed in non-logarithmic axis in Figure A6 (Appendix 1), is concordant with the global comparison between TOC content and marine PP published in (Felix, 2014), which was obtained from 121 locations.

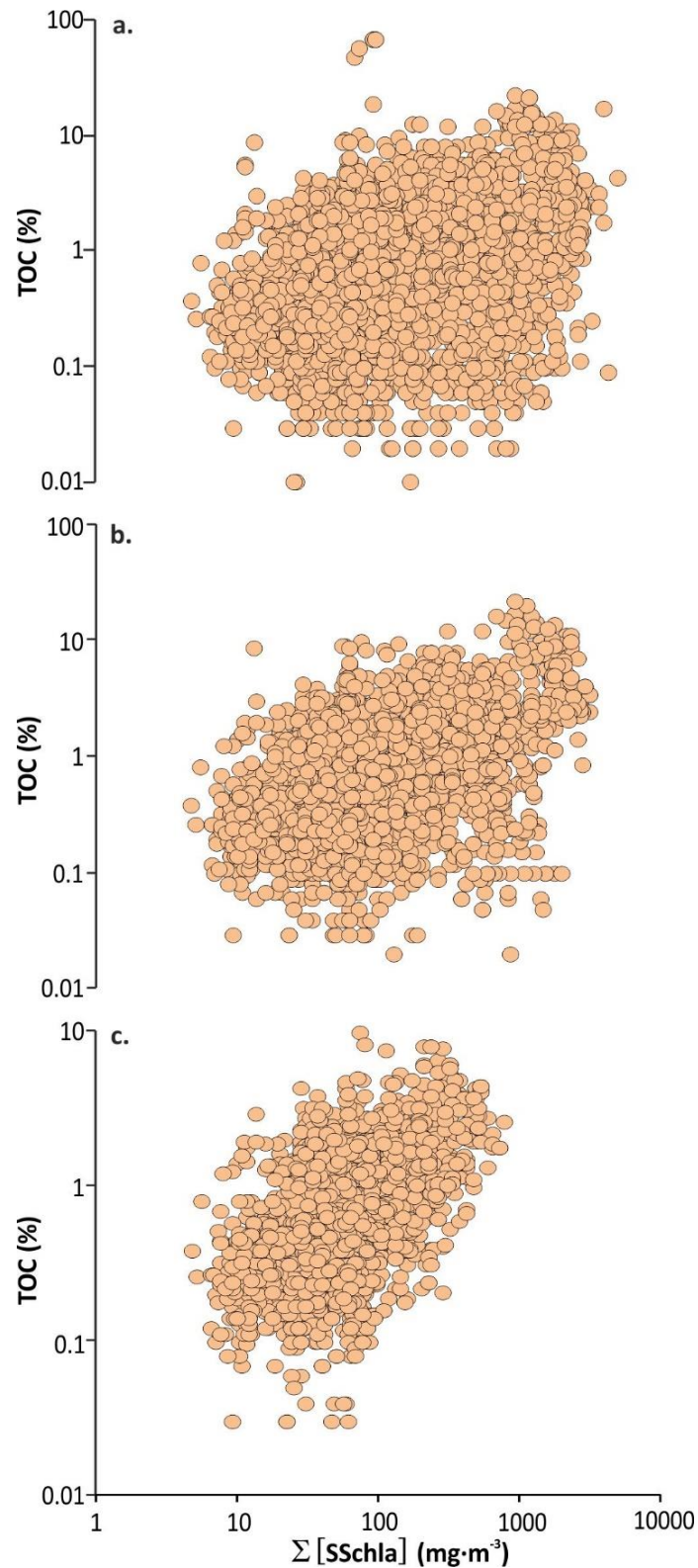


Figure 19. Global comparisons between sedimentary total organic carbon (TOC) content and the sum of sea-surface chlorophyll-*a* (SSchla) concentration from 1997 to 2017. **a.** includes the whole compilation, **b.** and **c.** include regions presenting RMS log errors lower than 31% between remote sensing and *in situ* SSchla, **c.** includes sediment samples below water columns deeper than 1,000 meters.

However, the obtained global correlation englobes different oceanic biogeochemical regions that present different ranges of PP and organic export efficiencies from the sea-surface to the sediment (Weber et al., 2016). In order to study the possible variations that the distinctive oceanic biogeochemical regions might reflect in the correlation between TOC and SSchl_a concentration, we divided the global ocean in different regions and obtained specific correlations for each region. Our classification is based on the regions defined in (Weber et al., 2016), which consider nutrient circulation, solar irradiance, temperature and phytoplankton community, but we differentiate between coastal and equatorial upwellings. Hence, we defined the following 5 regions: equatorial and coastal upwellings, and northern, southern and low latitudes (Figure 18). Since the use of TOC as a marine proxy might be constrained in coastal marine sediments, where almost half of the organic carbon that is buried becomes from river inputs (Schlünz & Schneider, 2000), we classified apart coastal regions where the organic carbon burial rates have been found disproportionately high relative to their surroundings (Bianchi et al., 2018).

Figure A7 (Appendix 1) shows TOC content variability is not the main factor related to SSchl_a concentration for the majority of the regions evaluated, as it was the case for the global ocean. The R^2 obtained in the linear correlation between TOC and SSchl_a concentration was lower than 0.25 for all regions with the exception of coastal upwellings, where we found a R^2 of 0.54 (Table A1, Appendix 1). Therefore, changes in TOC content in coastal upwellings can be mainly related to changes in SSchl_a concentration.

4.3.2. The link between preservation factors and TOC

Our results from the correlations between TOC and SSchl_a concentration (Figure 19) suggest besides PP, other factors have an important role in controlling TOC accumulation in sediments. These results are concordant with other studies that propose water depth, sedimentation rate and oxygen to have a key role in TOC export and burial processes (Mann & Zweigel, 2008; Müller & Suess, 1979; Schwarzkopf, 1993).

We studied the impact of a) water depth, b) oxygen concentration along the water column, c) oxygen concentration in bottom waters and d) sedimentation rate, in TOC at a global scale (Figure A8, Appendix 1). Sedimentation rates were extracted from the global map published in (Dunne et al., 2012) and oxygen concentration from NOAA database. The global comparisons obtained in this study are concordant with those published in (Felix, 2014), which were obtained from 121 locations (Figure A6, Appendix 1).

We did not find any strong linear correlation between TOC and the evaluated factors, R^2 was lower than 0.2 in all cases (Table A1, Appendix 1). Consequently, any of these factors seem to play a

major role in controlling TOC at a global scale. However, Figure A8 (Appendix 1) shows some general trends that can provide useful information about links between TOC and the assessed factors.

4.4. Discussion

4.4.1. TOC as a quantitative proxy for global past PP

TOC is commonly used as a paleoproductivity proxy. For instance, TOC has been used for tracking past PP variability for the time interval 48,000 to 28,000 years before present and during the Late Holocene in the Mediterranean (Moreno et al., 2004; Nieto-Moreno et al., 2011), during the last glacial maximum and the Late Quaternary in the eastern equatorial Pacific and the Inner Sea, respectively (Bunzel et al., 2017; Pedersen, 1983), and over the past 50,000 and 70,000 years in the Arctic Ocean and the Benguela Current upwelling system (Schubert et al., 2001; Summerhayes et al., 1995).

Despite of the wide use of TOC proxy for reconstructing marine changes in past PP, its applicability remains unclear, as environmental and preservation factors have been suggested to play also a role in controlling organic matter accumulation in sediment, and the predominant factor is still controversial (Chen et al., 2016; Fu et al., 2014; Li et al., 2017; Yu et al., 2019). Our results from the global comparison between TOC and SSchl_a concentration show a linear tendency between these two variables (Figure 19 b). However, this is only a broad trend as there is a lot of scatter and TOC content variability can only explain 25% of SSchl_a concentration variability ($R^2=0.25$, Table A1, Appendix 1).

These results suggest that indeed multiple factors are controlling TOC content. Organic matter accumulation in sediments involves biological, chemical and physical processes that occur from the sea-surface to the water-sediment interface. Hence, TOC content is the outcome of various ecological, oceanographic and sedimentological factors. PP, sedimentation rate, water depth and oxygen are the main factors discussed to play a role in controlling organic matter flux and TOC content (Betts & Holland, 1991; Canfield, 1994; Felix, 2014; Müller & Suess, 1979; Pace et al., 1987; Suess, 1980).

Shallow waters and low oxygen concentration through the water column reduce the degradation time of organic matter by reducing oxygen time exposure. Hence, differences in water depth and oxygen concentration through the water column might lead to differences in TOC (Hartnett et al., 1998). However, our results do not show a clear tendency between these two factors and TOC, and shallow waters and low oxygen concentration surprisingly present low TOC values (Figure A8,

Appendix 1). This might be because terrestrial inputs can alter the sedimentary composition, which might result in a dilution of TOC. In fact, dilution effects particularly occur in coastal margins, where shallow waters and low oxygen time exposure can be found.

As fluvial deposition is the greatest transport mechanism of terrestrial carbon to the marine environment, we did not include in Figure A8 (Appendix 1) oceanic regions where the organic carbon burial rates have been found disproportionately high relative to their surroundings because of river inputs (Bianchi et al., 2018). However, other mechanisms, such as atmospheric deposition, can also significantly alter TOC content by delivering terrestrial carbon into the coastal ocean (Lohmann et al., 2009) and thus, affect our comparisons and correlations. In order to avoid that dilution effects in coastal waters cover global oceanic tendencies that should be noticed in our comparisons and alter our correlations, we only consider sediments below water columns deeper than 1,000 meters in Figure 20.

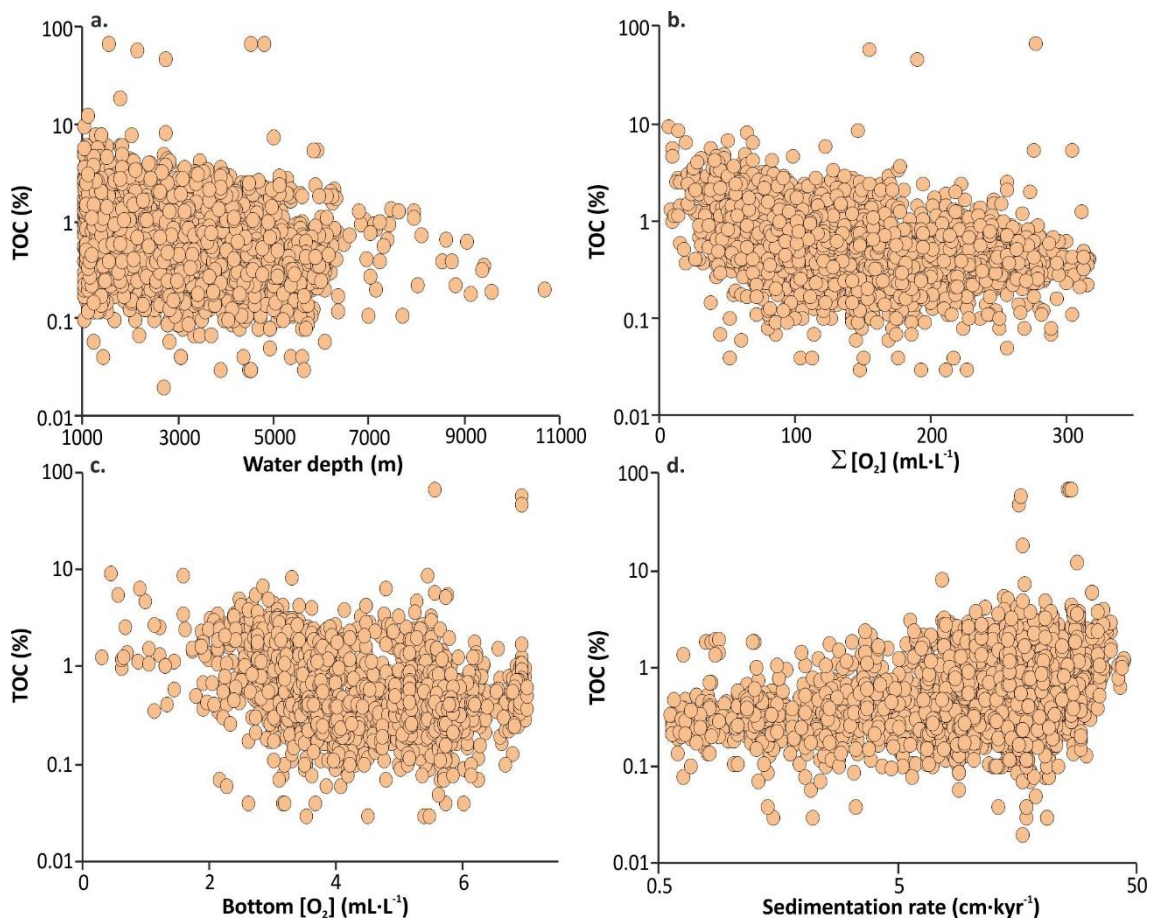


Figure 20. Global comparisons between sedimentary total organic carbon (TOC) content and **a.** water depth, **b.** oxygen concentration through the water column, **c.** oxygen concentration in bottom waters and **d.** sedimentation rate. These comparisons include sediment samples below water columns deeper than 1,000 meters.

Consequently, in Figure 20, water columns with low oxygen concentration are related to high TOC values, which can be explained by a better preservation in less oxic conditions. However, the big scatter in the correlation and $R^2=0.13$ indicate oxygen through the water column is not the predominant factor in controlling TOC (Table 3). Similarly, water depth also presents high scatter in its correlation with TOC and $R^2=0.11$, which suggest this is neither the primary factor controlling TOC, but might influence TOC variability (Table 3). Higher variability in TOC corresponds to shallow waters, meanwhile deep waters are related to low TOC content with low variability (Figure 20). Hence, lower TOC content in deeper waters can be explained by a major degradation due to a higher time exposure to oxygen along the water column.

Factor	Region	a	b	R ²	RMS log error (%)	n
Σ[SSchla]	Global	0.54	-1.15	0.30	22	2859
Σ[SSchla]	Nothern latitudes	0.59	-1.48	0.19	44	234
Σ[SSchla]	Low latitudes	0.52	-1.11	0.21	29	958
Σ[SSchla]	Southern latitudes	0.60	-1.45	0.23	30	334
Σ[SSchla]	Equatorial upwellings	0.49	-1.00	0.20	26	1001
Σ[SSchla]	Coastal upwellings	1.02	-2.16	0.54	23	351
WD	Global	-8x10 ⁻⁵	0.07	0.11	111126	4208
[O ₂]	Global	-2x10 ⁻³	0.03	0.13	5292	2194
Bottom [O ₂]	Global	-0.08	0.07	0.07	122	2194
LogSR	Global	0.25	-0.53	0.08	36	3453

Table 3. Coefficients and errors of total organic carbon (TOC) equations. $\text{LogTOC} = a \cdot \log \Sigma[\text{SSchla}] + b$. Data used in these equations include sediment samples below water columns deeper than 1,000 meters. Data used in these equations include regions presenting RMS log errors lower than 31% between remote sensing and *in situ* SSchla. Abbreviations: sea-surface chlorophyll-a (SSchla), water depth (WD), oxygen concentration through the water column ([O₂]), oxygen concentration in bottom waters (Bottom [O₂]), logarithm of sedimentation rate (LogSR), coefficient of determination (R²), root-mean square logarithmic error (RMS log error), number of samples (n).

Oxygen concentration in bottom waters has been also pointed out as an important factor affecting organic matter degradation in the water-sediment interface. It is suggested organic matter is degraded more efficiently in the presence of oxygen in the bottom waters than in anoxic environments (Canfield, 1994; Dauwe et al., 2001; Kristensen & Holmer, 2001). Accordingly, our results show that samples presenting high TOC values correspond to low oxygen concentration in bottom waters, but likewise the other variables assessed in this study, a lot of scatter can be

found in the correlation (Figure 20), which presents $R^2=0.07$ (Table 3). These results indicate oxygen concentration in bottom waters is not the dominant factor in regulating TOC.

Sedimentation rate is another environmental factor commonly inferred to have an effect on organic matter preservation. This relationship is expected because rapid deposition rates move organic matter more rapidly down through the diagenetically active zone (i.e. sediment-water interface), reducing time exposure to oxygen and microorganisms. In 1979, it was found an increasing linear tendency between organic matter accumulation and sedimentation rate from 6 sediments, mostly from upwelling regions, and the authors concluded TOC was mainly controlled by sedimentation rate (Müller & Suess, 1979). However, our results show a more complicated relationship and are in agreement with later studies that included a more extensive sediment compilation (Felix, 2014; Hedges & Keil, 1995). Our correlation between TOC and sedimentation rate, like the other correlations evaluated in this study, presents a big scatter (Figure 20), which together with a R^2 of 0.08, suggest sedimentation rate is not the main factor influencing TOC (Table 3).

One of the main challenges of understanding the relationship between sedimentation rate and TOC, is that sedimentation rate influences both preservation and dilution. Low sedimentation rates are related to low TOC, which can be explained by a high degradation of organic matter, as it remains longer in the diagenetically active zone. In contrast, high sedimentation rates reduce the degradation time of organic matter and results in a better preservation of organic matter and thus, higher TOC. Nevertheless, low TOC can also be found in some sediments accumulated under high sedimentation rate conditions, which might be caused by dilution. In fact, this dilution effect can be seen more clearly in Figure A8 (Appendix 1) as it includes coastal waters, which are more likely to be affected by dilution.

As the correlation we found between TOC and SSchla concentration might be also affected by dilution, we also obtained the correlation between these two parameters only considering sediments below water columns deeper than 1,000 meters (Figure 19 c, Table 3), as coastal waters are prone to be affected by dilution. In contrast to Figure 19 b, Figure 19 c does not show low TOC values for sediments accumulated below high PP waters (samples with high values of SSchla concentration). Consequently, Figure 19 c presents a lower degree of scatter and a higher value of R^2 ($R^2=0.30$).

Therefore, our results suggest SSchla concentration is the most relevant factor controlling TOC content in a global scale, among the factors evaluated in this study (SSchla concentration, oxygen through the water column, water depth, oxygen in bottom waters and sedimentation rate). However, SSchla concentration can only explain 30% of TOC variability, and all correlations

present a high degree of scatter. Thus, these data highlight the constraints in the use of TOC as a paleoproductivity proxy at a global scale, and present evidence of the high complexity of the global mechanisms that control organic matter deposition in marine sediments.

One plausible reason that might explain the huge scatter in our correlations is that TOC involves many different compounds that present different chemical composition and thus, different degradation pathways. Moreover, other factors not included in this study might affect organic matter accumulation. For instance, bioturbation and physical mixing also contribute to oxygen exposure time and thus, the preservation of TOC in sediments. Terrestrial inputs affecting deeper waters than 1,000 meters might be another source of uncertainty in our correlations.

4.4.2. TOC as a quantitative proxy for regional past PP

We have shown TOC abundance can explain 30% of SSchl_a concentration variability in a global scale. However, in this global correlation, different oceanic biogeochemical regions are included, which present different ranges of PP and depositional conditions (Weber et al., 2016) that might lead to different relationships between SSchl_a and TOC concentration. Our results from the regional comparison between TOC and SSchl_a concentration suggest differences among regions (Figure A7, Table A1, Appendix 1). Samples from coastal upwellings present the highest correlation with a R^2 of 0.54 and RMS log error of 24%. Samples from northern latitudes and equatorial upwellings present a R^2 around 0.2, the most similar R^2 to the global correlation; and southern and low latitudes present the lowest R^2 (less than 0.06). In southern latitudes, we can appreciate an overall linear tendency and some samples (those that present the highest SSchl_a concentration values) that do not follow this general trend.

These samples that present low TOC values are located in the western part of the southern Atlantic Ocean (red stars in Figure A9, Appendix 1). This site is not affected by coastal upwelling, but it is characterized by high PP due to the confluence of the Malvinas Current, which transports cold subantarctic water, and the warm Brazil Current. Moreover, it is influenced by the Rio de la Plata, which discharges freshwater from the second largest hydrographic basin in South America (Framiñan & Brown, 1996). These complex frontal motions and mixing patterns of warm- and cold-water masses lead to particular sedimentary settings, mainly characterized by an intense lateral particle transport (Ewing et al., 1964; Hensen et al., 2003; Hensen et al., 2000) and an impressive array of erosive, depositional and mixed contouritic features (Hernández-Molina et al., 2016).

Consequently, previous studies on the area found anomalous low organic carbon content in sediments (Hensen et al., 2000). The authors argued that organic matter is unlikely to be controlled

by export from surface waters, but by a combination of lateral transport processes, and suggested a strong dilution for explaining part of the observed discrepancy between sedimentary and flux values. Accordingly, the R^2 and RMS log error of our correlation between TOC and SSchl_a concentration in southern latitudes improve considerably when no considering the Brazil-Malvinas Confluence Zone (Table A1, Appendix 1).

Since dilution can also affect other oceanic regions and it mainly occurs in coastal waters, we also obtained the regional correlations between SSchl_a and TOC concentration only considering sediments below water columns deeper than 1,000 meters (Figure 21, Table 3), similar as we previously studied for the global correlation. Consequently, the R^2 obtained in the correlation of samples from low latitudes increase to 0.21, which is similar to the other evaluated regions, with the exception of coastal upwellings.

Therefore, it seems global organic matter accumulation in sediments is proportional to SSchl_a concentration, but can only explain around 20% of SSchl_a variability, with the exception of coastal upwellings, where changes in TOC abundance can explain 54% of SSchl_a concentration changes, with a RMS log error of 23%. Hence, TOC content changes in coastal upwellings can be mainly related to changes in SSchl_a concentration. Thus, our results suggest TOC can be used as a quantitative paleoproductivity proxy in upwelling regions and underline the limitations of its application in more general scenarios. This study also points out the importance of samples location in defining global processes, as the relationship obtained from a specific region, such as coastal upwellings, might not reflect the mechanisms occurring in the global ocean. Further research is needed to study TOC as a good tracer for quantifying past PP in more specific regions, rather than extensive areas, as it has been considered in our regional study.

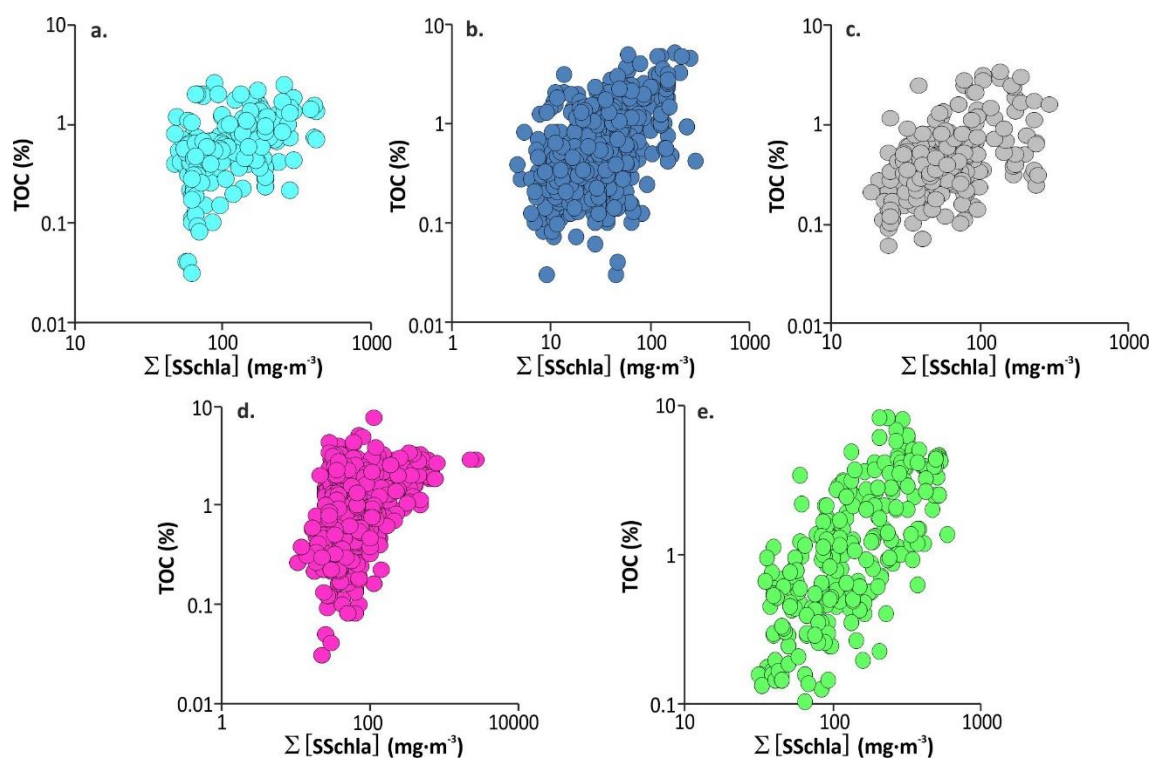


Figure 21. Regional comparisons between sedimentary total organic carbon (TOC) content and the sum of sea-surface chlorophyll-*a* (SSchla) concentration from 1997 to 2017. Different graphics present data from biogeochemical regions defined in Figure 18, **a.** northern latitudes, **b.** low latitudes, **c.** southern latitudes, **d.** equatorial upwellings and **e.** coastal upwellings. These comparisons include sediment samples below water columns deeper than 1,000 meters and regions presenting RMS log errors lower than 31% between remote sensing and *in situ* SSchla.

4.5. Conclusions

This study shows global changes in TOC content can explain 30% of SSchla concentration variability. However, the global correlation between TOC and SSchla concentration seems to reflect two different scenarios; TOC abundance can only explain around 20% of SSchla variability in the global ocean, meanwhile it can explain more than half the SSchla variability in coastal upwellings. Thus, our data suggest TOC content can be used as a quantitative paleoproductivity proxy in upwelling regions and underline the limitations of its application in a global scale. In this way, this study also points out the importance of samples location in defining global processes, as relationships obtained from specific regions might not reflect the mechanisms that influence the global ocean.

Our results also suggest organic matter accumulated in sediments is proportional to SSchla concentration, and exhibit the importance of SSchla in controlling global organic matter accumulation, as it has shown to be the most relevant factor controlling TOC content in a global scale, among the factors evaluated in this study (SSchla concentration, oxygen through the water column, water depth, oxygen in bottom waters and sedimentation rate). However, none of the

evaluated factors seems to be the dominant in regulating organic carbon accumulation in marine sediments. Therefore, our data support organic matter accumulation in marine sediments is controlled by the interaction of several environmental factors and presents more evidence about the high complexity of the global mechanisms that control organic matter deposition in marine sediments.

4.6. References

- Barbini, R., Colao, F., Fantoni, R., Fiorani, L., & Palucci, A. (2001). Remote sensing of the Southern Ocean: techniques and results. *Journal of Optoelectronics and Advanced Materials*, *3*(4), 817–830.
- Betts, J. N., & Holland, H. D. (1991). The oxygen content of ocean bottom waters, the burial efficiency of organic carbon, and the regulation of atmospheric oxygen. *Global and Planetary Change*, *5*(1–2), 5–18. [https://doi.org/10.1016/0921-8181\(91\)90123-E](https://doi.org/10.1016/0921-8181(91)90123-E)
- Bianchi, T. S., Cui, X., Blair, N. E., Burdige, D. J., Eglinton, T. I., & Galy, V. (2018). Centers of organic carbon burial and oxidation at the land-ocean interface. *Organic Geochemistry*, *115*, 138–155. <https://doi.org/10.1016/j.orggeochem.2017.09.008>
- Blondeau-Patissier, D., Gower, J. F. R., Dekker, A. G., Phinn, S. R., & Brando, V. E. (2014). A review of ocean color remote sensing methods and statistical techniques for the detection, mapping and analysis of phytoplankton blooms in coastal and open oceans. *Progress in Oceanography*, *123*, 123–144. <https://doi.org/10.1016/j.pocean.2013.12.008>
- Bradtmiller, L. I., Anderson, R. F., Sachs, J. P., & Fleisher, M. Q. (2010). A deeper respired carbon pool in the glacial equatorial Pacific Ocean. *Earth and Planetary Science Letters*, *299*(3–4), 417–425. <https://doi.org/10.1016/j.epsl.2010.09.022>
- Brown, C. W., & Yoder, J. A. (1994). Cocolithophorid blooms in the global ocean. *Journal of Geophysical Research*, *99*(C4), 7467–7482. <https://doi.org/10.1029/93JC02156>
- Bunzel, D., Schmiedl, G., Lindhorst, S., Mackensen, A., Reolid, J., Romahn, S., & Betzler, C. (2017). A multi-proxy analysis of late Quaternary Indian monsoon dynamics for the Maldives, Inner Sea. *Climate of the Past Discussions*, (April), 1–35. <https://doi.org/10.5194/cp-2017-54>
- Campbell, J. W. (1995). The lognormal distribution as a model for bio-optical variability in the sea. *Journal of Geophysical Research*, *100*(95), 13237–13254. <https://doi.org/10.1029/95JC00458>
- Canfield, D. E. (1994). Factors influencing organic carbon preservation in marine sediments. *Chemical Geology*, *114*(3–4), 315–329. [https://doi.org/10.1016/0009-2541\(94\)90061-2](https://doi.org/10.1016/0009-2541(94)90061-2)

- Chen, C., Mu, C. L., Zhou, K. K., Liang, W., Ge, X. Y., Wang, X. P., et al. (2016). The geochemical characteristics and factors controlling the organic matter accumulation of the Late Ordovician-Early Silurian black shale in the Upper Yangtze Basin, South China. *Marine and Petroleum Geology*, *76*, 159–175. <https://doi.org/10.1016/j.marpetgeo.2016.04.022>
- Claustre, H., & Maritoner, S. (2003). The Many Shades of Ocean Blue. *Ocean Science*, *302*(5650), 1514–1515.
- Claustre, H., Morel, A., Hooker, S. B., Babin, M., Antoine, D., Oubelkheir, K., et al. (2002). Is desert dust making oligotrophic waters greener? *Geophysical Research Letters*, *29*(10), 107-1-107–4. <https://doi.org/10.1029/2001GL014056>
- Cullen, J. J. (1982). The deep chlorophyll maximum: Comparing vertical profiles of chlorophyll a. *Canadian Journal of Fisheries and Aquatic Sciences*, *39*, 791–803.
- Dauwe, B., Middelburg, J. J., & Herman, P. M. J. (2001). Effect of oxygen on the degradability of organic matter in subtidal and intertidal sediments of the North Sea area. *Marine Ecology Progress Series*, *215*, 13–22.
- DeVries, T., & Weber, T. (2017). The export and fate of organic matter in the ocean: New constraints from combining satellite and oceanographic tracer observations. *Global Biogeochemical Cycles*, *31*(3), 535–555. <https://doi.org/10.1002/2016GB005551>
- Dierssen, H. M., & Smith, R. C. (2000). Bio-optical properties and remote sensing ocean color algorithms for Antarctic Peninsula waters, *105*(1999), 26301–26312.
- Dunne, J. P., Hales, B., & Toggweiler, J. R. (2012). Global calcite cycling constrained by sediment preservation controls. *Global Biogeochemical Cycles*, *26*(3), 1–14. <https://doi.org/10.1029/2010GB003935>
- Ewing, M., Ludwig, W. J., & Ewing, J. I. (1964). Sediment distribution in the oceans: The Argentine Basin. *J. Geophys. Res.*, *69*(10), 2003–2032.
- Felix, M. (2014). A comparison of equations commonly used to calculate organic carbon content and marine palaeoproductivity from sediment data. *Marine Geology*, *347*, 1–11. <https://doi.org/10.1016/j.margeo.2013.10.006>
- Framiñan, M. B., & Brown, O. B. (1996). Study of the Rio de la Plata turbidity front. Part I: Spatial and temporal distribution. *Continental Shelf Research*, *16*(10), 1259–1282. [https://doi.org/10.1016/0278-4343\(95\)00071-2](https://doi.org/10.1016/0278-4343(95)00071-2)
- Fu, X., Tan, F., Feng, X., Wang, D., Chen, W., Song, C., & Zeng, S. (2014). Early Jurassic anoxic conditions and organic accumulation in the eastern Tethys. *International Geology Review*,

- 56(12), 1450–1465. <https://doi.org/10.1080/00206814.2014.945103>
- Gregg, W. W., & Casey, N. W. (2004). Global and regional evaluation of the SeaWiFS chlorophyll data set. *Remote Sensing of Environment*, 93(4), 463–479.
<https://doi.org/10.1016/j.rse.2003.12.012>
- Hartnett, H. E., Keil, R. G., Hedges, J. I., & Devol, A. H. (1998). Influence of oxygen exposure time on organic carbon preservation in continental margin sediments. *Nature*, 391(February), 572–574.
- Hedges, J. I., & Keil, R. G. (1995). Sedimentary organic matter preservation: an assessment and speculative synthesis. *Marine Chemistry*, 49(2–3), 81–115. [https://doi.org/10.1016/0304-4203\(95\)00008-F](https://doi.org/10.1016/0304-4203(95)00008-F)
- Hensen, C., Pfeifer, Z. M., Schwenk, T., Kasten, S., Riedinger, N., Schulz, H. D., & Boetius, A. (2003). Control of sulfate pore-water profiles by sedimentary events and the significance of anaerobic oxidation of methane for the burial of sulfur in marine sediments. *Geochimica et Cosmochimica Acta*, 67(14), 2631–2647. [https://doi.org/10.1016/S0016-7037\(00\)00199-6](https://doi.org/10.1016/S0016-7037(00)00199-6)
- Hensen, Christian, Zabel, M., & Schulz, H. D. (2000). A comparison of benthic nutrient fluxes from deep-sea sediments off Namibia and Argentina. *Deep-Sea Research Part II: Topical Studies in Oceanography*, 47(9–11), 2029–2050. [https://doi.org/10.1016/S0967-0645\(00\)00015-1](https://doi.org/10.1016/S0967-0645(00)00015-1)
- Hernández-Molina, F. J., Soto, M., Piola, A. R., Tomasini, J., Preu, B., Thompson, P., et al. (2016). A contourite depositional system along the Uruguayan continental margin: Sedimentary, oceanographic and paleoceanographic implications. *Marine Geology*, 378, 333–349. <https://doi.org/10.1016/j.margeo.2015.10.008>
- Huisman, J., Pham Thi, N. N., Karl, D. M., & Sommeijer, B. (2006). Reduced mixing generates oscillations and chaos in the oceanic deep chlorophyll maximum. *Nature*, 439(7074), 322–325. <https://doi.org/10.1038/nature04245>
- Kahru, M., Kudela, R. M., Manzano-Sarabia, M., & Mitchell, B. G. (2012). Trends in the surface chlorophyll of the California Current: Merging data from multiple ocean color satellites. *Deep-Sea Research Part II: Topical Studies in Oceanography*, 77–80, 89–98.
<https://doi.org/10.1016/j.dsr2.2012.04.007>
- Kahru, M., Kudela, R. M., Anderson, C. R., Manzano-Sarabia, M., & Mitchell, B. G. (2014). Evaluation of satellite retrievals of ocean chlorophyll-a in the California current. *Remote Sensing*, 6(9), 8524–8540. <https://doi.org/10.3390/rs6098524>
- King, P., Kennedy, H., Newton, P. P., Jickells, T. D., Brand, T., Calvert, S., et al. (1998). Analysis of

- total and organic carbon and total nitrogen in settling oceanic particles and a marine sediment: An interlaboratory comparison. *Marine Chemistry*, 60(3–4), 203–216. [https://doi.org/10.1016/S0304-4203\(97\)00106-0](https://doi.org/10.1016/S0304-4203(97)00106-0)
- Kristensen, E., & Holmer, M. (2001). Decomposition of plant materials in marine sediment exposed to different electron acceptors (O_2 , NO_3^- , and SO_4^{2-}), with emphasis on substrate origin, degradation kinetics, and the role of bioturbation. *Geochimica et Cosmochimica Acta*, 65(3), 419–433. [https://doi.org/10.1016/S0016-7037\(00\)00532-9](https://doi.org/10.1016/S0016-7037(00)00532-9)
- Lee, Z., Marra, J., Perry, M. J., & Kahru, M. (2015). Estimating oceanic primary productivity from ocean color remote sensing: A strategic assessment. *Journal of Marine Systems*, 149, 50–59. <https://doi.org/10.1016/j.jmarsys.2014.11.015>
- Lewis, K. M., Mitchell, B. G., van Dijken, G. L., & Arrigo, K. R. (2016). Regional chlorophyll a algorithms in the Arctic Ocean and their effect on satellite-derived primary production estimates. *Deep-Sea Research Part II: Topical Studies in Oceanography*, 130, 14–27. <https://doi.org/10.1016/j.dsr2.2016.04.020>
- Li, Y., Zhang, T., Ellis, G. S., & Shao, D. (2017). Depositional environment and organic matter accumulation of Upper Ordovician–Lower Silurian marine shale in the Upper Yangtze Platform, South China. *Palaeogeography, Palaeoclimatology, Palaeoecology*, 466, 252–264. <https://doi.org/10.1016/j.palaeo.2016.11.037>
- Lohmann, R., Bollinger, K., Cantwell, M., Feichter, J., Fischer-Bruns, I., & Zabel, M. (2009). Fluxes of soot black carbon to South Atlantic sediments. *Global Biogeochemical Cycles*, 23(1), 1–13. <https://doi.org/10.1029/2008GB003253>
- Mann, U., & Zweigel, J. (2008). *Modelling Source-Rock Distribution and Quality Variations: The Organic Facies Modelling Approach. Analogue and Numerical Modelling of Sedimentary Systems: From Understanding to Prediction*. <https://doi.org/10.1002/9781444303131.ch11>
- Matsuoka, A., Huot, Y., Shimada, K., Saitoh, S. I., & Babin, M. (2007). Bio-optical characteristics of the western Arctic Ocean. *Can. J. Remote Sens.*, 33(6), 503–518. <https://doi.org/10.5589/m07-059>
- Matsuoka, Atsushi, Hill, V., Huot, Y., Babin, M., & Bricaud, A. (2011). Seasonal variability in the light absorption properties of western Arctic waters: Parameterization of the individual components of absorption for ocean color applications. *Journal of Geophysical Research: Oceans*, 116(2), 1–15. <https://doi.org/10.1029/2009JC005594>
- Mendonça, A., Martins, A., Figueiredo, M., Bashmachnikov, I., Couto, A., Lafon, V., & Aristegui, J.

- (2010). Evaluation of ocean color and sea surface temperature sensors algorithms using in situ data: a case study of temporal and spatial variability on two northeast Atlantic seamounts. *Journal of Applied Remote Sensing*, 4(1), 043506.
<https://doi.org/10.1117/1.3328872>
- Mitchell, B. G. (1992). Predictive bio-optical relationships for polar oceans and marginal ice zones. *Journal of Marine Systems*, 3(1–2), 91–105. [https://doi.org/10.1016/0924-7963\(92\)90032-4](https://doi.org/10.1016/0924-7963(92)90032-4)
- Moreno, A., Cacho, I., Canals, M., Grimalt, J. O., & Sanchez-Vidal, A. (2004). Millennial-scale variability in the productivity signal from the Alboran Sea record, Western Mediterranean Sea. *Palaeogeography, Palaeoclimatology, Palaeoecology*, 211(3–4), 205–219.
<https://doi.org/10.1016/j.palaeo.2004.05.007>
- Moulin, C., Gordon, H. R., Chomko, R. M., Banzon, V. F., & Evans, R. H. (2001). Atmospheric correction of ocean imagery through thick layers of Saharan dust. *Geophysical Research Letters*, 28(1), 5–8. <https://doi.org/10.1029/2000GL011803>
- Muller-Karger, F. E., Varela, R., Thunell, R., Luerssen, R., Hu, C., & Walsh, J. J. (2005). The importance of continental margins in the global carbon cycle. *Geophysical Research Letters*, 32(1), 1–4.
<https://doi.org/10.1029/2004GL021346>
- Müller, P. J., & Suess, E. (1979). Productivity, sedimentation rate, and sedimentary organic matter in the oceans: I. Organic carbon preservation. *Deep-Sea Research*, 26A, 1347–1362.
- Mustapha, S. Ben, Bélanger, S., & Larouche, P. (2012). Evaluation of ocean color algorithms in the southeastern beaufort sea, canadian arctic: New parameterization using SeaWiFS, MODIS, and MERIS spectral bands. *Canadian Journal of Remote Sensing*, 38(5), 535–556.
<https://doi.org/10.5589/m12-045>
- Nieto-Moreno, V., Martínez-Ruiz, F., Giralt, S., Jiménez-Espejo, F., Gallego-Torres, D., Rodrigo-Gámiz, M., et al. (2011). Tracking climate variability in the western Mediterranean during the Late Holocene: A multiproxy approach. *Climate of the Past*, 7(4), 1395–1414.
<https://doi.org/10.5194/cp-7-1395-2011>
- O'Reilly, J. E., Maritorena, S., O'Brien, M. C., Siegel, D. a, Toole, D., Menzies, D., et al. (2000). SeaWiFS Postlaunch Calibration and Validation Analyses, part 3. *NASA Tech. Memo.*, 11, 1–49.
- Pace, M. L., Knauer, G. a, Karl, D. M., & Martin, J. H. (1987). Primary production, new production and vertical flux in the eastern Pacific Ocean. *Nature*. <https://doi.org/10.1038/325803a0>
- Pedersen, T. F. (1983). Increased productivity in the eastern equatorial Pacific during the last glacial maximum (19000–14000 yr B.P.). *Geology*, 11(1971), 16–19.

- Sarmiento, J. L., & Gruber, N. (2006). *Ocean Biogeochemical Dynamics*. New Jersey: Princeton Univ. Press. <https://doi.org/10.1063/1.2754608>
- Sathyendranath, S., Cota, G., Stuart, V., Maass, H., & Platt, T. (2001). Remote sensing of phytoplankton pigments: A comparison of empirical and theoretical approaches. *International Journal of Remote Sensing*, *22*(2–3), 249–273. <https://doi.org/10.1080/014311601449925>
- Schlitzer, R. (2002). Carbon export fluxes in the Southern Ocean: Results from inverse modeling and comparison with satellite-based estimates. *Deep-Sea Research Part II: Topical Studies in Oceanography*, *49*(9–10), 1623–1644. [https://doi.org/10.1016/S0967-0645\(02\)00004-8](https://doi.org/10.1016/S0967-0645(02)00004-8)
- Schlünz, B., & Schneider, R. R. (2000). Transport of terrestrial organic carbon to the oceans by rivers: re-estimating flux- and burial rates. *International Journal of Earth Sciences*, *88*(4), 599–606. <https://doi.org/10.1007/s005310050290>
- Schoepfer, S. D., Shen, J., Wei, H., Tyson, R. V., Ingall, E., & Algeo, T. J. (2015). Total organic carbon, organic phosphorus, and biogenic barium fluxes as proxies for paleomarine productivity. *Earth-Science Reviews*, *149*, 23–52. <https://doi.org/10.1016/j.earscirev.2014.08.017>
- Schubert, C. J., Stein, R., & Calvert, S. E. (2001). Tracking nutrient and productivity variations over the last deglaciation in the Arctic Ocean. *Paleoceanography*, *16*(2), 199–211. <https://doi.org/10.1029/2000PA000503>
- Schwarzkopf, T. A. (1993). Model for prediction of organic carbon content in possible source rocks. *Marine and Petroleum Geology*, *10*(5), 478–492. [https://doi.org/10.1016/0264-8172\(93\)90049-X](https://doi.org/10.1016/0264-8172(93)90049-X)
- Siegel, D. A., Buesseler, K. O., Doney, S. C., Salliey, S. F., Behrenfeld, M. J., & Boyd, P. W. (2014). Global assessment of ocean carbon export by combining satellite observations and food-web models. *Global Biogeochemical Cycles*, *28*, 181–196. <https://doi.org/10.1002/2013GB004743>.Received
- Stramska, M., Stramski, D., Ryszard, H., Kaczmarek, S., & Joanna, S. (2003). Bio-optical relationships and ocean color algorithms for the north polar region of the Atlantic. *Journal of Geophysical Research*, *108*(C5), 3143. <https://doi.org/10.1029/2001JC001195>
- Stramski, D., & Tegowski, J. (2001). Effects of intermittent entrainment of air bubbles by breaking wind waves on ocean reflectance and underwater light field. *Journal of Geophysical Research*, *106*(C12), 31345–31360. <https://doi.org/10.1029/2000JC000461>
- Suess, E. (1980). Particulate organic carbon flux in the oceans - surface productivity and oxygen

- utilization. *Nature*, *288*(20), 260–263. <https://doi.org/10.1038/288260a0>
- Summerhayes, C. P., Kroon, D., Rosell-Mele, A., Jordan, R. W., Schrader, H.-J., Hearn, R., et al. (1995). Variability in the Benguela Current upwelling system over the past 70,000 years. *Progress in Oceanography*, *35*(3), 207–251. [https://doi.org/10.1016/0079-6611\(95\)00008-5](https://doi.org/10.1016/0079-6611(95)00008-5)
- Volpe, G., Santoleri, R., Vellucci, V., Ribera d'Alcalà, M., Marullo, S., & D'Ortenzio, F. (2007). The colour of the Mediterranean Sea: Global versus regional bio-optical algorithms evaluation and implication for satellite chlorophyll estimates. *Remote Sensing of Environment*, *107*(4), 625–638. <https://doi.org/10.1016/j.rse.2006.10.017>
- Waite, J. N., & Mueter, F. J. (2013). Spatial and temporal variability of chlorophyll-a concentrations in the coastal Gulf of Alaska, 1998–2011, using cloud-free reconstructions of SeaWiFS and MODIS-Aqua data. *Progress in Oceanography*, *116*, 179–192. <https://doi.org/10.1016/j.pocean.2013.07.006>
- Wang, J., & Cota, G. F. (2003). Remote-sensing reflectance in the Beaufort and Chukchi seas: observations and models. *Applied Optics*, *42*(15), 2754–2765. <https://doi.org/10.1364/AO.42.002754>
- Weber, T., Cram, J. A., Leung, S. W., DeVries, T., & Deutsch, C. (2016). Deep ocean nutrients imply large latitudinal variation in particle transfer efficiency. *Proceedings of the National Academy of Sciences*, *113*(31), 8606–8611. <https://doi.org/10.1073/pnas.1604414113>
- Werdell, P. J., McKinna, Lachlan, I. W., Boss, E., Ackleson, S. G., Craig, S. E., Gregg, W. W., et al. (2018). An overview of approaches and challenges for retrieving marine inherent optical properties from ocean color remote sensing. *Treatise on Geomorphology*, *160*, 186–212. <https://doi.org/10.1016/j.pocean.2018.01.001>
- Xu, Y., Wang, L., Yin, X., Ye, X., Li, D., Liu, S., et al. (2017). The influence of the Sunda Strait opening on paleoenvironmental changes in the eastern Indian Ocean. *Journal of Asian Earth Sciences*, *146*(December 2016), 402–411. <https://doi.org/10.1016/j.jseaes.2017.06.014>
- Yu, F., Fu, X., Xu, G., Wang, Z., Chen, W., Zeng, S., et al. (2019). Geochemical, palynological and organic matter characteristics of the Upper Triassic Bagong Formation from the North Qiangtang Basin, Tibetan Plateau. *Palaeogeography, Palaeoclimatology, Palaeoecology*, *515*(June 2017), 23–33. <https://doi.org/10.1016/j.palaeo.2017.12.002>
- Zhao, M., Mercer, J. L., Eglinton, G., Higginson, M. J., & Huang, C. Y. (2006). Comparative molecular biomarker assessment of phytoplankton paleoproductivity for the last 160 kyr off Cap Blanc, NW Africa. *Organic Geochemistry*, *37*(1), 72–97.

<https://doi.org/10.1016/j.orggeochem.2005.08.022>

Zonneveld, K. A. F., Versteegh, G. J. M., Kasten, S., Eglinton, T. I., Emeis, K., Huguet, C., & Koch, B. P. (2010). Selective preservation of OM in marine environment, 2010.pdf, 483–511.
<https://doi.org/10.5194/bg-7-483-2010>

Chapter 5

Nitrogen isotopes: constraints of nutrient proxies



Picture author: Caddo Pigment

5. Nitrogen isotopes: constraints of nutrient proxies

5.1. Introduction

Nutrients availability in the surface ocean is an important control on primary productivity (PP), as it is a limiting factor for carrying out phytoplankton photosynthesis in the vast majority of the global ocean. Phytoplankton requires several nutrients, such as nitrate, phosphate and iron. However, nitrate is the limiting nutrient in most of the ocean (70%) (Bristow et al., 2017). Therefore, nitrate availability can provide information on nutrient conditions and PP in the global ocean.

For studying nutrient conditions in past periods, paleoceanographers measure nitrogen isotopic ratios in marine sediments, as the preferential assimilation of ^{14}N relative to ^{15}N occurs when nutrients are abundant due to different uptake kinetics velocities (Wada & Hattori, 1978). Since the main source of nitrate in the surface ocean comes from deeper waters, where their isotopic composition is uniform ($\delta^{15}\text{N} \approx 5 \text{‰}$) (Sigman et al., 2000), variations in sea-surface $\delta^{15}\text{N}$ of nitrate and produced organic nitrogen, might mainly depend on phytoplankton nitrate depletion on surface waters.

Accordingly, nitrate concentrations in the surface ocean were found to be inversely correlated to $\delta^{15}\text{N}$ contents in plankton (Wada & Hattori, 1976). Later, the nitrate surface signal was found to be transferred and preserved in sediments (Altabet & Francois, 1994). Therefore, bulk sedimentary nitrogen isotopic signal ($\delta^{15}\text{N}_{\text{bulk}}$) has been considered a reliable proxy for tracking past changes in sea-surface nutrient conditions and infer past PP.

However, $\delta^{15}\text{N}_{\text{bulk}}$ is limited by the inherent heterogeneity and different diagenetic pathways of organic nitrogen accumulated in the sediment (Wada, 1980), which can overprint the nitrogen signal and thus, complicate the interpretation of the proxy (Enders et al., 2008; Junium et al., 2015; Sachs & Repeta, 1999; Tyler et al., 2010). Hence, in order to avoid the effect of multiple sources and diagenetic pathways on the isotopic signal, chlorin-specific nitrogen isotopic signal ($\delta^{15}\text{N}_{\text{chlorin}}$) has been proposed and applied as an alternative proxy for tracking past nutrient conditions and past PP (Enders et al., 2008; Fulton et al., 2018; Fulton et al., 2012; Kusch et al., 2010; Naeher et al., 2016a; Naeher et al., 2016b; Sachs & Repeta, 1999; Tyler et al., 2010). Chlorins include chlorophyll-*a* (Chl *a*), the main pigment used in photosynthesis, and its degradation products. Thus, in contrast to $\delta^{15}\text{N}_{\text{bulk}}$, $\delta^{15}\text{N}_{\text{chlorin}}$ provides exclusively information about nutrient conditions and past PP.

Nevertheless, the reliability in the use of $\delta^{15}\text{N}_{\text{bulk}}$ is not devoid of controversy. A global comparison between sediment traps and surface sediment (Robinson et al., 2012), and comparisons between $\delta^{15}\text{N}_{\text{bulk}}$ and $\delta^{15}\text{N}_{\text{chlorin}}$ have presented consistent agreement (Fulton et al., 2012; Higgins et al.,

2010; Kusch et al., 2010). Hence, the authors suggested $\delta^{15}\text{N}_{\text{bulk}}$ provides a good means for evaluating past nutrient conditions and past PP in the surface ocean. However, comparisons between $\delta^{15}\text{N}_{\text{bulk}}$ and $\delta^{15}\text{N}_{\text{chlorin}}$ have shown significant differences (Junium et al., 2015; Sachs & Repeta, 1999; Tyler et al., 2010), which leads to the authors suggest that the interpretation of $\delta^{15}\text{N}_{\text{bulk}}$ is compromised by multiple sources and diagenetic alteration.

Besides, the interpretation of $\delta^{15}\text{N}_{\text{chlorin}}$ proxy relies on the assumption that $\delta^{15}\text{N}_{\text{chlorin}}$ reflects the original Chl *a* nitrogen isotopic signal ($\delta^{15}\text{N}_{\text{chla}}$). This is based on the fact that the chemical bonds that are involved in the reaction from Chl *a* to the other chlorins do not link nitrogen atoms, so no nitrogen fractionation is expected during the transformation. In fact, Chl *a* derivatives were found to maintain the nitrogen isotopic signature from Chl *a* in some locations (Junium et al., 2015; Kusch et al., 2010; Tyler et al., 2010). However, nitrogen isotopic signal discrepancies between Chl *a* and the rest of chlorins, as well as among the different chlorins, were found in other sites (Kusch et al., 2010; Naeher et al., 2016b).

Therefore, the consistency between sedimentary bulk, chlorin and Chl *a* nitrogen isotopes is still controversial and the general limitations of the global applicability of these proxies are not well constrained. In this paper, we compare $\delta^{15}\text{N}_{\text{bulk}}$ with $\delta^{15}\text{N}_{\text{chlorin}}$ and $\delta^{15}\text{N}_{\text{chla}}$ from a global suite of core-top sediments, and study $\delta^{15}\text{N}_{\text{chlorin}}$ variability for evaluating general constraints in the use of these proxies for tracking past nutrient conditions and past PP.

5.2. Methods

We have assembled 137 nitrogen isotope measurements from 58 different locations, including marine and lacustrine sediments (Figure 22). Most of the data (70% of the compilation) are obtained from previous published studies (Appendix 2), while we have analysed the rest in the Japan Agency for Marine-Earth Science and Technology, following the methodology explained hereafter. Monthly SSchl_a concentration for the last 20 years were obtained from the GlobColour Project (<http://globcolour.info>), and oxygen concentration in bottom waters (bottom [O₂]) from NOAA database. Water depth covers the range from 16 to 5,200 meters.

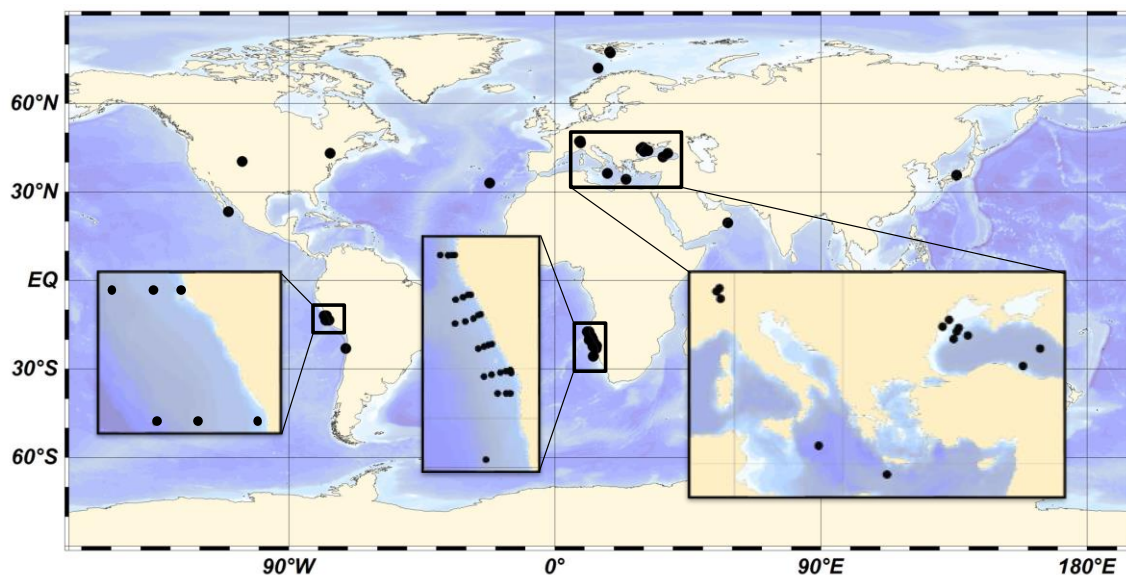


Figure 22. Global sediments distribution. The compilation includes 2,945 nitrogen isotopic measurements in 47 locations.

5.2.1. Bulk nitrogen isotopic analysis

Sediment samples were prepared for elemental analysis-isotope ratio mass spectrometry (EA-IRMS) by freeze-drying, powdering and sealed in tin capsules. EA-IRMS was performed using a Thermo Flash 1112 Elemental Analyzer interfaced to a DELTA V Advantage IRMS system via a ConFlo III interface (Thermo-Fisher). Standard deviations were better than 0.1 based on repeated analysis of the standard IAEA600. Data are reported using delta notation relative to atmospheric N_2 .

5.2.2. Chlorin-specific nitrogen isotopic analysis

Chlorin-specific nitrogen isotopes were analysed based on the method described in (Naeher, et al., 2016b). We did some modifications in the methodology for increasing the efficiency (the extraction time was reduced from 45 min to 15 min) and the amount of Chl *a* extracted (x1.7). In brief, freeze-dried sediment (5-25g) was extracted using acetone (x3 with twice the sample volume) and an ultrasonic probe (Test Branson Sonifier 450) during 5 min at 4 W, followed by centrifugation at 2,500 rpm and 17 °C during 10 min. The 3 supernatants were reduced under a cold stream of argon, sonicated and mixed before liquid-liquid extraction (x3) with MiliQ water (equal to the acetone volume) and hexane (8 mL). Then, the mixture was shaken during 1 min and centrifuged, and the hexane layer was recovered and dried under a cold stream of argon. All steps were carried out under careful exclusion of light irradiation.

For chlorins isolation, the sample was dissolved in 100 μ L (x2) of N,N-dimethylformamide (DMF), and filtered. Then, 50 μ L of the extracted sample was analysed (x4) by reversed-phase high performance liquid chromatography (HPLC), using an Agilent Infinity 1260 series HPLC equipped

with a photodiode array detector (PDA) and fraction collector. Chlorins separation was achieved using an Agilent Eclipse XDB-C18 column (250 mm × 4.6 mm; 5 μm) and an Agilent Eclipse XDB-C18 guard column (12.5 mm × 4.6 mm; 5 μm). The pigments were eluted isocratically with 75% A and 25% B for 5 min and then with a linear gradient to 50% B for 50 min at 1 mL·min⁻¹, where A=acetonitrile/pyridine (100:0.5; v:v) and B=ethyl acetate/pyridine (100:0.5; v:v). The oven temperature was kept constant at 30 °C and the range of recorded wavelengths of the PDA was set to 250–800 nm. Chlorins were identified by comparison with published UV–VIS spectra and relative retention times. The 4 eluted fractions of each chlorin were mixed and dried under a cold stream of argon.

For purification, the isolated chlorins were dissolved in 80 μL of DMF. Then, 40 μL were analysed (x2) using an Agilent Eclipse PAH column (250 mm × 4.6 mm; 5 μm) with an Agilent Eclipse PAH guard column (12.5 mm × 4.6 mm; 5 μm). Chlorins were eluted isocratically using 30% B for 7 min, followed by a linear gradient to 55% B for 7 min and then to 100% B for 4 min. The flow rate was constant at 1 mL·min⁻¹. The oven temperature was kept at 15°C for the isolation of Chl *a* and pheophytin-*a* (Phe *a*), whereas 30°C was used for all other pigments. The 2 eluted fractions of each chlorin were mixed and dried under a cold stream of argon.

For isotope analysis, samples were transferred to pre-cleaned tin cups by trichloromethane and dried at 35°C. EA-IRMS was performed using a modified Flash EA 1112 Automatic Elemental Analyser connected to a Thermo Finnigan Delta plus XP isotope ratio mass spectrometer via a ConFlo III (Ogawa et al., 2010). Data are reported using delta notation relative to atmospheric N₂. The analytical errors were within 0.9‰ based on repeated analysis of Nickel octaethylporphyrin ($\delta^{15}\text{N}=0.86\pm 0.03\text{‰}$).

5.3. Results and discussion

5.3.1. Bulk and chlorin-specific nitrogen isotopes

In Figure 23 we compare $\delta^{15}\text{N}_{\text{bulk}}$ with $\delta^{15}\text{N}_{\text{chl}a}$ and $\delta^{15}\text{N}_{\text{chlorin}}$ at global scale. Overall, there is a correlation between the nitrogen compound specific signature of pigments and the sedimentary bulk value, with considerable scatter.

Pooling together data from different studies allowed us to compare $\delta^{15}\text{N}_{\text{bulk}}$ and $\delta^{15}\text{N}_{\text{chl}a}$ values (Figure 23 a). We obtained a linear correlation with a coefficient of determination (R^2) of 0.53 between $\delta^{15}\text{N}_{\text{bulk}}$ and $\delta^{15}\text{N}_{\text{chl}a}$, which indicates that both measurements deliver a similar isotopic fingerprint at a global scale. The intercept of the regression that we obtained is 5.49, which is concordant with the discrepancy of $5.39\pm 0.67\text{‰}$ found between $\delta^{15}\text{N}_{\text{bulk}}$ and $\delta^{15}\text{N}_{\text{chl}a}$ in previous

studies, and probably reflect the nitrogen isotopic depletion of Chl *a* that occurs during its biosynthesis (Sachs et al., 1999).

It must be born in mind that Chl *a* is not present in all sediments. Hence, we compared $\delta^{15}\text{N}_{\text{bulk}}$ and $\delta^{15}\text{N}_{\text{chlorin}}$ in Figure 23 b and c. Chlorin nitrogen isotopic data is represented by individual chlorins in Figure 23 b, and by the average of the different chlorins present in each sample, with the standard deviation indicated by bars, in Figure 23 c. We obtained a linear correlation with a R^2 of 0.43 between $\delta^{15}\text{N}_{\text{bulk}}$ and the averaged $\delta^{15}\text{N}_{\text{chlorin}}$, which suggests both proxies are concordant at global scales.

Therefore, our results indicate that both bulk and chlorin compound specific nitrogen isotopic ratios provide similar information. Our results are in agreement with those that found essentially equal values of $\delta^{15}\text{N}_{\text{bulk}}$ in sinking flux and surface sediment (Altabet et al., 1999; Kienast et al., 2002; Thunell et al., 2004), and those that found a consistent offset of 5‰ between bulk and total chlorins in sediment (Higgins et al., 2010).

Nevertheless, high scatter is apparent in our graphics in Figure 23. $\delta^{15}\text{N}_{\text{bulk}}$ might present uncertainties related to diagenetic alteration of its complex chemical composition, since the diverse organic nitrogen compounds present in the sediment might have different pathways of degradation (Junium et al., 2015; Sachs & Repeta, 1999; Tyler et al., 2010; Wada, 1980). Besides, $\delta^{15}\text{N}_{\text{chlorin}}$ might present other uncertainties related to diagenetic and environmental factors. However, factors that control $\delta^{15}\text{N}_{\text{chlorin}}$ variability in sediment have not been thoroughly addressed in previous studies.

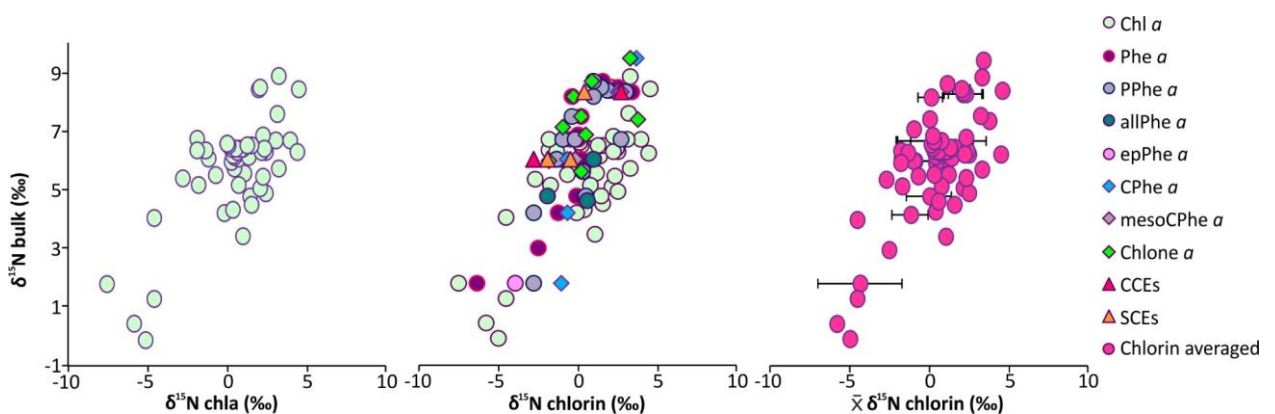


Figure 23. Comparison between the bulk nitrogen isotopic signal ($\delta^{15}\text{N}_{\text{bulk}}$) and **a.** the chlorophyll-*a* nitrogen isotopic signal ($\delta^{15}\text{N}_{\text{Chla}}$), **b.** the individual chlorin nitrogen isotopic signal ($\delta^{15}\text{N}_{\text{chlorin}}$) and **c.** the average of the different chlorins present in the samples ($\bar{x} \delta^{15}\text{N}_{\text{chlorin}}$), with the standard deviation indicated by bars.

5.3.2. Chlorin-compound specific nitrogen isotopic variability

$\delta^{15}\text{N}_{\text{chlorin}}$ variability can be gauged in Figure 24, which shows the spread of $\delta^{15}\text{N}_{\text{chlorin}}$ for every core-top location assembled in this study. Considerable differences on the nitrogen isotopic signal between the different chlorins were found in some of our core-top samples, such as those from the Barents sea, and Zurich, Rotsee and Green Fayetteville lakes. In contrast, other locations present similar values, which is the case of the California current. Otherwise, Black sea and Peru margin show both different and similar data depending on the sample. Therefore, no apparent patterns could be found related to samples location, which might represent the interplay of specific environmental conditions.

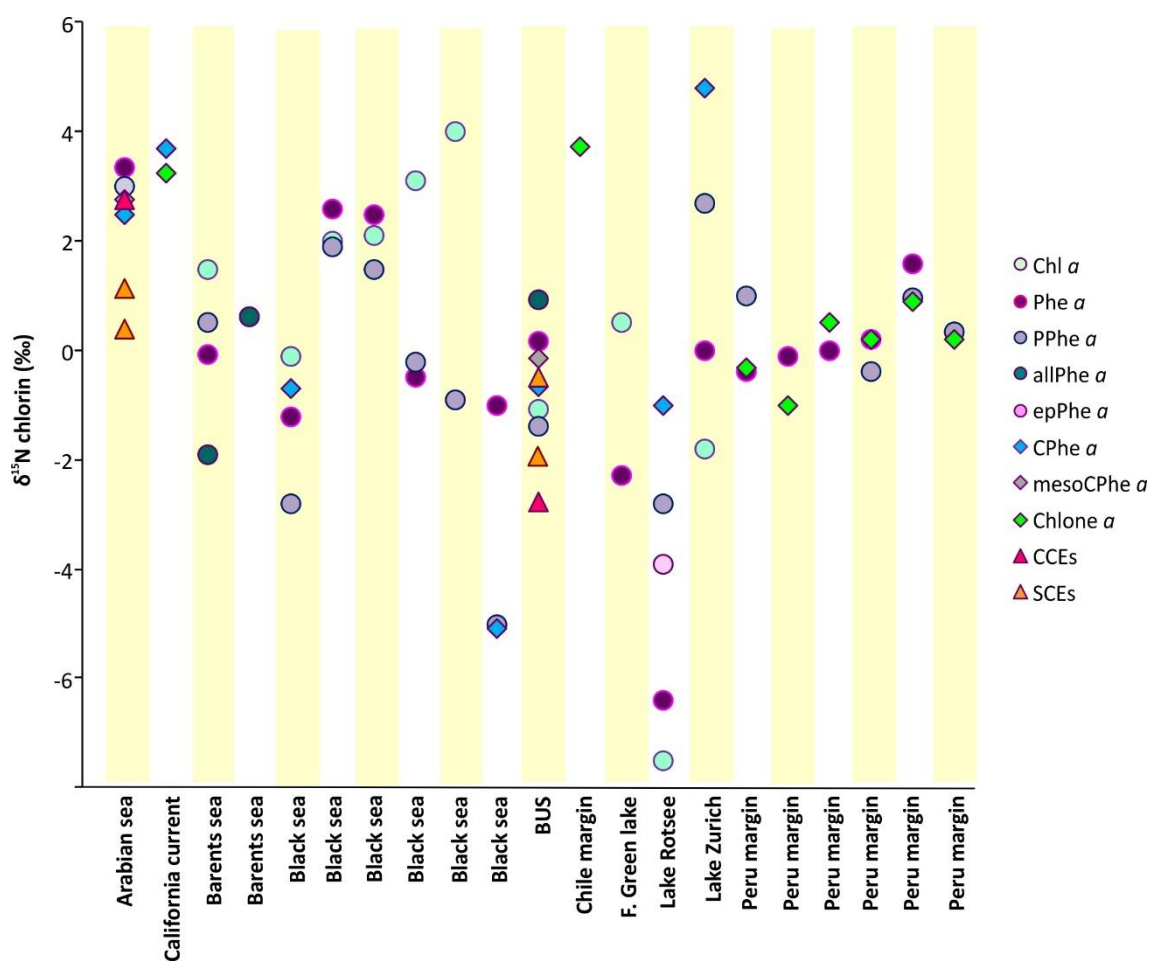


Figure 24. Chlorin nitrogen isotopic signal ($\delta^{15}\text{N}_{\text{chlorin}}$) from core-top sediment samples. Chlorin classification is based on their degradation pathway: senescence, zooplankton grazing and secondary degradation products are represented by circles, diamonds and triangles, respectively.

$\delta^{15}\text{N}_{\text{chlorin}}$ variability might be also affected by the nitrogen isotopic fractionation that might occur during the transformation from Chl *a* into its different degradation products. Compounds that undergo more alterations in their chemical structure, such as secondary degradation products and those that can be originated during zooplankton grazing, would be more likely to experience

isotopic fractionation than primary degradation products formed by senescence, whose formation pathways englobe less chemical reactions (Chikaraishi et al., 2007; Goericke et al., 1999; Louda et al., 2008). However, Figure 24 shows that PPhe *a*, a primary degradation product formed by senescence, and SCEs, secondary degradation products formed by sterols esterification, present similar nitrogen isotopic values than Chl *a* in the BUS, but different in the Arabian sea or Peru margin. Thus, discrepancies on nitrogen isotopic data do not seem to be primarily related with the specific pigment or its degradation pathway.

Nevertheless, $\delta^{15}\text{N}_{\text{chlorin}}$ variability in Figure 24 includes all conditions involved in altering $\delta^{15}\text{N}_{\text{chlorin}}$, which makes it difficult to interpret and obtain detailed information about the role of the different factors. To thoroughly evaluate the effect that Chl *a* transformations into its different degradation products might have on $\delta^{15}\text{N}_{\text{chlorin}}$, we calculated the differences between $\delta^{15}\text{N}_{\text{Chla}}$ and $\delta^{15}\text{N}_{\text{chlorin}}$ for each degradation product in each sample. Figure 25 shows the average of the differences of all samples corresponding to each degradation product. Since both Chl *a* and at least one derivative could only be found in 20 samples, we also considered Phe *a*, the first Chl *a* derivative, as a reference for calculating the differences with the rest of chlorins. Our results show no significant differences between Chl *a* or Phe *a* and the rest of chlorins, with the exception of an epimer of Phe *a* and CCEs, senescence and secondary products, respectively. Besides, the Phe *a* epimer and CCEs show no significant differences with other chlorins, whose ranges cover similar values than Chl *a* or Phe *a*. Thus, our data do not show evidence of significant differences in the $\delta^{15}\text{N}_{\text{chlorin}}$ based on the specific compound or the degree of degradation. Hence, $\delta^{15}\text{N}_{\text{chlorin}}$ variability observed in Figure 24 is not likely to be explained by nitrogen isotopic fractionation during the transformation of Chl *a* into its degradation products.

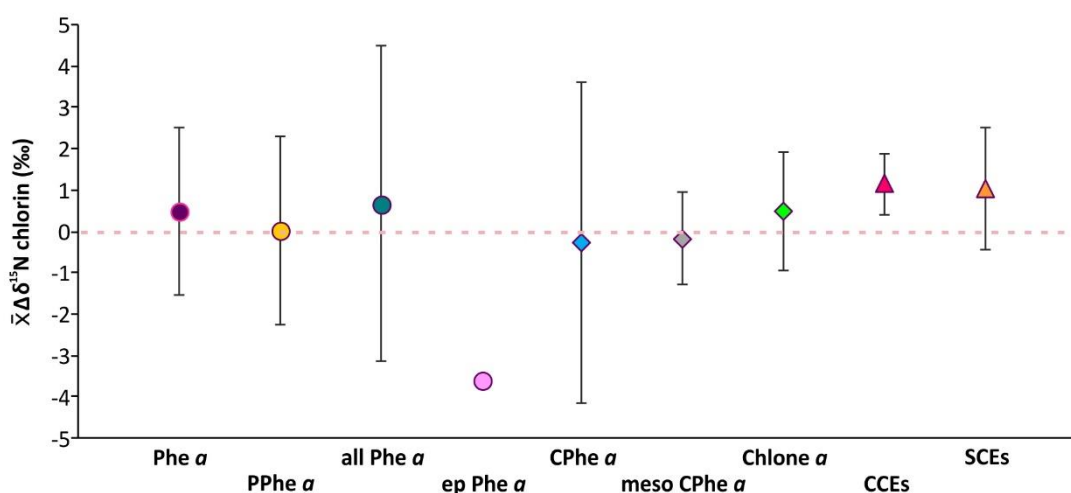


Figure 25. The averages and the standard deviations of the differences between chlorophyll-*a* or pheophytin-*a* nitrogen isotopic signal ($\delta^{15}\text{N}_{\text{Chla}}$ or $\delta^{15}\text{N}_{\text{Phea}}$) and the rest of chlorins. This graphic includes core-top sediment samples.

Phytoplankton blooms have also been discussed to potentially produce differences on the isotopic signal of individual chlorins accumulated in the sediment (Kusch et al., 2010; Naehler, et al., 2016b). It would be probably caused by the different isotopic signal of individual chlorins produced during blooms occurring at different times of the year by different phytoplankton communities (King, 1995). Hence, more episodic productivity regions might present higher variability on $\delta^{15}\text{N}_{\text{chlorin}}$ than more constant productivity regions. To study the influence that phytoplankton blooms might have on $\delta^{15}\text{N}_{\text{chlorin}}$ variability, we compared the differences between $\delta^{15}\text{N}_{\text{chla}}$ and $\delta^{15}\text{N}_{\text{chlorin}}$ with the seasonal variation index (SVI) (Lutz et al., 2007), for every core-top location (Figure 26 a). We determined the SVI for every location by calculating the average of every month for the whole period of satellite data available, which is 20 years, and then the average and the standard deviation of the calculated averages. It should be noted that this comparison could only be undertaken in very few locations, where sufficient data were available. Our results reveal that samples that present high SVI values, which represent more episodic productivity regions, are related to lower differences on $\delta^{15}\text{N}_{\text{chlorin}}$ between pigments than more constant productivity regions. Thus, our data do not suggest phytoplankton blooms as the main cause of $\delta^{15}\text{N}_{\text{chlorin}}$ variability.

Bottom $[\text{O}_2]$ might also play a role in modifying $\delta^{15}\text{N}_{\text{chlorin}}$, as the severity of the isotopic alteration of organic matter decomposition is generally suggested to be controlled by bottom $[\text{O}_2]$, arguably because aerobic and anaerobic bacteria use different metabolic pathways (Lehmann et al., 2002; Möbius et al., 2010; Sachs & Repeta, 1999). To approach the role that bottom $[\text{O}_2]$ might have on $\delta^{15}\text{N}_{\text{chlorin}}$ variability, we compared when available, bottom $[\text{O}_2]$ with the differences between $\delta^{15}\text{N}_{\text{chla}}$ and $\delta^{15}\text{N}_{\text{chlorin}}$ for every core-top location (Figure 26 b). Our results show nitrogen isotopes can be enriched and depleted in both, well-oxygenated and anoxic depositional environments, and present a huge range of nitrogen isotopic alteration in both environments. Hence, our results cannot confirm bottom $[\text{O}_2]$ as the principal factor in controlling $\delta^{15}\text{N}_{\text{chlorin}}$ variability.

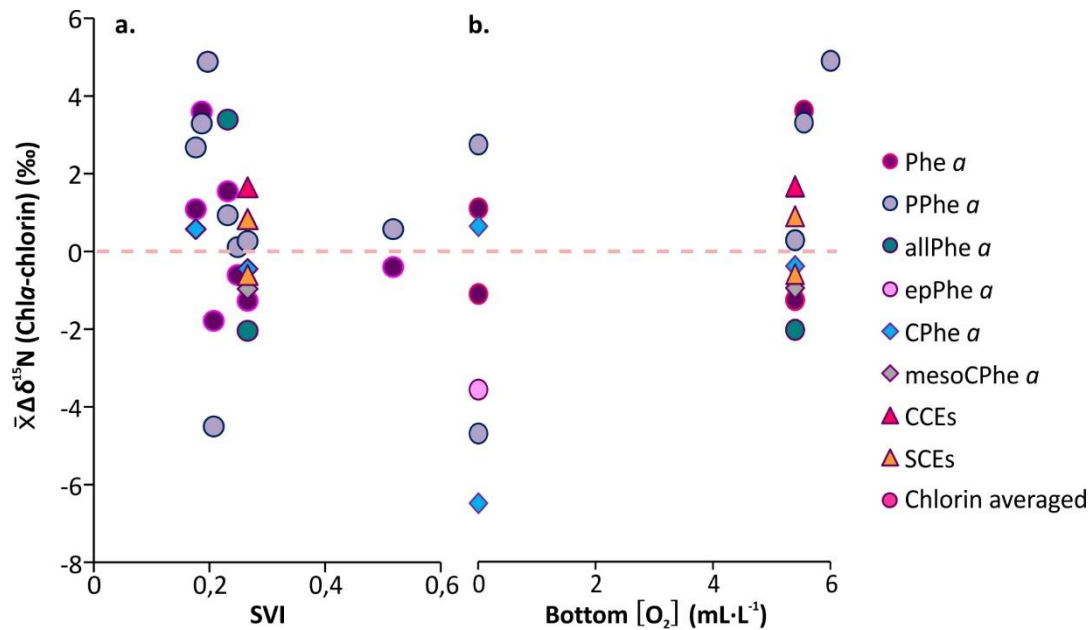


Figure 26. Comparison of the differences between chlorophyll-*a* and chlorin nitrogen isotopic signal ($\delta^{15}\text{N}_{\text{chl}a}$ and $\delta^{15}\text{N}_{\text{chlorin}}$) with **a.** the seasonal variation index (SVI) and **b.** oxygen concentration in bottom waters (Bottom $[\text{O}_2]$), for core-top sediment sample locations.

5.4. Conclusions

Bulk and chlorin nitrogen isotopic proxies provide equivalent information on past changes in nutrient conditions and past PP at a global scale. However, compound specific $\delta^{15}\text{N}_{\text{chlorin}}$ analysis requires a) high amount of sediment sample (>20 g), which can be an important limitation in paleoclimate studies; b) a modified EA-IRMS, which is not available in most of laboratories; and c) a tedious and time-consuming methodology, which needs high volume of solvents. Therefore, to obtain information on past surface ocean nutrient conditions, our study indicates that the use of $\delta^{15}\text{N}_{\text{bulk}}$ is far more straightforward and cheaper than compound specific $\delta^{15}\text{N}_{\text{chlorin}}$ analysis. Nevertheless, chlorophyll compound-specific analysis still might be needed in some specific regions where $\delta^{15}\text{N}_{\text{bulk}}$ is biased by postdepositional diagenetic alteration.

Our study on $\delta^{15}\text{N}_{\text{chlorin}}$ reflects high variability between individual chlorins, which suggests chemical, biological and physical processes occurring from the surface to the sediments might alter $\delta^{15}\text{N}_{\text{chlorin}}$. Hence, our results are at odds with the assumption that compound-specific $\delta^{15}\text{N}_{\text{chlorin}}$ variability in sediment can be used to track changes in sedimentary $\delta^{15}\text{N}_{\text{chl}a}$. Nevertheless, our results indicate there is no nitrogen isotopic fractionation during the transformation of Chl *a* into its degradation products. Besides, we cannot confirm that neither phytoplankton blooms nor oxygen depositional conditions are the main cause of $\delta^{15}\text{N}_{\text{chlorin}}$ variability. Therefore, further studies are needed to identify the principal factors controlling

$\delta^{15}\text{N}_{\text{chlorin}}$ variability to better constrain the applicability of compound-specific $\delta^{15}\text{N}_{\text{chlorin}}$ as a proxy for reconstructing past nutrient conditions and past PP at global scales.

5.5. References

- Altabet, M. a., Pilskaln, C., Thunell, R., Pride, C., Sigman, D., Chavez, F., & Francois, R. (1999). The nitrogen isotope biogeochemistry of sinking particles from the margin of the Eastern North Pacific. *Deep Sea Research Part I: Oceanographic Research Papers*, 46(4), 655–679. [https://doi.org/10.1016/S0967-0637\(98\)00084-3](https://doi.org/10.1016/S0967-0637(98)00084-3)
- Altabet, M. A., & Francois, R. (1994). Sedimentary nitrogen isotopic ratio as a recorder for surface ocean nitrate utilization. *Global Biogeochemical Cycles*, 8(1), 103–116. <https://doi.org/10.1029/93GB03396>
- Bristow, L. A., Mohr, W., Ahmerkamp, S., & Kuypers, M. M. M. (2017). Nutrients that limit growth in the ocean. *Current Biology*, 27(11), R474–R478. <https://doi.org/10.1016/j.cub.2017.03.030>
- Chikaraishi, Y., Matsumoto, K., Kitazato, H., & Ohkouchi, N. (2007). Sources and transformation processes of pheopigments: Stable carbon and hydrogen isotopic evidence. *Organic Geochemistry*, 38, 985–1001.
- Enders, S. K., Pagani, M., Pantoja, S., Baron, J. S., Wolfe, A. P., Pedentchouk, N., & Nunez, L. (2008). Compound-specific stable isotopes of organic compounds from lake sediments track recent environmental changes in an alpine ecosystem, Rocky Mountain National Park, Colorado. *Limnology and Oceanography*, 53(4), 1468–1478.
- Fulton, J. M., Arthur, M. A., Thomas, B., & Freeman, K. H. (2018). Pigment carbon and nitrogen isotopic signatures in euxinic basins. *Geobiology*, 16(4), 429–445. <https://doi.org/10.1111/gbi.12285>
- Fulton, James M., Arthur, M. A., & Freeman, K. H. (2012). Black Sea nitrogen cycling and the preservation of phytoplankton $\delta^{15}\text{N}$ signals during the Holocene. *Global Biogeochemical Cycles*, 26(2), n/a-n/a. <https://doi.org/10.1029/2011GB004196>
- Goericke, R., Shankle, A., & Repeta, D. J. (1999). Novel carotenol chlorin esters in marine sediments and water column particulate matter. *Geochimica et Cosmochimica Acta*, 63(18), 2825–2834. [https://doi.org/10.1016/S0016-7037\(99\)00155-6](https://doi.org/10.1016/S0016-7037(99)00155-6)
- Higgins, M. B., Robinson, R. S., Carter, S. J., & Pearson, A. (2010). Evidence from chlorin nitrogen isotopes for alternating nutrient regimes in the Eastern Mediterranean Sea. *Earth and Planetary Science Letters*, 290(1–2), 102–107. <https://doi.org/10.1016/j.epsl.2009.12.009>

- Junium, C. K., Arthur, M. A., & Freeman, K. H. (2015). Compound-specific $\delta^{15}\text{N}$ and chlorin preservation in surface sediments of the Peru Margin with implications for ancient bulk $\delta^{15}\text{N}$ records. *Geochimica et Cosmochimica Acta*, *160*, 306–318.
<https://doi.org/10.1016/j.gca.2014.12.018>
- Kienast, S. S., Calvert, S. E., & Pedersen, T. F. (2002). Nitrogen isotope and productivity variations along the northeast Pacific margin over the last 120 kyr: Surface and subsurface paleoceanography. *Paleoceanography*, *17*(4), 7-1-7–17.
<https://doi.org/10.1029/2001pa000650>
- King, L. L. (1995). A mass balance of chlorophyll degradation product accumulation in Black Sea sediments. *Deep-Sea Research Part I*, *42*(6), 919–942. [https://doi.org/10.1016/0967-0637\(95\)00029-6](https://doi.org/10.1016/0967-0637(95)00029-6)
- Kusch, S., Kashiyama, Y., Ogawa, N. O., Altabet, M., Butzin, M., Friedrich, J., et al. (2010). Implications for chloro- and pheopigment synthesis and preservation from combined compound-specific $\delta^{13}\text{C}$, $\delta^{15}\text{N}$, and $\Delta^{14}\text{C}$ analysis. *Biogeosciences*, *7*(12), 4105–4118.
<https://doi.org/10.5194/bg-7-4105-2010>
- Lehmann, M. F., Bernasconi, S. M., Barbieri, A., & McKenzie, J. A. (2002). Preservation of organic matter and alteration of its carbon and nitrogen isotope composition during simulated and in situ early sedimentary diagenesis. *Geochimica et Cosmochimica Acta*, *66*(20), 3573–3584.
[https://doi.org/10.1016/S0016-7037\(02\)00968-7](https://doi.org/10.1016/S0016-7037(02)00968-7)
- Louda, J. W., Neto, R. R., Magalhaes, A. R. M., & Schneider, V. F. (2008). Pigment alterations in the brown mussel *Perna perna*. *Comparative Biochemistry and Physiology - B Biochemistry and Molecular Biology*, *150*(4), 385–394. <https://doi.org/10.1016/j.cbpb.2008.04.008>
- Lutz, M. J., Caldeira, K., Dunbar, R. B., & Behrenfeld, M. J. (2007). Seasonal rhythms of net primary production and particulate organic carbon flux to depth describe the efficiency of biological pump in the global ocean. *Journal of Geophysical Research: Oceans*, *112*(10), C10011.
<https://doi.org/10.1029/2006JC003706>
- Möbius, J., Lahajnar, N., & Emeis, K. C. (2010). Diagenetic control of nitrogen isotope ratios in Holocene sapropels and recent sediments from the Eastern Mediterranean Sea. *Biogeosciences*, *7*(11), 3901–3914. <https://doi.org/10.5194/bg-7-3901-2010>
- Naeher, S., Suga, H., Ogawa, N. O., Schubert, C. J., Grice, K., & Ohkouchi, N. (2016a). Compound-specific carbon and nitrogen isotopic compositions of chlorophyll a and its derivatives reveal the eutrophication history of Lake Zurich (Switzerland). *Chemical Geology*, *443*, 210–219.
<https://doi.org/10.1016/j.chemgeo.2016.09.005>

- Naeher, S., Suga, H., Ogawa, N. O., Takano, Y., Schubert, C. J., Grice, K., & Ohkouchi, N. (2016b). Distributions and compound-specific isotopic signatures of sedimentary chlorins reflect the composition of photoautotrophic communities and their carbon and nitrogen sources in Swiss lakes and the Black Sea. *Chemical Geology*, *443*, 198–209. <https://doi.org/10.1016/j.chemgeo.2016.04.029>
- Ogawa, N. O., Nagata, T., Kitazato, H., & Ohkouchi, N. (2010). Ultrasensitive elemental analyzer/isotope ratio mass spectrometer for stable nitrogen and carbon isotope analyses. *Earth, Life and Isotopes, Kyoto Univ. Press*, (January 2010), 339–353.
- Robinson, R. S., Kienast, M., Luiza Albuquerque, A., Altabet, M., Contreras, S., De Pol Holz, R., et al. (2012). A review of nitrogen isotopic alteration in marine sediments. *Paleoceanography*, *27*(4), n/a-n/a. <https://doi.org/10.1029/2012PA002321>
- Sachs, J., Repeta, D., & Goericke, R. (1999). Nitrogen and carbon isotopic ratios of chlorophyll from marine phytoplankton. *Geochimica et Cosmochimica Acta*, *63*(9), 1431–1441. Retrieved from <http://faculty.washington.edu/jsachs/lab/www/Cultures-GCA.pdf>
- Sachs, J. P., & Repeta, D. J. (1999). Oligotrophy and Nitrogen Fixation During Eastern Mediterranean Sapropel Events. *Science*, *286*(5449), 2485–2488. <https://doi.org/10.1126/science.286.5449.2485>
- Sigman, D. M., Altabet, M. A., Mccorkle, D. C., Francois, R., & Fischer, G. (2000). The $\delta^{15}\text{N}$ of nitrate in the Southern Ocean: Nitrogen cycling and circulation interior. *Journal of Geophysical Research: Oceans*, *105*, 19599–19614.
- Thunell, R. C., Muller-Karger, F., Sigman, D. M., Astor, Y., & Varela, R. (2004). Nitrogen isotope dynamics of the Cariaco Basin, Venezuela. *Global Biogeochemical Cycles*, *18*(3), n/a-n/a. <https://doi.org/10.1029/2003gb002185>
- Tyler, J., Kashiwama, Y., Ohkouchi, N., Ogawa, N., Yokoyama, Y., Chikaraishi, Y., et al. (2010). Tracking aquatic change using chlorine-specific carbon and nitrogen isotopes: The last glacial-interglacial transition at Lake Suigetsu, Japan. *Geochemistry Geophysics Geosystems*, *11*(9), Q09010. <https://doi.org/10.1029/2010GC003186>
- Wada, E. (1980). Nitrogen isotope fractionation and its significance in biogeochemical processes occurring in marine environments. *Isotope Marine Chemistry*, 375–398. Retrieved from https://www.jamstec.go.jp/biogeochem/pdf/Wada_1980.pdf
- Wada, E., & Hattori, A. (1976). Natural abundance of ^{15}N in particulate organic matter in the North Pacific Ocean. *Geochimica et Cosmochimica Acta*, *40*(2), 249–251.

[https://doi.org/10.1016/0016-7037\(76\)90183-6](https://doi.org/10.1016/0016-7037(76)90183-6)

Wada, E., & Hattori, A. (1978). Nitrogen isotope effects in the assimilation of inorganic nitrogenous compounds by marine diatoms. *Geomicrobiology Journal*, *1*(1), 85–101.
<https://doi.org/10.1080/01490457809377725>

Chapter 6

Conclusions and further research



Picture author: Wildam

6. Conclusions and further research

6.1. Main conclusions

The aim of this thesis is to evaluate the applicability and constraints of some of the most frequently used organic proxies to study the marine carbon cycle through time. In order to achieve this goal, the following specific objectives have been addressed:

Objective 1. To evaluate the use of available organic export proxies for reconstructing past PP at global scale, and their potential as quantitative paleoproductivity proxies (*Chapter 2, 3 and 4*).

Objective 2. To evaluate global constraints of available nutrient proxies used for tracking past nutrient conditions and past PP (*Chapter 5*).

In order to reach **Objective 1**, we compared remote sensing sea-surface chlorophyll-*a* (SSchla) concentration estimates, as an indicator of primary productivity (PP), with global core-top sediment compilations of organic export proxies concentration: chlorins (*Chapter 2*), alkenones (*Chapter 3*) and total organic carbon (TOC) (*Chapter 4*). We used SSchla concentration rather than PP in our study since there is no consensus on the best approach to estimate PP globally using biogeochemical models (Palevsky et al., 2016).

To accomplish **Objective 1**, we tackled the following research questions:

Research question 1.1. Are organic export proxies concentration in sediment mainly related to PP?

Our results show that the global spatial distribution of chlorins and alkenones in sediments is primarily related to SSchla concentration, rather than to depositional conditions. Therefore, this study indicates that chlorins and alkenones can be used to reconstruct past PP at global scale. The obtained calibrations are independent of the biogeographic region, which implies that it is applicable globally despite any changes in biogeochemical regimes in a given site through time.

The global TOC content variability in sediments can also be explained in a major proportion by SSchla concentration rather than by the depositional conditions evaluated in this study (bottom oxygen concentration, oxygen concentration through the water column, sedimentation rate and water depth). However, we cannot confirm global TOC content distribution is mainly related to SSchla, but to other chemical, physical and biological processes, or a combination of them. Nevertheless, TOC content distribution seems to be mainly related to SSchla in coastal upwelling regions. Thus, our data suggest that TOC content provides quantitative information on past PP in coastal upwelling regions, and underline TOC limitations as a quantitative proxy in a global scale.

Linear relationships between export proxies and PP are generally assumed on past PP reconstructions. This work confirms that SSchl_a concentration is linearly related to alkenones and TOC, but shows it is logarithmically related to chlorins (Figure 27). Thus, the use of chlorins proxy in previous studies might lead to an overestimation on past PP, which would need to be revised using the logarithmic correlation obtained in this study.

Research question 1.2. Which organic proxy provides more accurate values on past PP quantitative reconstructions?

Current available paleoproductivity proxies do not provide quantitative information on past PP. The global correlations obtained in this thesis (Table 4) will permit to obtain absolute estimates of SSchl_a concentration in past periods, which would serve to quantitatively infer past PP. Therefore, besides relative past PP changes through downcore, past PP changes will be able for comparison between different locations at any site in the global ocean.

Our data show that concentration of specific biomarkers (chlorins and alkenones) presents lower scatter than TOC content in their correlation with SSchl_a concentration (Figure 27). Consequently, the errors on past PP estimation derived from our equations would be lower when using biomarkers proxies, in comparison with TOC. One plausible reason that might contribute to explain the greater scatter in TOC proxy is that TOC englobes all organic compounds preserved in the sediment, meanwhile biomarkers consider specific molecules with similar chemical and physical properties. Our data also suggest that estimates from chlorins records have a lower error than for alkenones. This might be explained because chlorins take into account all phytoplankton community, meanwhile alkenones only represent some species of coccolithophores. Hence, our data suggest specific biomarkers would provide more accurate information than bulk organic matter (TOC) on global past PP estimations.

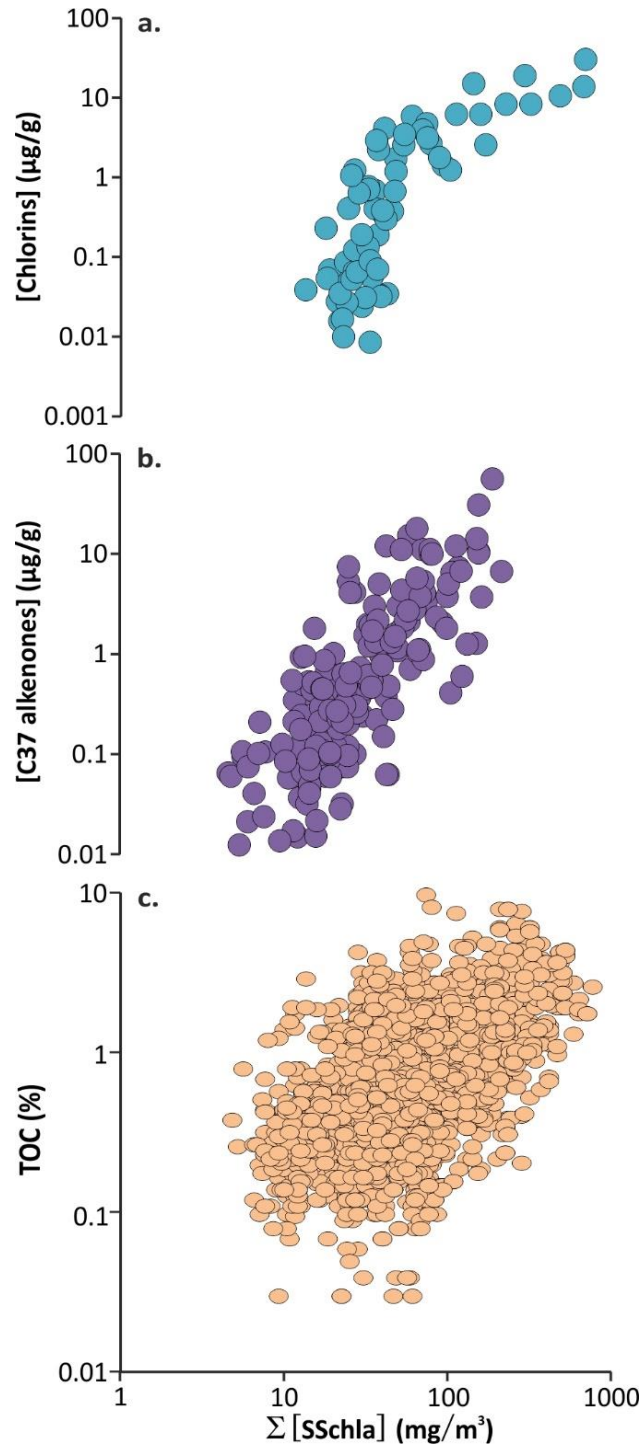


Figure 27. Global comparisons between the sum of sea-surface chlorophyll-*a* (SSchla) concentration from 1997 to 2017 and **a)** chlorins, **b)** C37 alkenones and **c)** total organic carbon (TOC) concentrations. This graphic includes regions presenting RMS log errors lower than 31% between remote sensing and *in situ* SSchla, and TOC graphic includes sediment samples below water columns deeper than 1,000 meters.

Proxy	y	x	Region	a	b	R ²	n
Chlorins	[Chlorins]	[SSchla]	Global	4.75	-16.16	0.68	70
Alkenones	Log[C37]	LogΣ[SSchla]	Global	1.26	-2.74	0.60	194
TOC	LogTOC	LogΣ[SSchla]	Coastal upwellings	1.02	-2.16	0.54	351

Table 4. Coefficients and errors of export proxies equations, with a R² higher than 0.5. These equations have been extracted from Chapter 1, 2 and 3. Data used in these equations include regions presenting RMS log errors lower than 31% between remote sensing and *in situ* SSchla. Data used in TOC equation include sediment samples below water columns deeper than 1,000 meters. *Abbreviations: sea-surface chlorophyll-a (SSchla), coefficient of determination (R²) and number of samples (n).*

In order to reach **Objective 2**, we compared bulk with chlorin and chlorophyll-*a* sedimentary nitrogen isotopic signal ($\delta^{15}\text{N}_{\text{bulk}}$, $\delta^{15}\text{N}_{\text{chlorin}}$ and $\delta^{15}\text{N}_{\text{chla}}$) from a global suite of core-top sediments, and study $\delta^{15}\text{N}_{\text{chlorin}}$ variability. We tested a) the transformation from chlorophyll-*a* (Chl *a*) into its degradation products, b) phytoplankton blooms and c) different oxygen content in bottom waters, as the main factors explaining $\delta^{15}\text{N}_{\text{chlorin}}$ variability.

Next, we answer the research questions set out to accomplish **Objective 2**:

Research question 2.1. Are nitrogen isotope proxies consistent on a global scale?

Our data indicate that bulk and chlorin nitrogen isotope proxies provide equivalent information on past nutrient conditions and past PP at global scale. However, $\delta^{15}\text{N}_{\text{chlorin}}$ analysis requires:

- high amount of sediment sample (>20 g), which can be an important limitation in paleoclimate studies,
- a modified EA-IRMS with higher analytical sensitivity, which would not be available in most laboratories, and
- a tedious analytical methodology, which would need high volume of solvents and time-consuming analysis.

Therefore, our study indicates that the use of $\delta^{15}\text{N}_{\text{bulk}}$ is far more straightforward and cheaper than compound specific $\delta^{15}\text{N}_{\text{chlorin}}$ analysis to obtain information on past surface ocean nutrient conditions and past PP. Nevertheless, compound-specific analysis might be needed in some specific regions where $\delta^{15}\text{N}_{\text{bulk}}$ is biased by postdepositional diagenetic alteration.

Hence, our results from the nutrient proxies study (*Chapter 5*) do not provide evidence for using specific compounds ($\delta^{15}\text{N}_{\text{chlorin}}$) rather than bulk sediment ($\delta^{15}\text{N}_{\text{bulk}}$) for estimating global past nutrient conditions and past PP. These results are in contrast to those obtained in the export proxies studies (*Chapter 2, 3 and 4*), which point out the potential of specific compounds

(biomarkers) to provide more accurate information than bulk organic matter (TOC) on global past PP estimations.

Research question 2.2. Can $\delta^{15}\text{N}_{\text{chlorin}}$ be used to track $\delta^{15}\text{N}_{\text{chla}}$ in sediment?

Our study on $\delta^{15}\text{N}_{\text{chlorin}}$ reflects high variability between individual chlorins, which suggests chemical, biological and physical processes might alter $\delta^{15}\text{N}_{\text{chlorin}}$. Hence, our results are at odds with the assumption that $\delta^{15}\text{N}_{\text{chlorin}}$ variability in sediment can be used to track changes in sedimentary $\delta^{15}\text{N}_{\text{chla}}$, which can complicate the interpretation of $\delta^{15}\text{N}_{\text{chlorin}}$ proxy for tracking past nutrient conditions and past PP. However, our data indicate that there is no nitrogen isotopic fractionation during the transformation of Chl *a* into its degradation products. Besides, we cannot confirm that neither phytoplankton blooms nor oxygen depositional conditions are the main cause of $\delta^{15}\text{N}_{\text{chlorin}}$ variability.

We must note that the data used in this study are spatially limited and might not define the global ocean dynamics, but provide some valuable information that should be taken into account in future research studies. Therefore, further studies are needed to identify the principal factors controlling $\delta^{15}\text{N}_{\text{chlorin}}$ variability to better constrain the applicability of $\delta^{15}\text{N}_{\text{chlorin}}$ as a proxy for reconstructing past nutrient conditions and past PP at global scale.

6.2. Further implications

Ocean surface and export processes are commonly studied by oceanographers using ocean biogeochemical models, meanwhile burial processes are studied by biogeochemists using diagenetic models. Hence, global processes that interplay and contribute to govern our climate are currently studied in the scientific community independently.

One of the big challenges of this thesis has been to provide an overall view of the chemical, physical and biological processes occurring from the surface to the sediments, on a global scale. Consequently, besides the main objectives, this thesis provides the following information about the global biological carbon pump.

6.2.1. The soft-tissue pump

Given the scarcity of observational data, export and buried PP estimations relies on ocean biogeochemical and early diagenetic models, respectively (Boudreau, 1996; Lutz et al., 2002; Martin et al., 1987; Stolpovsky et al., 2018; Suess, 1980; Wijsman et al., 2002). Using our chlorin and SSchla concentration data, we estimate that globally, the average fraction of the SSchla that is finally buried in the sediments in the form of chlorins is 0.33%, which is consistent with the fraction of global buried carbon estimated by modelling (Muller-Karger et al., 2005).

Moreover, our global correlations between SSchl_a and organic proxies concentration indicate that the spatial variability of surface organic matter is homogenised during export through the water column, driving to a spatially constant carbon flux from the sea-surface to the sediment. These results contribute to clarify the controversy on the spatial variability of the biological carbon export efficiency discussed on several studies (Henson et al., 2012; Lam et al., 2011; Marsay et al., 2015; Weber et al., 2016).

Furthermore, our data from the alkenones proxy study is concordant with previous studies that show picoplankton is dominant in terms of carbon sequestration (Dall'Olmo&Mork, 2014; Giering et al., 2016; Richardson et al., 2004; Richardson et al., 2006), and suggest photosynthetic picoeukaryotes (PPE) are the dominant phytoplankton in global carbon sequestration and burial in the sea-floor. Our results also indicate that PPE export contribution is proportional to total PP at global scale.

This thesis also points out the importance of samples location to describe global equations, as relationships obtained from specific regions might not reflect the global dynamics of the ocean. For instance, TOC content in sediments has been found to be mainly related to SSchl_a concentration in coastal upwellings, but the correlation found between them is much lower at global scale. Consequently, errors derived from TOC proxy would be higher in paleoreconstructions located out of coastal upwellings.

However, none of the preservation factors evaluated in this thesis (water depth, sedimentation rate and oxygen concentration in bottom waters and through the water column) seems to be the dominant in regulating TOC spatial distribution in sediments.

6.2.2. The carbonate pump

From our study of C₃₇ alkenones abundance and remote sensing sea-surface particulate inorganic carbon (SSPIC) concentration, it is deduced that SSPIC is not a good indicator of coccolithophore productivity. It might be because, in contrast to Chl *a* that is produced by living cells during photosynthesis, SSPIC is associated with detached coccoliths. Therefore, our data suggest SSPIC concentration does not provide information about coccolithophore fluxes from the sea-surface to the sediment and thus, neither about the global carbonate pump.

6.3. Future research

The results presented in this thesis also point out some questions that require further assessment in order to better constrain the global mechanisms governing our climate and provide data for

improving current tools used on oceanography and paleoclimate studies. Next, we suggest new research lines that can complement the results obtained in this thesis.

6.3.1. Ocean remote sensing validation

Currently, ocean remote sensing validation is based on comparison of remote sensing products with *in situ* discrete shipboard measurements. Consequently, short spatial and time coverages are used in the validations, which leads to a scarcity of validated data and limitations on describing natural processes that present temporal variability.

Therefore, we propose to use sedimentary data and the equations obtained in this thesis as a complementary tool for validating ocean remote sensing products. In this way, we can estimate global SSchl_a from sedimentary biomarkers using the equations obtained in *Chapters 2 and 3*. This new approach would enhance spatial coverage by incorporating new field data from global sedimentary compilations and would permit to consider longer time-scales to better assess natural processes by using the sedimentary record.

Thus, the equations derived from this thesis would enable the identification of oceanographic areas with optical properties that diverge from the global and needs specific algorithms for estimating SSchl_a concentration and PP. In this sense, the results of this thesis would provide a new tool for improving ocean biogeochemical models and their estimates of PP.

6.3.2. Implications of logarithmic relationship between chlorins and PP

A linear relationship between chlorins abundance and PP is generally assumed on past PP reconstructions. However, changes in past PP can be overestimated when using a linear, rather than a logarithmic, relationship (*see Chapter 2*). Therefore, a reinterpretation of chlorins proxy in paleorecords is needed applying the new logarithmic relationship obtained in this thesis.

The principal factor causing the logarithmic relationship, however, remains unknown after this work. We tested some depositional factors that might influence chlorins concentration in sediment. But, our data suggest neither bottom oxygen concentration nor sedimentation rates nor water column are the main factors controlling chlorins concentration. One plausible process that might contribute to the drastically drop of chlorins concentration is the opening of the tetrapyrrolic ring. This change in chlorins chemical structure will hamper the detection of the derived compound as the analytical techniques used for their detection are based on the absorbance and fluorescence properties of the aromatic ring. In this sense, the logarithmic relationship obtained in this thesis would serve as a start point to study past environmental conditions that can be linked to the marked decrease of chlorins concentration in sediment.

6.3.3. Constraining $\delta^{15}\text{N}_{\text{chlorin}}$ proxy

In this thesis we evaluated the global constraints of $\delta^{15}\text{N}_{\text{chlorin}}$ as a proxy for tracking past nutrient conditions and past PP. In this way, our results indicate changes in individual sedimentary $\delta^{15}\text{N}_{\text{chlorin}}$ cannot be used to track changes in sedimentary $\delta^{15}\text{N}_{\text{chla}}$, which can complicate the interpretation of $\delta^{15}\text{N}_{\text{chlorin}}$ proxy for tracking past nutrient conditions and past PP. Nevertheless, our results indicate there is no nitrogen isotopic fractionation during the transformation of Chl *a* into its degradation products. Besides, we cannot confirm that neither phytoplankton blooms nor oxygen depositional conditions are the main cause of $\delta^{15}\text{N}_{\text{chlorin}}$ variability. Hence, further studies are needed to identify the principal factors controlling $\delta^{15}\text{N}_{\text{chlorin}}$ variability to better constrain the applicability of $\delta^{15}\text{N}_{\text{chlorin}}$ proxy.

Taking into consideration the mentioned results, which indicate $\delta^{15}\text{N}_{\text{chlorin}}$ might not track $\delta^{15}\text{N}_{\text{chla}}$, and the main factor controlling $\delta^{15}\text{N}_{\text{chlorin}}$ variability remains unclear, our suggestion for estimating past nutrient conditions and past PP by using nitrogen isotopes would be to use the original signal of $\delta^{15}\text{N}_{\text{chla}}$. However, since Chl *a* might be relatively easily degraded in sedimentary records, an alternative option could be to measure the nitrogen isotopic signal of the total chlorin fraction (all chlorin compounds present in the sample), which has been used in the Mediterranean sea (Higgins et al., 2010). The total chlorins approach would stand between $\delta^{15}\text{N}_{\text{bulk}}$ proxy, which considers all accumulated nitrogen compounds, and $\delta^{15}\text{N}_{\text{chlorin}}$ proxy, which avoids diagenetic alterations from nitrogen compounds present in the sediment, such as aminoacids and proteins.

6.4. References

- Boudreau, B. P. (1996). A method-of-line code for carbon and nutrient daigenesis in aquatic sediments. *Computer & Geosciences*, 22(5), 479–496.
- Dall’Olmo, G., & Mork, K. A. (2014). Carbon export by small particles in the Norwegian Sea. *Geophysical Research Letters*, 1–6. <https://doi.org/10.1002/2014GL059244.1>.
- Giering, S. L. C., Sanders, R., Martin, A. P., Lindemann, C., Möller, K. O., Daniels, C. J., et al. (2016). High export via small particles before the onset of the North Atlantic spring bloom. *Journal of Geophysical Research: Oceans*, 121, 2268–2285. <https://doi.org/10.1002/2016JC011882>.Received
- Henson, S. A., Sanders, R., & Madsen, E. (2012). Global patterns in efficiency of particulate organic carbon export and transfer to the deep ocean. *Global Biogeochemical Cycles*, 26(1), 1–14. <https://doi.org/10.1029/2011GB004099>

- Higgins, M. B., Robinson, R. S., Carter, S. J., & Pearson, A. (2010). Evidence from chlorin nitrogen isotopes for alternating nutrient regimes in the Eastern Mediterranean Sea. *Earth and Planetary Science Letters*, *290*(1–2), 102–107. <https://doi.org/10.1016/j.epsl.2009.12.009>
- Lam, P. J., Doney, S. C., & Bishop, J. K. B. (2011). The dynamic ocean biological pump: Insights from a global compilation of particulate organic carbon, CaCO₃, and opal concentration profiles from the mesopelagic. *Global Biogeochemical Cycles*, *25*(3), 1–14. <https://doi.org/10.1029/2010GB003868>
- Lutz, M., Dunbar, R., & Caldeira, K. (2002). Regional variability in the vertical flux of particulate organic carbon in the ocean interior. *Global Biogeochemical Cycles*, *16*(3), 11–11–18. <https://doi.org/10.1029/2000GB001383>
- Marsay, C. M., Sanders, R. J., Henson, S. A., Pabortsava, K., Achterberg, E. P., & Lampitt, R. S. (2015). Attenuation of sinking particulate organic carbon flux through the mesopelagic ocean. *Proceedings of the National Academy of Sciences*, *112*(4), 1089–1094. <https://doi.org/10.1073/pnas.1415311112>
- Martin, J. H., Knauer, G. A., Karl, D. M., & Broenkow, W. W. (1987). VERTEX: carbon cycling in the northast Pacific, *34*(2), 267–285.
- Muller-Karger, F. E., Varela, R., Thunell, R., Luerssen, R., Hu, C., & Walsh, J. J. (2005). The importance of continental margins in the global carbon cycle. *Geophysical Research Letters*, *32*(1), 1–4. <https://doi.org/10.1029/2004GL021346>
- Palevsky, H. I., Quay, P. D., & Nicholson, D. P. (2016). Discrepant estimates of primary and export production from satellite algorithms, a biogeochemical model, and geochemical tracer measurements in the North Pacific Ocean. *Geophysical Research Letters*, *43*(16), 8645–8653. <https://doi.org/10.1002/2016GL070226>
- Richardson, T. L., Jackson, G. A., Ducklow, H. W., & Roman, M. R. (2004). Carbon fluxes through food webs of the eastern equatorial Pacific: An inverse approach. *Deep-Sea Research Part I: Oceanographic Research Papers*, *51*(9), 1245–1274. <https://doi.org/10.1016/j.dsr.2004.05.005>
- Richardson, T. L., Jackson, G. A., Ducklow, H. W., & Roman, M. R. (2006). Spatial and seasonal patterns of carbon cycling through planktonic food webs of the Arabian Sea determined by inverse analysis. *Deep-Sea Research Part II: Topical Studies in Oceanography*, *53*(5–7), 555–575. <https://doi.org/10.1016/j.dsr2.2006.01.015>

- Stolpovsky, K., Dale, A. W., & Wallmann, K. (2018). A new look at the multi-G model for organic carbon degradation in surface marine sediments for coupled benthic-pelagic simulations of the global ocean, (September), 1–26. <https://doi.org/10.5194/bg-15-3391-2018>
- Suess, E. (1980). Particulate organic carbon flux in the oceans—surface productivity and oxygen utilization. *Nature*, *288*(5788), 260–263. <https://doi.org/10.1038/288260a0>
- Weber, T., Cram, J. A., Leung, S. W., DeVries, T., & Deutsch, C. (2016). Deep ocean nutrients imply large latitudinal variation in particle transfer efficiency. *Proceedings of the National Academy of Sciences*, *113*(31), 8606–8611. <https://doi.org/10.1073/pnas.1604414113>
- Wijsman, J. W. M., Herman, P. M. J., Middelburg, J. J., & Soetaert, K. (2002). A model for early diagenetic processes in sediments of the continental shelf of the Black Sea. *Estuarine, Coastal and Shelf Science*, *54*(3), 403–421. <https://doi.org/10.1006/ecss.2000.0655>

Appendix



Picture author: MagicJS

Appendix 1. Supplementary figures and tables

Chapter 2

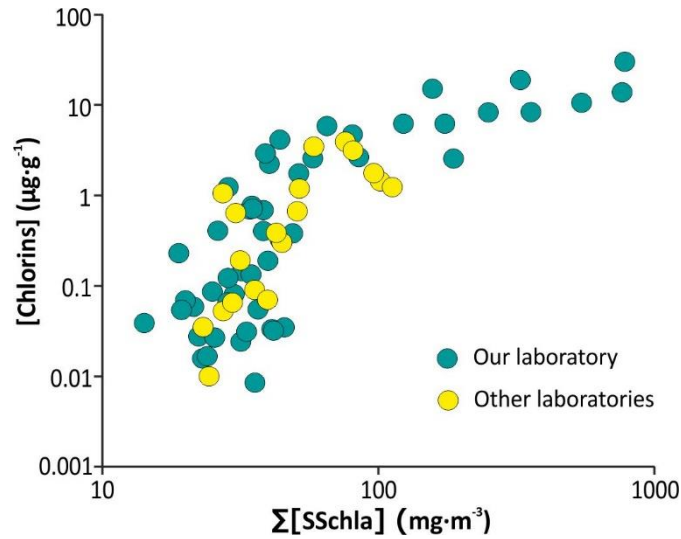


Figure A1. Global comparison between sedimentary chlorins concentration and the sum of sea-surface chlorophyll-*a* (SSchla) concentration from 1997 to 2017. This graphic includes regions presenting RMS log errors lower than 31% between remote sensing and *in situ* SSchla. Samples are classified according the laboratory that carried out the chlorins analysis: our laboratory (green) and other laboratories (yellow).

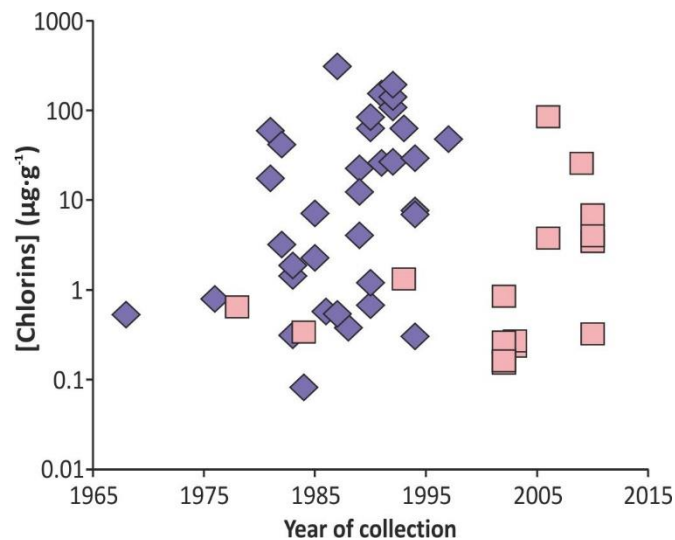


Figure A2. Global comparison between chlorins concentration and the year of sample collection. Samples are classified by core type: box corer and multicorer (pink squares), and gravity and piston core (purple diamonds).

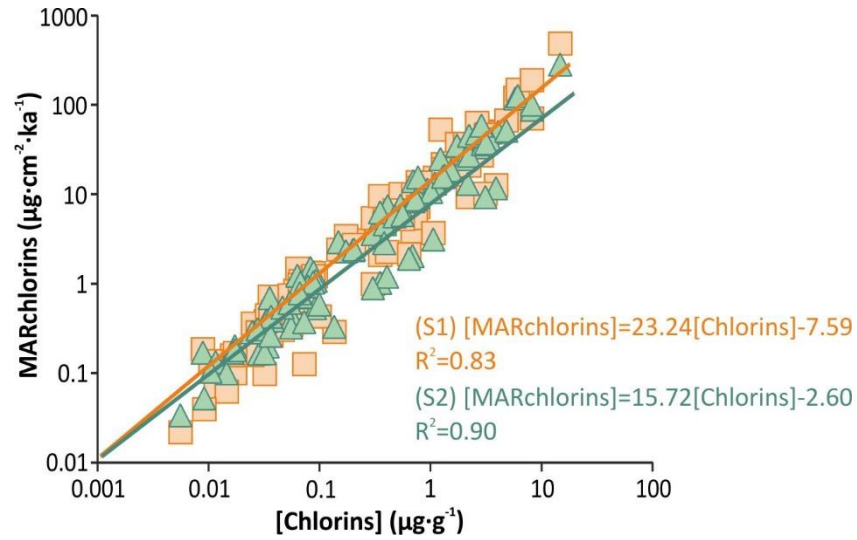


Figure A3. Global correlation between chlorin mass accumulation rate (MARchlorins) and chlorins concentration. MARchlorins was calculated from sedimentation rates published in [Dunne et al., 2012] (orange) and [Jahnke, 1996] (green).

Chapter 3

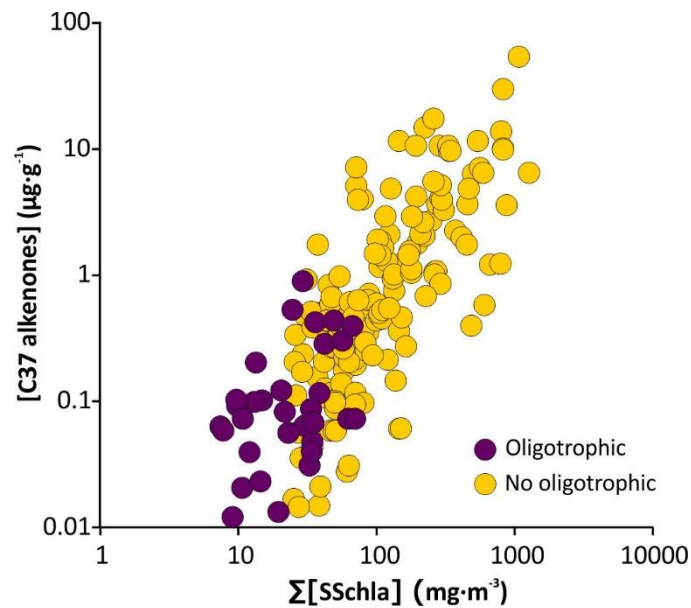


Figure A4. Global comparison between alkenones concentration and the sum of sea-surface chlorophyll-*a* (SSchla) concentration from 1997 to 2017. This graphic includes regions presenting RMS log errors lower than 31% between remote sensing and *in situ* SSchla. Purple and yellow dots represent samples located in oligotrophic and no oligotrophic areas, respectively.

Chapter 4

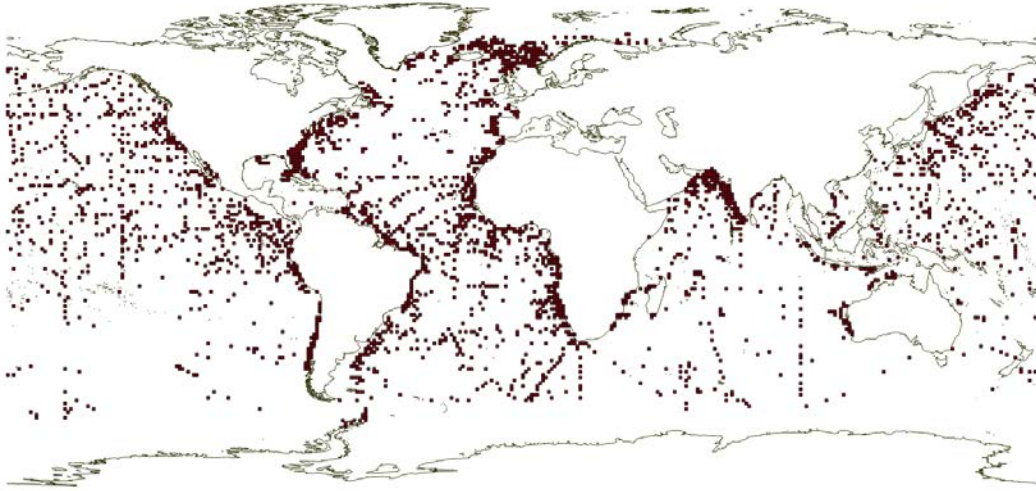


Figure A5. Combined map of our global core-top sediments location map (Figure 18) and a $1^\circ \times 1^\circ$ grid layer. Each $1^\circ \times 1^\circ$ cell contains averages values of sea-surface chlorophyll-*a* (SSchla) concentration from 1997 to 2017 and total organic carbon (TOC) content, from all the samples located inside the cell.

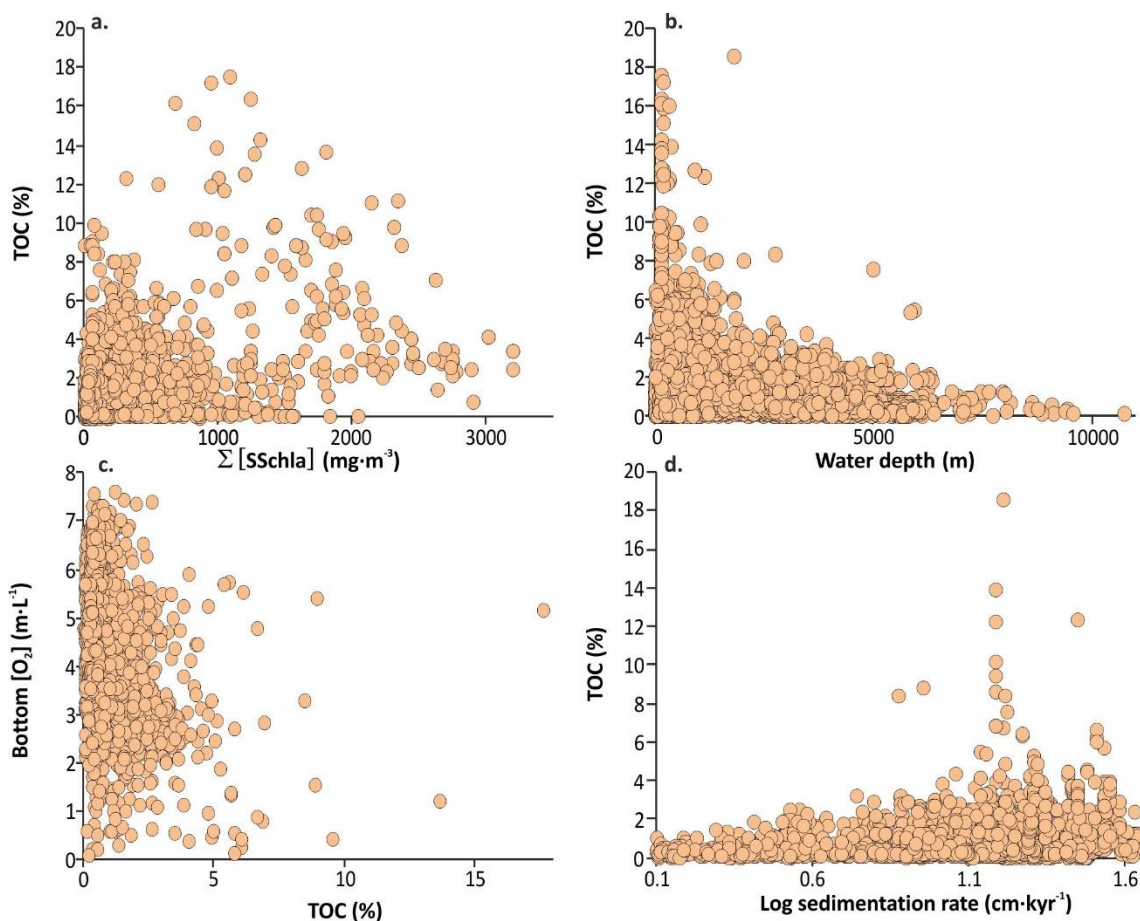


Figure A6. Global comparisons in non-logarithmic scale axis between sedimentary total organic carbon (TOC) content and **a.** sea-surface chlorophyll-*a* (SSchla) concentration from 1997 to 2017, **b.** water depth, **c.** oxygen concentration in bottom waters and **d.** the logarithm of sedimentation rate. These comparisons includes regions presenting RMS log errors lower than 31% between remote sensing and *in situ* SSchla

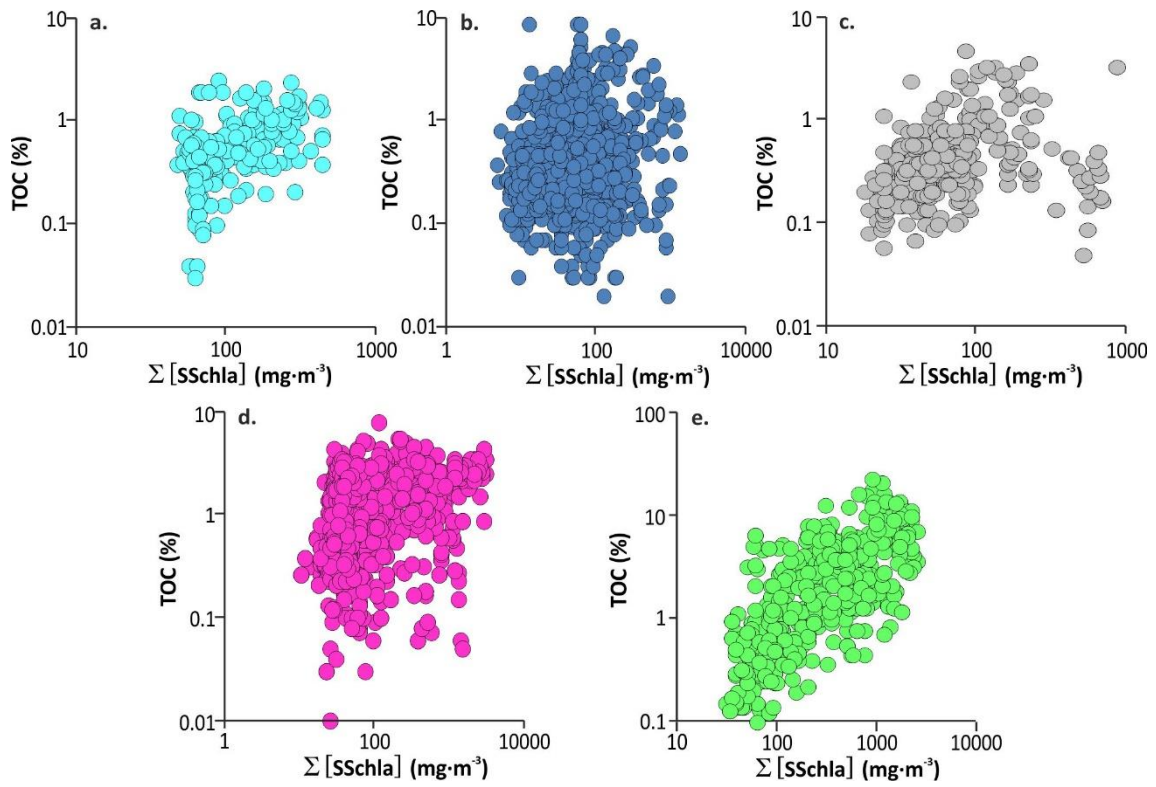


Figure A7. Regional comparisons between sedimentary total organic carbon (TOC) content and the sum of sea-surface chlorophyll-*a* (SSchla) concentration from 1997 to 2017. Different graphics present data from biogeochemical regions defined in Figure 18: **a.** northern latitudes, **b.** low latitudes, **c.** southern latitudes, **d.** equatorial upwellings, and **e.** coastal upwellings. These comparisons include regions presenting RMS log errors lower than 31% between remote sensing and *in situ* SSchla.

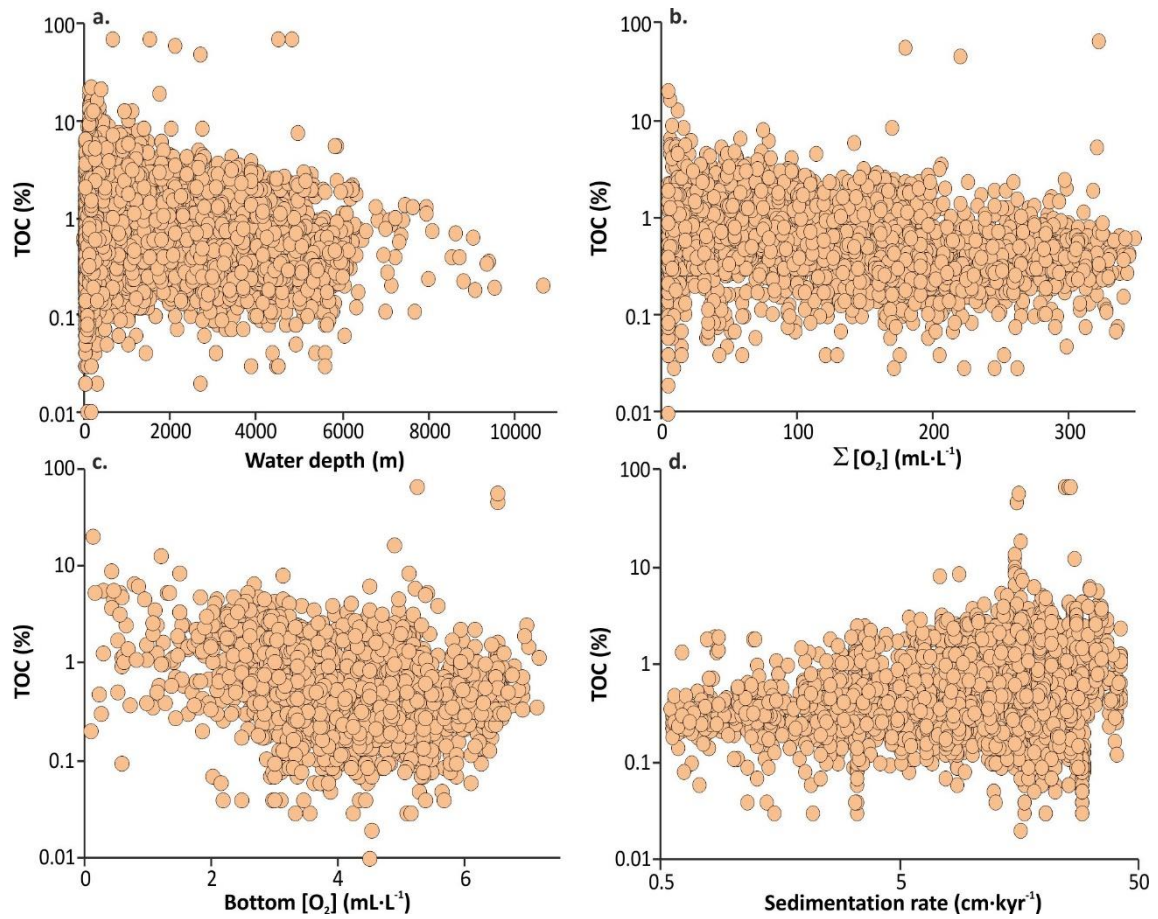


Figure A8. Global comparisons between sedimentary total organic carbon (TOC) content and **a.** water depth, **b.** oxygen concentration through the water column, **c.** oxygen concentration in bottom waters and **d.** sedimentation rate. These comparisons include the whole compilation.

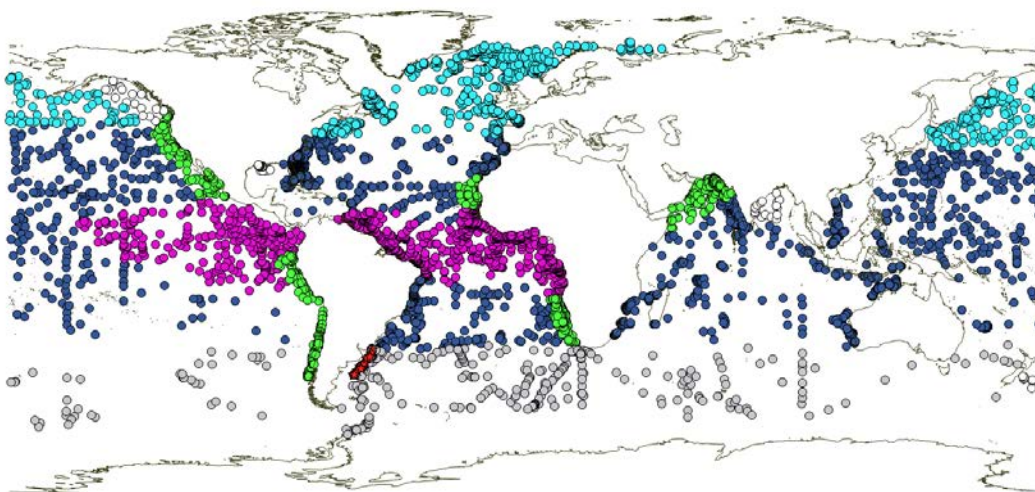


Figure A9. Global core-top sediments distribution. Coloured circles indicate distinct biogeochemical regions defined on the basis of temperature and nutrient concentration (Weber et al., 2016), and red stars indicate samples from the Brazil/Malvinas Confluence Zone.

Factor	Region	a	b	R ²	RMS log error (%)	n
$\Sigma[\text{Sschla}]$	Global	0.43	-0.99	0.25	22	4701
$\Sigma[\text{SSchla}]$	Nothern latitudes	0.62	-1.55	0.21	49	226
$\Sigma[\text{SSchla}]$	Low latitudes	0.17	-0.65	0.03	83	1756
$\Sigma[\text{SSchla}]$	Southern latitudes	0.22 0.69*	-0.79 1.61*	0.05 0.28*	68 38*	439 221*
$\Sigma[\text{SSchla}]$	Equatorial upwellings	0.32	-0.71	0.17	39	1362
$\Sigma[\text{SSchla}]$	Coastal upwellings	0.72	-1.52	0.54	24	689
WD	Global	-4×10^{-5}	-0.09	0.03	203681	6967
[O ₂]	Global	-1×10^{-3}	-0.10	0.06	11755	2589
Bottom [O ₂]	Global	-0.07	0.05	0.06	164	2589
LogSR	Global	0.18	-0.48	0.04	51	4457

Table A1. Equations coefficients and errors of total organic carbon equations. $\text{LogTOC} = a \cdot \log \Sigma[\text{SSchla}] + b$. Data used in these equations include regions presenting RMS log errors lower than 31% between remote sensing and *in situ* SSchla. Data identified with (*) have been calculated by not considering samples from the Brazil-Malvinas Confluence Zone. *Abbreviations:* sea-surface chlorophyll-a (SSchla) concentration from 1997 to 2018, water depth (WD), oxygen concentration through the water column ([O₂]), oxygen concentration in bottom waters (Bottom [O₂]), logarithm of sedimentation rate (LogSR), coefficient of determination (R²), root-mean square logarithmic error (RMS log error), number of samples (n).

Appendix 2. Database references

Chapter 3

Abrantes, Fatima F; Lebreiro, Susana Martin; Rodrigues, Teresa; Gil, Isabelle M; Bartels-Jonsdottir, Helga B; Oliveira, Paulo; Kissel, Catherine; Grimalt, Joan O (2005): Sea surface temperature reconstruction from biomarker in sediment core POS287-26-1B. PANGAEA, <https://doi.org/10.1594/PANGAEA.761848>

Álvarez, M. C., Flores, J. A., Sierro, F. J., Diz, P., Francés, G., Pelejero, C., & Grimalt, J. (2005). Millennial surface water dynamics in the Ría de Vigo during the last 3000 years as revealed by coccoliths and molecular biomarkers. *Palaeogeography, Palaeoclimatology, Palaeoecology*, 218(1–2), 1–13. <https://doi.org/10.1016/j.palaeo.2004.12.002>

Budziak, Dörte (2003): Alkenones data of surface sediments. PANGAEA, <https://doi.org/10.1594/PANGAEA.98753>

Budziak, Dörte; Schneider, Ralph R; Rostek, Frauke; Müller, Peter J; Bard, Édouard; Wefer, Gerold (2000): Alkenones, TOC and stable oxygen isotope ratios of *Neogloboquadrina dutertrei* of sediment core GeoB3005-1. PANGAEA, <https://doi.org/10.1594/PANGAEA.104770>

Chen, Wenwen; Mohtadi, Mahyar; Schefuß, Enno; Mollenhauer, Gesine (2014): Organic-geochemical proxies (UK'37 and TEXH86) records in surface sediments of the tropical Eastern Indian Ocean. PANGAEA, <https://doi.org/10.1594/PANGAEA.823057>

Goni, M. A., Woodworth, M. P., Aceves, H. L., Thunell, R. C., Tappa, E., Black, D., et al. (2004). Generation, transport, and preservation of the alkenone-based UK'37 sea surface temperature index in the water column and sediments of the Cariaco Basin (Venezuela). *Global Biogeochemical Cycles*, 18(2), 1–21. <https://doi.org/10.1029/2003GB002132>

Hinrichs, K. U., Schneider, R. R., Müller, P. J., & Rullkötter, J. (1999). A biomarker perspective on paleoproductivity variations in two Late Quaternary sediment sections from the Southeast Atlantic Ocean. *Organic Geochemistry*, 30(5), 341–366. [https://doi.org/10.1016/S0146-6380\(99\)00007-8](https://doi.org/10.1016/S0146-6380(99)00007-8)

Kennedy, J. A., & Brassell, S. C. (1992). Molecular records of twentieth-century El Niño events in laminated sediments from the Santa Barbara basin.

Kienast, M., MacIntyre, G., Dubois, N., Higginson, S., Normandeau, C., Chazen, C., & Herbert, T. D. (2012). Alkenone unsaturation in surface sediments from the eastern equatorial pacific: Implications for SST reconstructions. *Paleoceanography*, 27(1), 1–11.

<https://doi.org/10.1029/2011PA002254>

Méjanelle, L., & Laureillard, J. (2008). Lipid biomarker record in surface sediments at three sites of contrasting productivity in the tropical North Eastern Atlantic. *Marine Chemistry*, 108(1–2), 59–76.

<https://doi.org/10.1016/j.marchem.2007.10.002>

Mollenhauer, Gesine; Müller, Peter J (2003): TOC and C37-alkenones of sediment core IOW226660-5. Leibniz Institute for Baltic Sea Research, Warnemünde, PANGAEA, <https://doi.org/10.1594/PANGAEA.132785>

Mollenhauer, Gesine; Müller, Peter J (2003): TOC and C37-alkenones of sediment core IOW226920-3. Leibniz Institute for Baltic Sea Research, Warnemünde, PANGAEA, <https://doi.org/10.1594/PANGAEA.132790>

Müller, P. J., & Fischer, G. (2001). A 4-year sediment trap record of alkenones from the filamentous upwelling region off Cape Blanc, NW Africa and a comparison with distributions in underlying sediments. *Deep-Sea Research Part I: Oceanographic Research Papers*, 48(8), 1877–1903.

[https://doi.org/10.1016/S0967-0637\(00\)00109-6](https://doi.org/10.1016/S0967-0637(00)00109-6)

Ohkouchi, N., Kawamura, K., Kawahata, H., & Okada, H. (1999). Depth ranges of alkenone production in the central Pacific Ocean, *13(1998)*, 695–704

Pelejero, C., Grimalt, J. O., Sarnthein, M., Wang, L., & Flores, J. A. (1999). Molecular biomarker record of sea surface temperature and climatic change in the South China Sea during the last 140,000 years. *Marine Geology*, 156(1–4), 109–121.

[https://doi.org/10.1016/S0025-3227\(98\)00175-3](https://doi.org/10.1016/S0025-3227(98)00175-3)

Prahl, F. G., Rontani, J. F., Zabeti, N., Walinsky, S. E., & Sparrow, M. A. (2010). Systematic pattern in U37K'- Temperature residuals for surface sediments from high latitude and other oceanographic settings. *Geochimica et Cosmochimica Acta*, 74(1), 131–143.

<https://doi.org/10.1016/j.gca.2009.09.027>

Rostek, F., Bard, E., Beaufort, L., Sonzogni, C., & Ganssen, G. (1997). Sea surface temperature and productivity records for the past 240kyr in the Arabian Sea. *Deep-Sea Research*, 44(97), 1461–1480

Schefuß, Enno; Versteegh, Gerard J M; Jansen, J H Fred; Sinninghe Damsté, Jaap S (2004): (Table 4) Lipid biomarker concentrations from surface sediments, Southeast Atlantic. PANGAEA, <https://doi.org/10.1594/PANGAEA.205715>

Schwab, C., Kinkel, H., Weinelt, M., & Repschlger, J. (2012). Coccolithophore paleoproductivity and ecology response to deglacial and Holocene changes in the Azores Current System. *Paleoceanography*, 27(3), 1–18.

<https://doi.org/10.1029/2012PA002281>

Sikes, Elisabeth L; Volkman, J K; Robertson, L G; Pichon, Jean-Jacques (1997): (Table 2) Concentration of long chained alkenones and alkenes in sediment surface samples. PANGAEA, <https://doi.org/10.1594/PANGAEA.735810>

Weijers, Johan W H; Schouten, Stefan; Schefuß, Enno; Schneider, Ralph R; Sinninghe Damsté, Jaap S (2009): Bulk and molecular proxies of sediment core GeoB6518-1. PANGAEA, <https://doi.org/10.1594/PANGAEA.745616>

Chapter 4

The references of the total organic carbon global compilation are included in the attached CD / Appendix2-Chapter4 file.

Chapter 5

Enders, S. K., Pagani, M., Pantoja, S., Baron, J. S., Wolfe, A. P., Pedentchouk, N., & Nunez, L. (2008). Compound-specific stable isotopes of organic compounds from lake sediments track recent environmental changes in an alpine ecosystem, Rocky Mountain National Park, Colorado. *Limnology and Oceanography*, 53(4), 1468–1478.

Fulton, James M., Arthur, M. A., & Freeman, K. H. (2012). Black Sea nitrogen cycling and the preservation of phytoplankton $\delta^{15}\text{N}$ signals during the Holocene. *Global Biogeochemical Cycles*, 26(2), n/a-n/a. <https://doi.org/10.1029/2011GB004196>

Fulton, J. M., Arthur, M. A., Thomas, B., & Freeman, K. H. (2018). Pigment carbon and nitrogen isotopic signatures in euxinic basins. *Geobiology*, 16(4), 429–445.

<https://doi.org/10.1111/gbi.12285>

Higgins, Meytal B; Robinson, Rebecca S; Carter, Susan J; Pearson, Ann (2010): (Appendix) Carbon and nitrogen isotope ratios of ODP Site 160-964. PANGAEA,

<https://doi.org/10.1594/PANGAEA.786705>

Junium, C. K., Arthur, M. A., & Freeman, K. H. (2015). Compound-specific $\delta^{15}\text{N}$ and chlorin preservation in surface sediments of the Peru Margin with implications for ancient bulk $\delta^{15}\text{N}$ records. *Geochimica et Cosmochimica Acta*, 160, 306–318.

<https://doi.org/10.1016/j.gca.2014.12.018>

Kusch, Stephanie; Kashiyama, Y; Ogawa, Nanako O; Altabet, Mark A; Butzin, Martin; Friedrich, Jana; Ohkouchi, Naohiko; Mollenhauer, Gesine (2010): (Table 1) Radiocarbon and stable isotopic compositions of purified chloro- and pheopigments, bivalve shells, total organic carbon, and bulk sediment. PANGAEA, <https://doi.org/10.1594/PANGAEA.758102>

Naeher, S., Suga, H., Ogawa, N. O., Schubert, C. J., Grice, K., & Ohkouchi, N. (2016a). Compound-specific carbon and nitrogen isotopic compositions of chlorophyll a and its derivatives reveal the eutrophication history of Lake Zurich (Switzerland). *Chemical Geology*, 443, 210–219. <https://doi.org/10.1016/j.chemgeo.2016.09.005>

Naeher, S., Suga, H., Ogawa, N. O., Takano, Y., Schubert, C. J., Grice, K., & Ohkouchi, N. (2016b). Distributions and compound-specific isotopic signatures of sedimentary chlorins reflect the composition of photoautotrophic communities and their carbon and nitrogen sources in Swiss lakes and the Black Sea. *Chemical Geology*, 443, 198–209.

<https://doi.org/10.1016/j.chemgeo.2016.04.029>

Tyler, J., Kashiyama, Y., Ohkouchi, N., Ogawa, N., Yokoyama, Y., Chikaraishi, Y., et al. (2010). Tracking aquatic change using chlorine-specific carbon and nitrogen isotopes: The last glacial-interglacial transition at Lake Suigetsu, Japan. *Geochemistry Geophysics Geosystems*, 11(9), Q09010. <https://doi.org/10.1029/2010GC003186>

Xin, Y. (2015). Nitrogen cycling in the northern Benguela Upwelling System based on the $\delta^{15}\text{N}$ of chlorophyll pigment Dissertation, 149.

